

**Characterization of new proteins involved in chloroplast biogenesis
from *Arabidopsis thaliana***

Dissertation
der Fakultät für Biologie
der Ludwig-Maximilians-Universität München

vorgelegt von
Roberto Andres Espinoza Corral

München
März 2019

Diese Dissertation wurde angefertigt unter der Leitung von Prof. Dr. Jürgen Soll an der Fakultät für Biologie der Ludwig-Maximilians-Universität München.

Erstgutachter: Prof. Dr. Jürgen Soll
Zweitgutachter: Prof. Dr. Wolfgang Frank
Tag der Abgabe: 29.01.2019
Tag der mündlichen Prüfung: 21.03.2019

Printed with the support of the German Academic Exchange Service.

Table of Contents

SUMMARY	1
ZUSAMMENFASSUNG	2
ABBREVIATIONS	3
1 INTRODUCTION	6
1.1 ORIGIN OF PLASTIDS	6
1.2 PROTEIN TARGETING AND IMPORT INTO THE PLASTID	6
1.3 CHLOROPLAST BIOGENESIS AND MATURATION	8
1.4 THYLAKOID BIOGENESIS	10
1.5 THE FUNCTION OF PLASTOGLOBULI	13
1.6 AIM OF THIS WORK	16
2 MATERIAL AND METHODS	17
2.1 MATERIAL	17
2.1.1 <i>Chemicals</i>	17
2.1.2 <i>Molecular weight and size markers</i>	17
2.1.3 <i>Oligonucleotides</i>	17
2.1.4 <i>Vectors</i>	19
2.1.5 <i>Enzymes</i>	20
2.1.6 <i>Bacterial strains</i>	20
2.1.7 <i>Membranes</i>	20
2.1.8 <i>Antisera</i>	20
2.1.9 <i>Accession numbers</i>	21
2.1.10 <i>Computational analyses</i>	21
2.2 MOLECULAR BIOLOGICAL METHODS	22
2.2.1 <i>Cloning strategies</i>	22
2.2.2 <i>Polymerase chain reaction (PCR)</i>	23
2.2.3 <i>Isolation of plasmid DNA from E. coli</i>	23
2.2.4 <i>Sequencing</i>	23
2.2.5 <i>Isolation of genomic DNA from A. thaliana for genotyping PCR</i>	23
2.2.6 <i>Isolation of RNA from A. thaliana</i>	24
2.2.7 <i>cDNA synthesis</i>	24
2.2.8 <i>Protein precipitation with trichloroacetic acid (TCA)</i>	24
2.3 BIOCHEMICAL METHODS	24
2.3.1 <i>Overexpression of recombinant proteins</i>	24
2.3.2 <i>Purification of soluble proteins</i>	25
2.3.3 <i>Purification of proteins out of inclusion bodies</i>	25
2.3.4 <i>Isolation of proteins from A. thaliana</i>	26
2.3.5 <i>Determination of protein concentration</i>	26
2.3.6 <i>SDS polyacrylamide gel electrophoresis (SDS-PAGE)</i>	26
2.3.7 <i>Semi-dry electro blot and immunodetection of proteins</i>	27
2.3.8 <i>Detection of radiolabeled proteins</i>	27
2.3.9 <i>Blue Native PAGE (BN-PAGE)</i>	27
2.3.10 <i>Silver staining of SDS gels</i>	28

2.3.11	<i>Mass spectrometry</i>	28
2.3.12	<i>Transformation of A. tumefacium</i>	28
2.3.13	<i>Pigment analysis</i>	28
2.3.14	<i>In vitro transcription</i>	29
2.3.15	<i>In vitro translation</i>	29
2.3.16	<i>Agarose gel electrophoresis</i>	30
2.3.17	<i>Electrophoretic mobility shift assay (EMSA)</i>	30
2.3.18	<i>RNAse assay</i>	30
2.3.19	<i>Northern Blot</i>	31
2.4	CELL BIOLOGICAL METHODS	32
2.4.1	<i>Isolation of intact chloroplasts from P. sativum</i>	32
2.4.2	<i>Isolation of inner and outer chloroplast envelope from P. sativum</i>	32
2.4.3	<i>Isolation of plastoglobuli from P. sativum</i>	33
2.4.4	<i>Isolation of thylakoid membranes</i>	33
2.4.5	<i>Solubilization of thylakoid membranes</i>	34
2.4.6	<i>Thylakoid membrane wash from A. thaliana</i>	34
2.4.7	<i>Trypsin digestion of thylakoid membranes from A. thaliana</i>	34
2.4.8	<i>In vitro import into chloroplasts from P. sativum</i>	35
2.4.9	<i>In vivo translation of proteins in Arabidopsis seedlings</i>	35
2.4.10	<i>RNAse A treatment</i>	36
2.5	PLANT BIOLOGICAL METHODS	36
2.5.1	<i>Plant growth conditions</i>	36
2.5.2	<i>Stable transformation of A. thaliana with A. tumefacium</i>	36
2.5.3	<i>Transient transformation of N. benthamiana</i>	37
2.5.4	<i>Isolation of protoplast from N. benthamiana for GFP localization</i>	37
2.5.5	<i>Photosynthetic performance by pulse amplitude modulation analysis (PAM)</i>	38
2.6	MICROSCOPY	39
2.6.1	<i>Analysis of chloroplast ultrastructure</i>	39
3	RESULTS	40
3.1	RV-1	40
3.1.1	<i>Phylogenetic conservation of RV-1</i>	40
3.1.2	<i>RV-1 localization in chloroplasts</i>	42
3.1.3	<i>Isolation of rv-1 mutant lines</i>	44
3.1.4	<i>Translation is impaired in rv-1</i>	48
3.1.5	<i>Analysis of a putative RNAse activity of RV-1</i>	50
3.1.6	<i>Characterization of the RV-1-like gene</i>	55
3.2	PG18	58
3.2.1	<i>Characterization of PG18</i>	58
3.2.2	<i>Characterization of pg18 mutant lines</i>	63
3.2.3	<i>Arabidopsis pg18 mutant plants show symptoms of light stress</i>	67
3.2.4	<i>Photosynthetic performance is affected in pg18 mutant plants</i>	70
3.2.5	<i>Loss of PG18 has an impact on the accumulation of thylakoid membrane complexes</i>	74
4	DISCUSSION	76

4.1 RV-1	77
4.2 PG18	79
5 LITERATURE	84
CURRICULUM VITAE	95
VERÖFFENTLICHUNGEN	96
EIDESSTATTLICHE VERSICHERUNG	97
DANKSAGUNG	98

Summary

Chloroplasts consist of highly organized membranes with a double envelope and an inner stacked membranous system called thylakoids wherein photosynthesis takes place. The biogenesis of chloroplasts requires the expression of genes encoded in the nucleus and their product translated into proteins that have to be imported into the organelle, as well as from genes encoded in the chloroplast. In this way, organelles cannot form *de novo* but rather are generally maternally inherited and multiply by division.

The biogenesis of chloroplasts starts from undifferentiated plastids lacking thylakoids. Upon light, differentiation is triggered in angiosperms, and thylakoids are built up progressively to form photosynthetic chloroplasts. In spite of what is known about the composition of the photosynthetic machinery, the making of the thylakoid components is not well understood and even less is known about the proteins involved in the differentiation from proplastids into chloroplasts. Here, we identify two proteins namely RV-1 and PG18, which loss of function in *A. thaliana* impact chloroplast biogenesis as well as function. RV-1 is a protein located in the stroma of the chloroplast which loss of function causes a seedling lethal phenotype with plants which form only albino cotyledons and leaves. Biochemical studies revealed that RV-1 partially comigrates with ribosomes but the exact function is still unknown. On the other hand, PG18 is a protein located in the plastoglobuli of chloroplasts and plays a role in thylakoid formation and function. The characterization of loss of function mutant plants reveals that it is important for the photosynthetic activity. Mutant plants are pale with a reduction of PSI subunits as well as the ATP synthase. Additionally, PG18 loss of function impacts the ultrastructure of chloroplasts by reducing their size, shortening the stroma lamellae and a higher grana stacking degree in the thylakoid membranes compared to wild type.

Zusammenfassung

Chloroplasten bestehen aus hochorganisierten Membranen mit einer doppelten Hülle und einem inneren, gestapelten Membransystem, den Thylakoiden, an denen die Photosynthese stattfindet. Die Biogenese von Chloroplasten erfordert die Expression von Genen, welche direkt in den Plastiden kodiert sind. Darüberhinaus werden Proteine benötigt, deren Gene im Kern kodiert sind. Diese Proteine müssen post-translational in den Chloroplasten importiert werden. Daher können Organellen nicht *de novo* gebildet werden, sondern werden in der Regel mütterlich vererbt und durch Teilung vermehrt.

Die Biogenese von Chloroplasten beginnt mit undifferenzierten Plastiden ohne Thylakoide, den sogenannten Proplastiden. Durch Licht wird in Angiospermen eine Differenzierung ausgelöst und die Thylakoide werden nach und nach zu photosynthetischen Einheiten aufgebaut. Trotz des Wissens über die Zusammensetzung der Photosynthesemaschine ist die Entstehung der Thylakoidkomponenten noch ungeklärt. Gleiches gilt für die Proteine, die an der Differenzierung von Proplastiden zu Chloroplasten beteiligt sind. Hier identifizieren wir zwei Proteine, nämlich RV-1 und PG18, deren Funktionsverluste bei *A. thaliana* sowohl die Chloroplastenbiogenese als auch die Funktion beeinflussen. RV-1 ist ein Protein, das sich im Stroma des Chloroplasten befindet, dessen Funktionsverlust einen keimlingsletalen Phänotyp verursacht, wobei die Pflanzen nur albinotische Kotyledonen und -blätter erzeugen. Biochemische Studien haben gezeigt, dass RV-1 teilweise mit Ribosomen komigriert, obwohl die genaue Funktion noch unbekannt ist. Auf der anderen Seite ist PG18 ein Protein, das sich in den Plastoglobuli der Chloroplasten befindet und eine Rolle bei der Bildung und Funktion von Thylakoiden spielt. Die Charakterisierung des Funktionsverlustes von Mutantpflanzen zeigt, dass PG18 für die photosynthetische Aktivität wichtig ist. Mutantpflanzen sind blass mit einer Reduktion von PSI-Untereinheiten sowie der ATP-Synthase. Zudem beeinflusst der PG18-Funktionsverlust die Ultrastruktur von Chloroplasten, indem er deren Größe reduziert, die Stromalamellen verkürzt und einen höheren Grad von Granastapel in den Thylakoidmembranen im Vergleich zum Wildtyp aufweist.

Abbreviations

ATP	Adenosine triphosphate
BCA	Bicinchoninic acid
BLAST	Basic local alignment search tool
BN-PAGE	Blue native polyacrylamide gel electrophoresis
BSA	Bovine serum albumin
CDS	Coding sequence
Col-0	<i>Arabidopsis thaliana</i> ecotype Columbia
cpSEC	Chloroplast Secretory pathway
cpTAT	Chloroplast Twin Arginine Translocase
Cyt	Cytochrome
DGDG	Digalactosyl diacylglycerol
DMF	Dimethyl formamide
DNA	Deoxyribonucleic acid
DTT	Dithiothreitol
ECL	Enhanced chemiluminescence
EDTA	Ethylene-diamine-tetra-acetic acid
EGTA	Ethylene glycol bis (aminoethyl ether) -N, N, N', N'-tetraacetic acid
EMSA	Electrophoretic Mobility Shift Assay
ETR	Electron Transfer Rate
ER	Endoplasmic reticulum
FBN	Fibrillin
gDNA	Genomic DNA
GFP	Green fluorescent protein
GTP	Guanosine triphosphate
H	Homozygous
h	Heterozygous
HEPES	2- (4- (2-hydroxyethyl) -1-piperazinyl) ethanesulfonic acid
His tag	Hexa or deca histidine tag
Hsp	Heat shock protein

IE	Inner envelope of the chloroplast
IL	Increased light
IPTG	Isopropyl- β -D-thiogalactopyranoside
kDa	Kilodalton
LDS	Lithium dodecyl sulfate
LHC	Light harvesting complex
MBP	Maltose binding protein
MDGD	Mono galactosyl diacylglycerol
MES	2- (N-Morpholino) ethanesulfonic acid
MOPS	3- (N-Morpholino) propanesulfonic acid
mRNA	Messenger RNA
mt	Mutant
NADPH	Nicotinamide adenine dinucleotide phosphate
Ni-NTA	Nickel-nitrilotriacetic acid
NL	Normal light
NPQ	Non-photochemical quenching
PAGE	Polyacrylamid gel electrophoresis
PAM	Pulse Amplitude Modulation
pb	Pair base
PCR	Polymerase chain reaction
PG	Platoglobuli
PLBs	Prolamellar bodies
PMSF	Phenylmethylsulfonyl fluoride
PS	Photosystem
PVDF	Polyvinylidene fluoride
PVP	Polyvinylpyrrolidone
RNA	Ribonucleic acid
rRNA	Ribosomal RNA
RT	Room temperature
ROS	Reactive oxygen species
RSH	RelA and SpoT homolog

OE	Outer envelope of the chloroplast
SDS	Sodium dodecyl sulfate
SGDG	Sulfoquinovosyl diacylglycerol
SPP	Stromal processing peptidase
T-DNA	Transferred DNA
TCA	Trichloroacetic acid
TBST	Tris-buffered saline and Polysorbate 20
TEM	Transmission electron microscopy
TIC	Translocase of the inner membrane of chloroplasts
tRNA	Transfer RNA
TOC	Translocase of the outer membrane of chloroplasts
TP	Transit peptide
TPP	Thylakoidal processing peptidase
WT	Wildtype
Y	Quantum yield of photosystem
β -DM	β -dodecyl maltoside

1 Introduction

1.1 Origin of plastids

Life as we know it today is the result of successful adaptation and evolution throughout billions of years. In the beginning of this process, our planet had a toxic and warmer atmosphere deprived of oxygen with abundant greenhouse gases and dramatically different ocean chemistries (Kerr, 2005). In this scenario, life appeared 3,5 billions of years ago as self-replicable organisms with the fundamental components such as RNAs, DNAs, amino acids, and membranes (Brasier *et al.*, 2015; Lake *et al.*, 2018). Among all the components that were changing on early earth, one constant that shaped the rest of life's story is the sun. About 2.5 billions of years ago emerged the first organism able to convert solar radiation into chemical energy and releasing oxygen to the atmosphere, a process called oxygenic photosynthesis (Shih, 2015). This event dramatically changed the earth's fate by producing oxygen from water splitting and using its electrons to drive biosynthetic metabolism (De Marais, 2000). In order to do so, this photosynthetic ancestor had to develop systems of protein complexes to split water and transport electrons to oxidized acceptors (Cardona, 2018; Ponce-Toledo *et al.*, 2017). It was not until 1.5 billions of years ago when a heterotrophic protist engulfed an ancestral photosynthetic cyanobacterium marking the birth of modern plastids such as chloroplasts (de Vries & Archibald, 2017; Douzery *et al.*, 2004).

1.2 Protein targeting and import into the plastid

The endosymbiotic event resulted in a massive transfer of genetic material to the host cell leading the cyanobacterial guest into a semiautonomous state (Stiller, 2007). In spite of this, plastids retained their own genome, today encoding for just a small number of their proteins. Modern plastids contain between 2100 to 4800 proteins, for which plastid genomes encode for between 60 to 200 proteins in various lineages (Richly & Leister, 2004; Timmis *et al.*, 2004). Ever since, plastids necessitate a system for trafficking of translated proteins encoded by nuclear genes through the organelle membranes which gave rise to the translocons of the outer and inner

envelope membrane of the modern chloroplast (TOC and TIC respectively) (Gross & Bhattacharya, 2009). The right sorting of proteins destined to the plastid and other organelles was accomplished by sequence information to facilitate their correct trafficking within the cell. Although in most cases this information resides in a cleavable N-terminal sequence the different organelle-targeting sequences have distinct properties (Kim & Hwang, 2013). The N-terminal sequences for chloroplast localization is highly heterologous and have a net positive charge due to lack of acidic residues (Schwenkert *et al.*, 2011).

The proteins encoded by nuclear genes that are localized to the plastid are translated in the cytosol and recognized at the surface of the organelle in order to proceed with their import. At this point, the pre-proteins are assisted by chaperones in the cytosol to prevent their aggregation (Schwenkert *et al.*, 2011). Once the complex of pre-protein and chaperones reaches the plastid surface, the N-terminal transit peptide (TP) is recognized by members of the TOC apparatus. Its core components are Toc159, Toc34 and Toc75. Depending on the chaperones bound to the pre-protein, the TP makes first contact with either Toc34 or Toc159 receptors in a GTP depending manner (Demarsy *et al.*, 2014; Hirsch *et al.*, 1994; Kessler *et al.*, 1994). Afterwards the import across the outer envelope continues through Toc75, which forms a β -barrel protein acting as a channel embedded in the membrane (Hinnah *et al.*, 2002). Once the pre-protein passes across the outer envelope, it reaches the TIC apparatus composed of Tic110, Tic40 and Hsp93 as the minimal functional unit and Tic32, Tic55 and Tic62, which form the redox regulon. At the inner membrane, the first point of contact is assumed to be Tic110, which was identified decades ago (Schnell *et al.*, 1994). This has been thought to be the major channel of the TIC apparatus (Balsera *et al.*, 2009; Heins *et al.*, 2002; Kovacheva *et al.*, 2005), however Tic20 has also been proposed as a channel at the inner envelope (Kikuchi *et al.*, 2009; Kouranov *et al.*, 1998). Tic40 and Hsp93 assist the import of the pre-protein through the inner envelope along with the consumption of ATP (Chou *et al.*, 2006; Kovacheva *et al.*, 2005). This process has been reported to be regulated by the NADP⁺/NADPH ratio in the interaction of Tic32 and Tic62 with Tic110 (Benz *et al.*, 2009; Chigri *et al.*, 2006). Additionally, Tic55 has been identified as a potential

thioredoxin target (Bartsch *et al.*, 2008). Once the pre-protein crosses the inner and outer envelopes, its TP is cleaved off by the stromal processing peptidase (SPP) (Trosch & Jarvis, 2011) and the mature protein is folded with the assistance of Hsp70 (Flores-Perez & Jarvis, 2013; Yalovsky *et al.*, 1992).

Imported proteins can still continue their transit to the thylakoid membranes or the lumen inside the thylakoids. These proteins bear a bipartite TP, wherein its first part is used for translocation across the envelopes and the second part guides the intermediate to thylakoids where it is processed by a thylakoidal processing peptidase (TPP) (Chaal *et al.*, 1998; Schackleton & Robinson, 1991). Then the protein in transit can follow one of four pathways; for membrane proteins spontaneous insertion or the Signal Recognition Particle (SRP) dependent pathway, and for luminal proteins the Secretory (cpSec) or the Twin Arginine Translocase (cpTat) pathways (Albiniak *et al.*, 2012; Schunemann, 2007).

1.3 Chloroplast biogenesis and maturation

Plastids, while functionally and structurally distinct, are present in all plant cells. They originate from the differentiation of proplastids, requiring thylakoid membrane formation and protein synthesis (Barsan *et al.*, 2012; Enami *et al.*, 2011; Rottet *et al.*, 2015). Proplastids are colorless round organelles deprived of internal membranes which in the presence of light undergo differentiation into chloroplasts in angiosperms by building up consecutive phases of internal membrane systems, a process during which often vesicles or small saccular structures have been observed (Muhlethaler, 1959; Vothknecht & Westhoff, 2001). However, in absence of light, plastids turn into etioplasts, which contain few internal membranes but a characteristic prolamellar body, rich in Mg-tetrapyrrole protochlorophyllide and NADPH dependent protochlorophyllide oxidoreductase (Sperling *et al.*, 1998). Upon illumination, etioplasts can continue their differentiation into chloroplasts (Solymosi & Schoefs, 2010).

Plastids are not synthesized *de-novo* but rather originate from division - similar to prokaryotes. Plastid division happens in developing tissues such as new leaves and meristems, i.e. chloroplasts as well as proplastids can undergo division

(Miyagishima, 2011). Depending on the tissue and developmental stage, proplastids differentiate into multiple organelles with distinct functions (Figure 1). Among these we find chromoplasts, which are non-photosynthetic carotenoid accumulating plastids abundant in flowers, fruits and roots (Egea *et al.*, 2010). Alternatively, proplastids can differentiate into amyloplasts, located in root cells and specialized in starch accumulation. Recently, these plastids have been found to play an important role in gravitropism of roots (Toyota *et al.*, 2013). Finally, proplastids can differentiate into chloroplast. Their maturation starts with the elongation of a first lamella, which ultimately forms stacks known as grana (Westphal *et al.*, 2003). The specific steps that lead to the initial thylakoid formation are still unknown. Nevertheless the observation of vesicles in early stages of chloroplast maturation suggests that vesicle trafficking is involved in thylakoid biogenesis (Morre *et al.*, 1991). Moreover, in some plants such as maize and sorghum vesicles have also been observed in fully mature chloroplasts (Rosado-Alberio *et al.*, 1968).

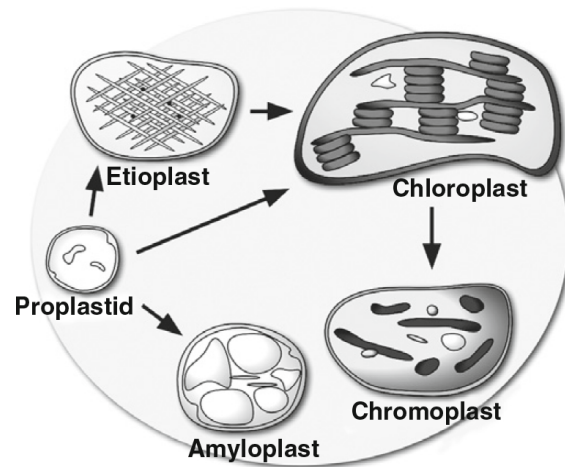


Figure 1. Proplastid differentiation fates. In absence of light, proplastids differentiate into etioplasts which then turn into chloroplasts upon light exposure. Additionally, proplastids can differentiate into amyloplast in tissues such as roots. Depending on the developmental stage, chloroplast can further differentiate into plastids rich in carotenoids known as chromoplast which are present in tissues such as fruits and flowers. Modified from Kato and Sakamoto (2010).

In addition to membrane re-modeling and protein import, chloroplast maturation requires the coordination of other processes happening inside the organelle such as transcription and translation. Plastid genes are highly regulated at RNA level by RNA splicing, editing and processing (Mullet, 1993; Suzuki *et al.*, 2003). Besides, it has been shown that plastid rRNAs undergo multiple maturation steps for ribosome assembly by various nuclear encoded RNases. Chloroplast RNases have been shown to play a role also in the maturation of tRNAs and other transcripts as well as for RNA decay. The importance of these RNases has been confirmed by their deletions which often leads to lethal phenotypes (Stoppel & Meurer, 2012). Protein synthesis inside the chloroplast is performed by bacterial-type 70S ribosomes, composed of a large subunit (50S) and a small subunit (30S) containing one (16S rRNA) and three rRNAs species (23S rRNA, 5S rRNA, and 4.5S rRNA), respectively (Zoschke & Bock, 2018). Just recently, the structure of the chloroplast ribosome has been resolved which reveals plastid specific extensions remodeling the mRNA entry and exit sites (Bieri *et al.*, 2017).

1.4 Thylakoid biogenesis

Thylakoids house the photosystems (PSs), wherein light energy is used to split water and use its electrons to produce NADPH and the chemical potential for ATP synthesis to fuel anabolic metabolism. These membranes are organized in two recognizable regions namely grana stacks and stroma lamellae (Figure 2). These are not just structurally different but also differ in their protein composition wherein PSII and the Cyt *b₆f* complex are enriched in the grana stacks and PSI and the ATP synthase in the stroma lamellae (Danielsson *et al.*, 2004; Dumas *et al.*, 2016). The synthesis of these complexes is achieved by the coordinated expression of their respective nuclear and plastid encoded subunits. The proper assembly and stoichiometry of thylakoid complexes is ensured by a number of auxiliary assembly factor such as in the case of the retrograde signaling regulation of nuclear encoded genes expression (Chan *et al.*, 2016). The *de novo* synthesis of thylakoid complexes is highly dependent on the developmental stage of the tissue in higher plants (Roberts *et al.*, 1987), with a half-life that can be up to one week for Cyt *b₆f* complex

(Schottler *et al.*, 2007). In contrast, the reaction center subunit D1 of PSII has the highest turnover ranging from once per day to once per hour due to its susceptibility to oxidative damage (Aro *et al.*, 1993). In spite of the high turnover rate of D1, PSII is not synthesized *de novo* but rather disassembled by phosphorylation of its core proteins and light harvesting complexes (LHC) to facilitate the replacement of a newly synthesized D1 subunit (Tikkanen *et al.*, 2008). The proper assembly of the thylakoid complexes is assisted by nuclear encoded assembly factors and while the majority of them are conserved in photosynthetic organisms the molecular mechanisms are not always identical (Chi *et al.*, 2012).

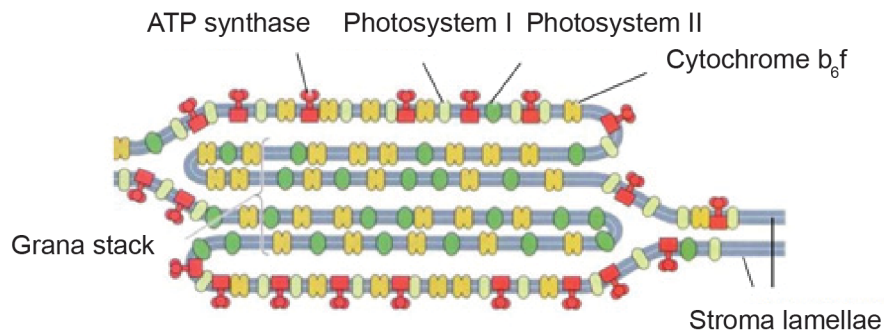


Figure 2. Thylakoid membrane organization. Schematic model of thylakoid membrane organization into their two major sections - grana stacks and stroma lamellae. Additionally, complexes involved in photosynthesis are represented according on their location on the thylakoid membrane. Modified from Voet *et al.* (2008).

Although thylakoids are typical bilayer membranes with embedded protein complexes, the proportion of protein to lipid content is higher than in any other membrane with about 80% proteins (Kirchhoff, 2008). The lipid composition of thylakoids is very unique with the presence mainly of non-phosphorus lipids unlike most biological membranes. Thylakoid membranes are composed of mono- and digalactosyldiacylglycerols (MGDG and DGDG respectively) constituting about 53% and 27% of the lipids respectively. Other lipids present in the thylakoids are

sulfoquinovosyldiacylglycerol (SQDG) and phosphatidylglycerol (PG), which are anionic lipids with a negative charge in their head groups (Kobayashi, 2016). The biosynthesis of thylakoid lipids takes place at the inner envelope where the MGDG synthase is located (Kobayashi *et al.*, 2007), and also at the outer envelope where the DGDG synthase transfers a second galactose to MGDG (Froehlich *et al.*, 2001). Since lipids cannot diffuse freely from one membrane to another without assistance, i.e. from the inner envelope to the thylakoid membranes, it has been theorized that chloroplast could use vesicle trafficking to mobilize lipids for thylakoid membrane formation (Benning *et al.*, 2006). This hypothesis has also been formulated by the observation of fatty acid desaturase mutants in *Arabidopsis*, which are localized in the endoplasmic reticulum (ER). These mutants showed a strong reduction on MGDG species suggesting the necessity of lipid transport from the ER to the thylakoid membrane (Miquel & Browse, 1992; Slack *et al.*, 1977).

Besides the fatty acid and protein content of the thylakoid membrane, several pigments play a crucial role in thylakoid function. Chlorophyll is the most abundant pigment in thylakoids and is associated with proteins such as LHCs and both PSI and PSII, thus allowing the harvest of light to power photosynthesis (Eckhardt *et al.*, 2004). Among other relevant pigments that play a role in photosynthesis, there are compounds related to photo protection such as the members of the xanthophyll cycle. When light intensity is not higher than the capacity of the photosystems, the Δ pH across the thylakoid membrane leads to the lumen being more acidic than the stroma. However, during higher light intensities, photosystems reach their maximum capacity to transfer electrons, thus prolonging the chlorophyll excitation state lifetime, which in turn leads to the production of reactive oxygen species (ROS) (Johnson *et al.*, 2012). In addition to the latter, the lumen pH drops due to the limitation of the ATP synthase to relax the Δ pH. This causes the de-epoxidation of violaxanthin to antheraxanthin further de-epoxidation of the latter to the photo protective pigment zeaxanthin (Rockholm & Yamamoto, 1996). Thus, zeaxanthin attached to the LHC quenches the excited state of chlorophyll preventing the production of ROS by a process called Non Photochemical Quenching (NPQ) (Jahns & Holzwarth, 2012).

1.5 The function of Plastoglobuli

Beside vesicles, that might transport lipid and protein components to the thylakoids, lipid bodies persistently attached to the thylakoid membrane have been observed, which are called plastoglobuli (PGs). Early descriptions of these compartments were performed during the sixties and they were first described as osmiophilic globules due to their ability to get stained with osmium tetroxide during the preparation of TEM pictures. These early observations led to the study of their composition and they were initially described as lipid bodies containing plastoquinone and galactolipids (Greenwood *et al.*, 1963). Later it was found that PGs are present throughout the plant's life and propagate in distinct developmental stages and tissues. For instance, PGs propagate and are bigger in size in chromoplasts especially in flowers and fruits (Hansmann & Sitte, 1982). This holds true for several plant species. Further investigation of the composition of PGs in chromoplasts revealed that they are rich in carotenoids. Moreover, this led to the identification of fibrillin (FBN) as the core protein of PGs (Deruere, Bouvier, *et al.*, 1994; Deruere, Romer, *et al.*, 1994). Additionally, it was observed that during senescence the number and size of PGs increased in chloroplasts and that they play a role in the accumulation of break down intermediates of chlorophyll degradation such as phytol (Tevini & Steinmuller, 1985; Vom Dorp *et al.*, 2015). In this stage, plastid metabolism is solely catabolic losing stroma and storing thylakoid breakdown content into PGs. Moreover, PGs are also accumulating under stress conditions such as drought (Langenkamper *et al.*, 2001), high light stress (Zhang *et al.*, 2010) and nitrogen limiting conditions (Gaude *et al.*, 2007).

Electron tomography studies on the structure of PGs have revealed that they are composed of a neutral lipid core and a lipid monolayer, which is physically attached and continuous with the stroma-side leaflet of the thylakoid membrane (Figure 3).

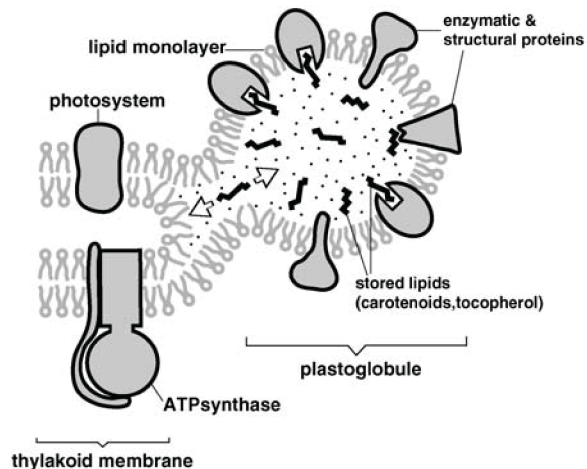


Figure 3. Plastoglobuli organization. Scheme representing a PG in relation with the thylakoid membrane. Proteins are represented as shapes on the monolayer of the PG. Modified from Austin *et al.* (2006).

Besides, it was shown that even though PGs propagate they always maintain at least one contact site with another PG or the thylakoid membrane, i.e. PGs are not found as individual components (Austin *et al.*, 2006). Further analyses on the composition of PGs have shown that certain variations in their lipid composition can occur depending on the developmental stage of the plant or the plant tissue. Under non-stress conditions, PGs are composed of high levels of tocopherols and quinones as well as neutral lipids such as triacylglycerol and free fatty acids (Steinmuller & Tevini, 1985; Vidi *et al.*, 2006; Zbierzak *et al.*, 2009). Other less abundant components are galactolipids, carotenoids and phytol esters, which increase in senescent chloroplasts (Gaude *et al.*, 2007; Tevini & Steinmuller, 1985) or during chromoplast differentiation, i.e. carotenoids (Deruere, Romer, *et al.*, 1994; Hansmann & Sitte, 1982). The proteome of PGs was identified by mass-spectrometry of isolated PGs from chromoplasts and chloroplasts (Vidi *et al.*, 2006; Ytterberg *et al.*, 2006). This revealed that in normal conditions PGs are composed of 30 proteins, the most abundant of which are FBNs (Lundquist *et al.*, 2012). This family of proteins is well conserved from plants to cyanobacteria (Cunningham *et al.*, 2010; Singh & McNellis, 2011). Initially, they were called fibrillins due of their ability to form fibers in the

presence of carotenoids and polar lipids, a phenomenon that was also observed in chromoplasts (Deruere, Romer, *et al.*, 1994). Furthermore, the second most abundant family of proteins in PGs is the ABC1K kinase family two of which were shown to play a role in vitamin E synthesis (Martinis *et al.*, 2013; Martinis *et al.*, 2014). Other proteins present in PGs are related to isoprenoid and neutral lipid metabolism (Lundquist *et al.*, 2012).

Analyses of mutant knockout plants for many of the PG's proteins lead to the conclusion that the function PGs is related to stress conditions or specific developmental stages. (Fatihi *et al.*, 2015; Singh *et al.*, 2010; Youssef *et al.*, 2010). Thus, PGs are assumed not to be essential for plant survival but rather relevant in their adaptation to different conditions and successful tissue differentiation.

1.6 Aim of this work

The central question to be answered in this thesis was: which are the crucial factors required for chloroplast biogenesis that are still unknown?

To date, the process by which proplastids undergo thylakoid formation and arrange their membranes along with the different embedded photosynthetic complexes embedded is still obscure. In order to tackle this question, a chloroplast proteome analysis from young plants should be utilized to identify proteins without known function. This should provide insights into proteins that might be involved in either early development of thylakoid formation (and therefore differentiation from proplastids to chloroplasts) or chloroplast biogenesis in general. To understand those processes the study of proteins with either unknown domains or function is crucial. In this work two proteins with unknown function, RV-1 and PG18, were selected to pursue a molecular characterization and investigate their role in plant development using knockout mutant plants in Arabidopsis.

2 Material and methods

2.1 Material

2.1.1 Chemicals

If not noted otherwise, all used chemicals were received from Sigma Aldrich (Taufkirchen, Germany), Roth (Karlsruhe, Germany), Merck (Darmstadt, Germany), Thermo Fisher Scientific (Braunschweig, Germany) or Serva (Heidelberg, Germany).

2.1.2 Molecular weight and size markers

For SDS-PAGE pepGOLD protein marker I (VWR, Ismaning, Germany) was used. EcoRI and HindIII digested lambda phage DNA (Thermo Fisher Scientific) was used as a marker for agarose gel electrophoresis. HMW Calibration Kit for Native Electrophoresis (GE Healthcare, Munich, Germany) was used for BN-PAGE.

2.1.3 Oligonucleotides

DNA oligonucleotides were ordered from Metabion (Martinsried, Germany) and are listed in Table 1.

Table 1. Oligonucleotides used for this work.

Oligonucleotide	5'-3' oligonucleotide sequence	Purpose
Gabi Kat F	ATATTGACCATCATACTCATTGC	Genotyping
AT1G36320 GT F	GGGGACAAGTTTGTACAAAAAAG CAGGCTTCTGAAGGAGATAGAACC ATGGTTTCAGTGTT	pK7FWG2
AT1G36320 GT R -stop	GGGGACCACTTTGTACAAGAAAG CTGGGTCTCCACCTCCGGACATA TACTTCTTTT	pK7FWG2
AT4g37920 F EcoRV -TP	GATATCGCGGAAGTAAAAAGCTC	pMAL-c5x
AT4g37920 R EcoRI Histag -stop	GAATTCGTGATGGTGATGGTGAT GGTTCAAAAAAT	pMAL-c5x

AT4g37920 GT F	GGGGACAAGTTTGTACAAAAAAG CAGGCTTCGAAGGAGATAGAACC ATGGCGAATTTACTG	gateway vectors, Genotyping
AT4g37920 GT R -stop	GGGGACCACTTTGTACAAGAAAG CTGGGTCTCCACCTCCGGAGTTC AAAAAATCTTCA	pK7FWG2
AT4g37920 GT R +stop	GGGGACCACTTTGTACAAGAAAG CTGGGTCTCCACCTCCGGATCAG TTCAAAAAATC	pDest14, pDest17, Genotyping
AT4g37920 GT F -TP	GGGGACAAGTTTGTACAAAAAAG CAGGCTTCCTGGAAGTTCTGTTT CAGGGCCCGGCGGAAGTAAAAA GCTC	pDest17
AT4g37920 R cDNA	AGTCGTAATTGCAATTATAGCTGA	Genotyping
AT4g37920 RNAi F	GGGGACAAGTTTGTACAAAAAAG CAGGCTTTAGTTTTAACATTTT	pOpOff2
AT4g37920 RNAi R	GGGGACCACTTTGTACAAGAAAG CTGGGTCTTTGTAAGTGACAGTG	pOpOff2
ATCG00920 rRNA 16S F	TCTCATGGAGAGTTTCGATCCT	pSP64
ATCG00920 rRNA 16S R	AAAGGAGGTGATCCAGCCG	pSP64
ATCG00950 rRNA 23S F	TTCAAACGAGGAAAGGCTT	pSP64
ATCG00950 rRNA 23S R	AGGAGAGCACTCATCTTGG	pSP64
AT1G36320 F	TGATCACTAAAGCTTGGTCG	Genotyping
AT1G36320 R	TCACATATACTTCTTTTCAA	Genotyping
AT4G13200 GT F	GGGGACAAGTTTGTACAAAAAAG CAGGCTTCGAAGGAGATAGAACC ATGAGTAGCTTCACGA	gateway vectors, Genotyping
AT4G13200 GT F -TP	GGGGACAAGTTTGTACAAAAAAG CAGGCTTCCTGGAAGTTCTGTTT CAGGGCCCGGAGTCTCGAAG	pDest17
AT4G13200 GT R -stop	GGGGACCACTTTGTACAAGAAAG CTGGGTCTCCACCTCCGGATCAG TCTTCATCACT	pK7FWG2

AT4G13200 GT R +stop	GGGGACCACTTTGTACAAGAAAG CTGGGTCTCCACCTCCGGATCAG TCTTCATCA	pDest17, Genotyping
23S F NW	TTCAAACGAGGAAAGGCTTA	Northern Blot
23S R NW	AGGAGAGCACTCATCTTG	Northern Blot
16S F NW	GTAAAGCGTCTGTAGGTG	Northern Blot
16S R NW	GCCTAGTATCCATCGTTT	Northern Blot

2.1.4 Vectors

To overproduce proteins fused to an N-terminal His-tag pDest17 vector was used (Thermo Fisher Scientific). The vector pMAL-c5x (New England Biolabs) was used to overproduce proteins fused to MBP at their N-terminal. pDest14 (Thermo Fisher Scientific) and pSP64 (Promega) vectors were used for *in vitro* transcription and translation. For plant transformation the following binary vectors were used: pK7FWG2 for expression under 35S promoter and pOpOff2 for expression of interference RNA (both Plant Systems Biology, Zwijnaarde, Belgium). Cloning into binary vectors as well as pDest14 and pDest17, was performed using the Gateway system (Thermo Fisher Scientific) via pDONR207 vector. Restriction site cloning was performed by using the entry vector Zero blunt (Thermo Fisher Scientific). All plasmids used for this thesis are listed in Table 2.

Table 2. List of plasmids used for this work.

Gene	Description	vector	Restriction sites	purpose
AT4g37920	- stop	pDONR207	-	localization
AT4g37920	+ stop	pDONR207	-	in-vitro translation
AT4g37920	- TP / + stop	pDONR207	-	over-expression
AT4g37920	- stop	pK7FWG2	-	localization
AT4g37920	- TP / + stop	pDest17	-	over-expression
AT4g37920	+ stop	pDest14	-	in-vitro translation
AT4g37920	Histag / - TP / - stop	pCR-Blunt	EcoRV / EcoRI	over-expression
AT4g37920	Histag / - TP / - stop	pMAL-c5x	EcoRV / EcoRI	over-expression
AT4g37920	-	pDONR207	-	RNAi
AT4g37920	-	pOpOff2	-	RNAi
AT1G20020	+ stop	pF3A	-	in-vitro translation

ATCG00920	-	pCR-Blunt	-	In-vitro transcription
ATCG00950	-	pCR-Blunt	-	In-vitro transcription
ATCG00920	-	pSP64	-	In-vitro transcription
ATCG00950	-	pSP64	-	In-vitro transcription
AT1G36320	- stop	pDONR207	-	localization
AT1G36320	- stop	pK7FWG2	-	localization
AT4G13200	- stop	pDONR207	-	localization
AT4G13200	- TP / + stop	pDONR207	-	over-expression
AT4G13200	- stop	pK7FWG2	-	localization
AT4G13200	- TP / + stop	pDest17	-	over-expression

2.1.5 Enzymes

Restriction endonucleases were purchased either from Thermo Fisher Scientific or from New England BioLabs (Frankfurt am Main, Germany). T4 DNA ligase was received from Thermo Fisher Scientific, Phusion DNA polymerase from New England BioLabs, Taq DNA polymerase from Bioron (Ludwigshafen, Germany).

2.1.6 Bacterial strains

E. coli TOP10 cells were used for propagation of plasmid DNA. Overexpression of heterologous proteins was performed using RIPL (BL21-CodonPlus (DE3)-RIPL strain) cells. For stable transformation of *A. thaliana* plants *A. tumefaciens* GV3101 (pMP90RK) cells were used. *A. tumefaciens* AGL1 cells were used for transient transformation of *Nicotiana tabacum* with GFP tagged proteins.

2.1.7 Membranes

PVDF transfer membrane for western blotting was received from Macherey-Nagel (Düren, Germany), blotting paper was obtained from Millipore (Darmstadt, Germany).

2.1.8 Antisera

Antisera against Arabidopsis proteins were purchased from Agrisera (Vännäs, Sweden), i.e. PGL35 (AS06 116), D1 (AS05 084), CP47 (AS04 038), PsaF (AS06 104), PsaD (AS09 461), Cyt *f* (AS08 306), LHCal (AS01 005), LHCall (AS01 006)

and LHCbII (AS01 003). Phycocyanin antiserum was purchased from ABBIOTEC (250488). ATP synthase, D1 and OE33 antisera were kindly provided by Stephan Greiner, TIC110 and FBPase antisera from Bettina Bölter and PsaG antiserum from Jörg Meurer. RV-1 and PG18 antisera were produced by Biogenes (Berlin, Germany).

2.1.9 Accession numbers

The gene accession numbers of the proteins involved in this work can be seen in Table 3.

Table 3. Gene accession numbers of proteins involved in this work.

Gene name	Accession number
RV-1	AT4g37920
RV-1-like	AT1G36320
PG18	AT4G13200
rRNA 16S	ATCG00920
rRNA 23S	ATCG00950
FNR	AT1G20020

2.1.10 Computational analyses

Sequences for RV-1, RV-1-like PG18 from *Arabidopsis* were obtained from TAIR (<https://www.arabidopsis.org>). Homologs of RV-1, RV-1-like PG18 from other species were collected from NCBI/BLAST (<http://blast.ncbi.nlm.nih.gov/Blast.cgi>) and Phytozome (<https://phytozome.jgi.doe.gov/pz/portal.html>). Phylogenetic trees were generated by using the MEGA7 software (Kumar *et al.*, 2016). The accessions for each sequence used for phylogenetic trees are indicated in table 4. Alignments were generated by using the algorithm provided by CLC Main Workbench (developed by QIAGEN Aarhus).

Graphs and statistical analyses were generated by using GraphPad Prism version 6.0, GraphPad Software, La Jolla, California, USA (www.graphpad.com). Image analyses were done by using the software ImageJ.

Table 4. Gene accession numbers of proteins used for phylogenetic analyses.

Species	RV-1	RV-1-like	PG18
<i>Arabidopsis thaliana</i>	AT4g37920	AT1G36320	AT4G13200
<i>Physcomitrella patens</i>	-	-	Pp3c16_19690V3.2
<i>Citrus sinensis</i>	orange1.1g013676m	orange1.1g048140m	A0A067FRT7_CITSI
<i>Fragaria vesca</i>	mrna05566.1-v1.0-hybrid	mrna31319.1-v1.0-hybrid	mrna17524.1-v1.0-hybrid
<i>Solanum tuberosum</i>	PGSC0003DMT400078670	PGSC0003DMT400070893	PGSC0003DMT400071989
<i>Solanum lycopersicum</i>	Solyc02g091640.2.1	Solyc04g072400.2.1	Solyc09g061440.2.1
<i>Sorghum bicolor</i>	Sobic.010G157700.1	Sobic.001G530900.1	Sobic.006G145200.1
<i>Zea mays</i>	B6TPX9_MAIZE	C0PEL6_MAIZE	B6TBJ2_MAIZE
<i>Oryza sativa</i>	LOC_Os01g20110.1	A3A5Q9_ORYSJ	LOC_Os04g43350.1
<i>Sphagnum fallax</i>	-	-	Sphfalx0010s0144.1
<i>Micromonas pusilla</i>	-	-	189112
<i>Calothrix</i> sp. 336/3	-	-	WP_035149421
<i>Synechocystis</i> sp. PCC 6803	-	-	WP_010872303
<i>Anabaena</i> sp. WA113	-	-	WP_066381343

2.2 Molecular biological methods

General methods not listed below were performed according to Sambrook and Russell (2001). Competent cells for DNA transformation were prepared according to Hanahan (1985).

2.2.1 Cloning strategies

For over-expression of proteins fused to an N-terminal MBP tag pMAL-c5x vector and *in vitro* transcription of rRNAs, PCR product created with primers containing the appropriate restriction site were digested with EcorV and EcoRI for RV-1 and with XbaI and BamHI for rRNAs. Ligation was carried out for 1 h at RT using T4 ligase into the vector pCR-Blunt. Afterwards, the corresponding plasmids were digested with EcorV and EcoRI, as well as the pMAL-c5x vector. Additionally, the corresponding plasmids with rRNA were digested with XbaI and BamHI as well as the vector pSP64 for its ligation as described above. For stable plant transformation,

over-expression of proteins and *in vitro* transcription and translation, Gateway system (Thermo Fisher Scientific) was used to clone constructs via homologous recombination from pDONR207 into binary vectors pk7FWG2, pDest14, pDest17 or pOpOff2. Cloning was performed according to the manufacturer's instructions.

2.2.2 Polymerase chain reaction (PCR)

PCR was performed with gDNA, cDNA or plasmid DNA as templates. For subsequent cloning proof-reading Phusion polymerase was used. For genotyping and colony PCR Taq polymerase was chosen. Annealing temperature and elongation time were adapted concerning oligonucleotides and length of constructs. PCR products for cloning were excised from 1% agarose gels run in TAE buffer (40 mM Tris, 2.5 mM EDTA, 1% acetic acid) and purified using NucleoSpin Gel and PCR Clean-up kit (Macherey-Nagel).

2.2.3 Isolation of plasmid DNA from *E. coli*

Plasmid DNA was isolated from 2 ml overnight *E. coli* culture using the NucleoSpin Plasmid EasyPure kit (Macherey-Nagel) according to the manufacturer's instructions.

2.2.4 Sequencing

Each plasmid was confirmed by sequencing which was performed by the sequencing service of the Faculty of Biology (Ludwig-Maximilians-Universität München, Germany) using 100 – 200 ng of vector with appropriate primer.

2.2.5 Isolation of genomic DNA from *A. thaliana* for genotyping PCR

One leaf was homogenized in 500 µl of extraction buffer (1 M Tris-HCl pH 7.5, 50 mM NaCl, 50 mM EDTA, 1% (w/v) PVP 40) by a mixing mill for 3 min in a tube with a tungsten carbide 3 mm ball. Afterwards, 66 µl of 10% (w/v) SDS were added and the samples were mixed by inverting them several times followed by the addition of 166 µl of 5 M potassium acetate. The sample was then centrifuged for 15 min at 15000 gRT. The supernatant was rescued and mixed with 0.7 vol of isopropanol and

incubated for 15 min at -20 °C. The sample was then centrifuged for 15 min at 15000 g and 4 °C and the supernatant was discarded. The pellet was washed with 500 µl of 70% (v/v) ethanol and mixed by inverting the tube and then centrifuged for 5 min at 15000 g and 4 °C. The pellet was dried at RT and dissolved in 50 µl of H₂O.

2.2.6 Isolation of RNA from *A. thaliana*

RNA from *A. thaliana* leaves was isolated using the Rneasy Plant Mini kit (Qiagen) according to the manufacturer's instructions. Digestion with Dnase was either performed during RNA isolation (DnaseI, Roche, Mannheim, Germany).

2.2.7 cDNA synthesis

cDNA was synthesized in 10 µl reaction volume from 1 µg RNA using M-MLV reverse transcriptase (Promega) according to the manufacturer's instructions.

2.2.8 Protein precipitation with trichloroacetic acid (TCA)

Proteins were precipitated by adding TCA (final percentage 10% [v/v]) and incubating the samples for 30 min at -20 °C. Afterwards, proteins were centrifuged for 15 min at 16000 g and 4°C and the supernatant was discarded. The pellet was washed twice by adding 1 ml of 100% ethanol and centrifuging for 5 min at 16000 g and 4 °C. The pellet was dried at Rtf for 15 min and resuspended in loading buffer (100 mM Tris pH 7.5, 2% SDS, 10% glycerol, 5% β-mercaptoethanol, 0.004% bromphenol blue).

2.3 Biochemical methods

2.3.1 Overexpression of recombinant proteins

Transformed *E. coli* bacteria were grown in LB medium (1% peptone from casein, 0.5% yeast extract, 171 mM NaCl) at 37°C to an OD600 of 0.6 – 0.8. Overexpression was induced by the addition of 1 mM isopropyl β-D-1-thiogalactopyranoside. *E. coli* strains and conditions for overexpression were depending on the construct and are

listed in Table 5.

Table 5. Conditions for overexpression and way of purification of recombinant proteins

Construct	Vector	<i>E. coli</i> strain	Temperature	Time	Purification
RV-1	pDest17	RIPL	37 °C	overnight	inclusion bodies
RV-1	pMAL-c5x	RIPL	12 °C	overnight	soluble
PG18	pDest17	RIPL	37 °C	overnight	inclusion bodies

2.3.2 Purification of soluble proteins

Pelleted bacteria from 1 l overexpression of constructs with His-tags were resuspended in 25 ml lysis buffer (20 mM Tris pH 7.5, 200 mM NaCl, 15 mM imidazole). After cell disruption by a microfluidizer (Microfluidics, Westwood, USA) the solution was centrifuged at 20000 g, 4°C for 30 min and the supernatant was rotated with 250 µl Ni-Sepharose at 4°C for 2 h. The beads were washed three times with 5 ml wash buffer (20 mM Tris pH 7.5, 200 mM NaCl, 15 mM imidazole). Recombinant proteins were eluted in 200 – 400 µl fractions with elution buffer (20 mM Tris pH 7.5, 200 mM NaCl, 500 mM imidazole). Samples were then dialyzed to remove imidazole in bags with a molecular weight cut-off of 3.5 kDa (Spectra/Por 3) against 2 l of lysis buffer without imidazole overnight at 4 °C with agitation.

2.3.3 Purification of proteins out of inclusion bodies

Insoluble proteins were purified out of inclusion bodies. Pelleted bacteria from 0.5 – 1 l overexpression were resuspended in 25 ml resuspension buffer (50 mM Tris pH 8.0, 200 mM NaCl, 5 mM β-mercaptoethanol). Cells were disrupted and centrifuged as described in 2.3.4. The pellet was washed one time with 20 ml detergent buffer (20 mM Tris pH 7.5, 200 mM NaCl, 1% deoxycholic acid, 1% nonidet P-40, 10 mM β-mercaptoethanol), two times with Triton buffer (20 mM Tris pH 7.5, 0.5% Triton X-100, 5 mM β-mercaptoethanol) and two times with Tris buffer (20 mM Tris pH 8.0, 10 mM DTT). Centrifugation was done at 12000 g, 4°C for 10 min. Finally, the pellet was resuspended in 5 ml urea buffer (50 mM Tris pH 8.0, 100 mM NaCl, 7 M urea) and rotated for overnight at 4 °C. After centrifugation at 20000 g, 4 °C for 15 min denaturated proteins were present in the supernatant. In order to get rid of urea from

the buffer, samples were dialyzed as described in section 2.3.2.

2.3.4 Isolation of proteins from *A. thaliana*

A. thaliana leaves were homogenized in 300 μ l homogenization medium (50 mM Tris pH 8.0, 10 mM EDTA, 2 mM EGTA, 10 mM DTT) using an electronic micropestle. The suspension was incubated for 10 min in the dark on ice then filtered and centrifuged at 9300 g for 10 min and 4 °C. Supernatant contained soluble proteins, pellet resuspended in homogenization medium contained membrane proteins. For total protein extraction, leaves were grinded with liquid nitrogen and the powder was then transferred into a tube and resuspended by adding equal volume of extraction buffer (50 mM Tris-HCl pH 8, 2% [w/v] LDS, 0.1 mM PMSF). The sample was vortexed and then incubated on ice for 30 min and centrifuged for 15 min at 16000 g and 4 °C. The supernatant was rescued, and protein concentration was measured by BCA test. Finally, EDTA and DTT were added immediately to a final concentration of 50 mM and 10 mM respectively.

2.3.5 Determination of protein concentration

Concentration of proteins was determined using Bradford reagent (Bio-rad). 10 μ l protein was mixed with 1:5 diluted Bradford reagent and absorption was measured against buffer at 595 nm. When indicated, protein concentrations were also quantified by using the kit Pierce™ BCA protein assay according to the manufacturer's instructions (Thermo Fisher Scientific).

2.3.6 SDS polyacrylamide gel electrophoresis (SDS-PAGE)

Proteins were separated by SDS-PAGE using discontinuous gels according to (Laemmli, 1970) consisting of a stacking gel (5% polyacrylamide) and a running gel (10 – 15% polyacrylamide). Samples were loaded with SDS loading buffer (62.5 mM Tris pH 6.8, 2% SDS, 10% glycerol, 5% β -mercaptoethanol, 0.004% bromphenol blue). Gels were run in SDS running buffer (25 mM Tris, 192 mM glycine, 0.1% SDS) and afterwards either stained with 2600massie (45% methanol, 9% acetic acid, 0.2% 2600massie brilliant blue R-250) or used for western blotting (see 2.3.7).

2.3.7 Semi-dry electro blot and immunodetection of proteins

Proteins were electrotransferred out of an SDS gel onto a PVDF membrane using a semi-dry blotting apparatus. The blot was assembled as follows on the anode: three blotting papers in anode I buffer (20% methanol, 300 mM Tris), two blotting papers in anode II buffer (20% methanol, 25 mM Tris), activated membrane, gel, three blotting papers in cathode buffer (20% methanol, 40 mM aminocaproic acid). Transfer was carried out for 1 h at 0.8 mA/cm², proteins on membrane were stained with ponceau solution (5% acetic acid, 0.3% ponceau S). For immunodetection of proteins membrane was blocked for 30 min with 5% skimmed milk in TBST (20 mM Tris pH 7.6, 137 mM NaCl, 0.075% Tween). Incubation with primary antibody was performed over night at 4°C. After three times 10 min washing in TBST membrane was incubated for 2 h at RT with horse radish peroxidase conjugated secondary antibody. After three times 10 min washing in TBST membrane was incubated in equal volumes of development solution I (100 mM Tris pH 8.5, 1% luminol, 0.44% coumaric acid) and II (100 mM Tris pH 8.5, 0.018% H₂O₂) and signal was detected with enhanced chemiluminescence using Image Quant LAS 400 (GE Healthcare).

2.3.8 Detection of radiolabeled proteins

To visualize radiolabeled proteins dried SDS gels were exposed overnight to BAS-MS phosphor imaging plates (FUJIFILM) which were analyzed using a Typhoon scanner (GE healthcare).

2.3.9 Blue Native PAGE (BN-PAGE)

Solubilized samples (thylakoid membranes) were separated on native acrylamide gradient Bis-Tris gel (5 – 12% polyacrylamide). Samples were loaded with BN loading buffer (750 mM aminocaproic acid, 5% Serva-G 250), gel was run with cathode buffer (50 mM tricine, 15 mM Bis-Tris pH 7.0, 0.2% Serva-G 250) and anode buffer (50 mM Bis-Tris pH 7.0). For second dimension one lane of the BN gel was placed on top of an SDS gel containing 4 M urea which was either silver stained to visualize proteins.

2.3.10 Silver staining of SDS gels

Gels were incubated for 1 h in fixation solution (50% [v/v] ethanol, 12% [v/v] acetic acid, 0.05% [v/v] formaldehyde) then washed three times for 30 min in 50% (v/v) ethanol. After 90 sec pre-impregnation in 0.02% (v/v) sodium thiosulfate and three times 30 sec washing in water impregnation of the gel was performed for 30 min in darkness using 0.2% (w/v) silver nitrate and 0.075% (v/v) formaldehyde. Gels were washed again in water then stained with development solution (6% [w/v] Na₂CO₃, 0.05% [v/v] formaldehyde, 0.0004% [v/v] sodium thiosulfate). After protein signals became visible reaction was stopped with stopping solution (50% [v/v] ethanol, 12% [v/v] acetic acid).

2.3.11 Mass spectrometry

Mass spectrometric analyses were performed at the MSBioLMU core facility (Department Biology I, Ludwig-Maximilians-Universität München).

2.3.12 Transformation of *A. tumefacium*

1 – 2 µg plasmid was added to either to competent GV2101 or AGL1 cells which were incubated 5 min on ice then for 5 min in liquid nitrogen. Heat shock was performed for 5 min at 37 °C then 800 µl LB was added and cells were incubated shaking for 3 h at 28 °C before plated on LB plates with appropriate antibiotics. Cells were grown for 2 days at 28 °C.

2.3.13 Pigment analysis

Pigment measurements were done by Prof. Dr Peter Jahns (Plant Biochemistry, Heinrich-Heine-University Düsseldorf, Düsseldorf). Leaf samples were frozen in liquid N₂ and either used directly for pigment extraction or stored at -80°C for up to 2 weeks until further use. Pigments were extracted by grinding frozen leaf material in a mortar after addition of 1 ml 100% acetone. After short centrifugation, the supernatant was filtered through a 0.2-µm membrane filter (GE Healthcare, Little Chalfont, Buckinghamshire, UK) and then subjected to HPLC analysis. Separation

and quantification of pigments was done by reversed-phase chromatography as described in Farber *et al.* (1997).

2.3.14 *In vitro* transcription

Vectors including either a T7 or SP6 promoter sequence were used for *in vitro* transcription of various genes (see Table 2). For the transcription reaction, 1 µg plasmid, 0.05% BSA, 2 mM DTT, 0.25 mM m⁷G(5')ppp(5')G Cap analog (Ambion), 0.4 mM ACU (Roche), 50 U RibolockRI (Thermo Fisher Scientific), 30 U T7 or SP6 RNA polymerase (Thermo Fisher Scientific), 1x transcription buffer (Thermo Fisher Scientific) were added in a total volume of 50 µl and incubated at 37°C for 15 min for RNA capping. To this capped RNA, 1.2 mM GTP was added and reaction was incubated at 37 °C for 120 min for final mRNA generation. For transcription and simultaneous radiolabeling, the transcription reaction was set up as follows: 1 µg plasmid, 0.5 mM AGU (Roche), 12 µM CTP (Roche), 40 U RibolockRI (Thermo Fisher Scientific), 20 U SP6 RNA polymerase (Thermo Fisher Scientific), 1x transcription buffer (Thermo Fisher Scientific), 2.5 µCi/µl [α ³²P] CTP (sp. act. 800 Ci/mmol) (Perkin Elmer, Walluf, Germany) in a total volume of 20 µl. The reaction was performed at 37 °C for 120 min and then 2 U of Dnase I (Roche) were added and incubated for extra 15 min 37 °C. The reaction was stopped by adding 230 µl of buffer G50 (20 mM Tris-HCl pH 7.5, 300 mM sodium acetate, 2 mM EDTA, 0.25% [w/v] SDS). 500 µl of 25:24:1 phenol/chloroform/isoamylalcohol and the solution was vortexed. The sample was then centrifuged for 5 min at 14000 g at 4 °C and the upper aqueous phase was transferred into a new tube. 600 µl of 100% ethanol were added to the sample and then centrifuged for 10 min at 14000 g and 4°C discarding the supernatant and the pellet was dried for 10 min at RT. The pellet was resuspended in 10 µl of distilled, deionized H₂O.

2.3.15 *In vitro* translation

In vitro translation of radiolabeled proteins was done using reticulocyte lysate (Promega). 1 µl *in vitro* transcription product was used for 10 µl translation reaction with 30 µCi ³⁵S methionine (Perkin Elmer, Walluf, Germany), 80 µM amino acid

mixture without methionine, 66% reticulocyte lysate and 70 mM KCl. Translation was carried out at 30°C for 50 min.

2.3.16 Agarose gel electrophoresis

DNA samples were separated on 1% agarose gels containing 0.5 µg/ml ethidium bromide in TAE 1X buffer (40 mM Tris, 20 mM acetate, 1 mM EDTA). Samples were loaded into the gel by adding loading buffer (5% (v/v) glycerol, 0.042% (w/v) bromophenol blue 0.042% (w/v) xylene cyanol FF).

RNA samples were separated on 1.2% agarose gels in buffer MOPS (20 mM MOPS pH 7.5 mM sodium acetate, 1 mM EDTA) and 1X MOPS running buffer. The RNA was prepared by incubating the sample for 10 min at 60°C in 3.5% DMSO (v/v), 0.4% glyoxal, \cong 10 µg RNA in 1X MOPS buffer (total volume of 10 µl) and then 5 µl of loading buffer were added as mentioned above. EMSA samples were separated on a 1% agarose gels without ethidium bromide in buffer TBE 1X (89 mM Tris pH 8, 89 mM boric acid, 2 mM EDTA). Samples were loaded using the loading buffer indicated above and the gels were run in buffer TBE.

2.3.17 Electrophoretic mobility shift assay (EMSA)

RNA synthesized as described in section 2.3.14 was used along with soluble purified proteins as described in section 2.3.2. Binding was performed by preparing a 15 µl sample containing 0-10 µg of protein and 0.125 µCi RNA [α 32 P] in binding buffer (40 mM Tris-HCl pH 8, 30 mM KCl, 1 mM MgCl₂, 1 mM DTT, 0.01% [v/v] NP40). The reaction was performed for 30 min at 20°C and samples were further separated on agarose gels as described in section 2.3.15.

2.3.18 RNase assay

Total RNA extracted from plants as described in section 2.2.6 or *in vitro* transcribed RNA as described in section 2.3.14 was used to performed RNase assays. Soluble proteins purified as described in section 2.3.2 were used for preparing 20 µl of reaction mix containing 1 µg of RNA, 5 µg of protein in RNase buffer (50 mM HEPES

pH 7, 10 mM MgCl₂). The reaction was incubated for 30 min at RT and separated on an agarose gel as described in section 2.3.15.

2.3.19 Northern Blot

EMSA samples that were run on an agarose gel were transferred onto a nylon membrane (Biodyne, Pall). The agarose gel was rinsed twice in buffer 20X SSC (3 M NaCl, 300 mM sodium citrate pH 7) and placed onto wet whatman paper connected to a beaker with 20X SSC buffer. Transfer was done by putting the nylon membrane onto the agarose gel and whatman paper, letting it transfer by capillarity overnight at RT. Afterwards, the membrane was exposed overnight to BAS-MS phosphor imaging plates (FUJIFILM).

In case of transferring RNA, the samples isolated as described in section 2.2.6 were separated in agarose gels as described in section 2.3.16 containing 0.925% formaldehyde. The gels were then washed twice for 15 min in 20X SSC buffer and transferred onto a nylon membrane as described above. The membrane was then expose to UV light (0.12 J, Stratalinker). The RNA onto the membrane was hybridized with probes obtained by PCR (section 2.2.2) using Digoxigenin-11-UDP (Roche) and specific primers for the 16S and 23S rRNAs. Hybridization mix was prepared with probes incubated for 30 min at 68 °C at a concentration of 2.5 ng probe/ml in prehybridization mix (0.25 M Na₂HPO₄ pH 7.2, 1 mM EDTA, 20% SDS, 0.5% Blocking reagent [10 g Blocking (Roche) in 0.1 M maleic acid, pH 8, 0.15 M NaCl]). The membrane was transferred into a tube containing pre-heated hybridization mix for 1 h at 68 °C. Denaturation of DIG-labeled DNA probes were done by adding 25 ng of each probe to 100 µL of water in a clean microreaction tube and incubate for 10 min at 99°C, immediately the probe was placed on ice for at least 1 min. These probes were then added into the membrane with hybridization mix incubating it overnight at 68 °C. Later the membrane was washed for 20 min at 65 °C three times with pre-heated hybridization wash buffer (20 mM Na₂HPO₄, 1 mM EDTA, 1% SDS). The membrane was brought to RT and washed with buffer I (0.1 M maleic acid, pH 8.0, 3 M NaCl, 0.3% Tween 20) and then transferred into blocking buffer II (19 mL wash buffer I plus 1 ml 20 x blocking) and incubated for 1 h at RT.

For immunodetection of the probes onto the membrane, conjugate buffer III was prepared by diluting α -DIG-AP 1: 20000 with blocking buffer II (0.5 μ L antibody / 10 mL). The membrane was incubated for 1 h in conjugate buffer containing α -DIG-AP and then washed four times for 10 min with buffer I. Then the membrane was incubated for 5 min in substrate buffer IV (0.1 M Tris-HCl pH 9.5, 0.1 M NaCl, 50 mM $MgCl_2$) and transferred from tube onto a plastic foil, pipet substrate buffer V (0.12 mM CDP* [1:100, Roche] 50 μ L/ 5 mL substrate buffer IV) onto membrane and incubate for 5 minutes and the membrane expose in ECL reader.

2.4 Cell biological methods

2.4.1 Isolation of intact chloroplasts from *P. sativum*

Approximately 200 g leaf material of 9 – 14 days old peas was mixed in isolation buffer (330 mM sorbitol, 20 mM MOPS, 13 mM Tris pH 7.6, 3 mM $MgCl_2$, 0.1% BSA) filtered and centrifuged for 1 min at 1900 g, 4°C. Intact chloroplasts were isolated out of the pellet via a discontinuous percoll gradient of 12 ml 40% percoll solution (330 mM sorbitol, 50 mM HEPES pH 7.6, 40% percoll) and 8 ml 80% percoll solution (330 mM sorbitol, 50 mM HEPES pH 7.6, 80% percoll) for 5 min at 8000 g, 4°C and washed twice with washing buffer (330 mM sorbitol, 25 mM HEPES pH 7.6, 3 mM $MgCl_2$). The chlorophyll concentration was determined by measuring the absorption of 1 μ l chloroplast solution in 1 ml 80% acetone and calculated with the following formula:

$$\text{mg chlorophyll / ml} = 8.02 \times (E663 - E750) + 20.2 \times (E645 - E750)$$

2.4.2 Isolation of inner and outer chloroplast envelope from *P. sativum*

Plant material from 20 trays of 9-11 days old pea seedlings was harvested in dark and homogenized in 5-7 l of isolation medium (330 mM sorbitol, 20 mM MOPS, 13 mM Tris, 0.1 mM $MgCl_2$, 0.02% (w/v) BSA). The suspension was filtered through four layers of mull and one layer of gauze (30 μ m pore size) and centrifuged for 5 min at 1500 g. Using a soft brush, the pellet was gently resuspended in small volume of isolation medium and overlaid onto discontinuous Percoll gradient (as described

in section 2.4.1). Intact chloroplasts separated at the interface were transferred to 250 ml beakers and washed twice with wash media (330 mM sorbitol, Tris-base pH 7.6). The chloroplasts were burst by incubation in a hypotonic 0.7 M sucrose buffer for 10 min on ice in darkness and subsequent pottering in down's homogenizer. The suspension was further treated according to the modification of Waegemann *et al.* (1992) of the previously described method by Keegstra and Yousif (1986). Afterwards, the suspension was centrifugated for 1 h at 100000 g and 4 °C and the pellet carefully resuspended in buffer Tricine (10 mM Tricine pH 7.9, 1 mM EDTA). This was then loaded onto a discontinuous sucrose gradient (composed by three phases of 0.996 M, 0.8 M and 0.465 M sucrose) and centrifuged for 3 h at 100000 g and 4 °C. The gradients were fractionated and further precipitated by using TCA as described in section 2.2.8.

2.4.3 Isolation of plastoglobuli from *P. sativum*

Intact chloroplasts from 3-week-old peas were isolated as described in section 2.4.2. The chloroplasts were then separated in a discontinuous sucrose gradient according to Vidi *et al.* (2006). Intact chloroplasts were resuspended in osmotic buffer (10 mM Tricine pH 7.9, 0.6 M sucrose, 1 mM EDTA) and incubated for 30 min on ice and then centrifugated for 1 h at 100000 g and 4 °C. The pellet was resuspended in TED buffer plus sucrose (50 mM Tricine pH 7.9, 2 mM DTT, 2 mM EDTA, 48% sucrose) and subsequently potted in down's homogenizer. The solution was further treated with three sonication pulses of 1 min separated by intervals of 5 min. The final solution was used as the bottom solution for the discontinuous gradient by adding four extra phases (38%, 20%, 15% and 5% sucrose with 1 mM EDTA pH 7.9). The gradient was then centrifuged over night at 100000 g and 4°C and then fractionated by taking 1 ml samples. The proteins in each fraction were precipitated with trichloroacetic acid as described in section 2.2.8.

2.4.4 Isolation of thylakoid membranes

Approximately 1 g leaf material of 21 days old Arabidopsis plants grown on soil was mixed in 25 ml isolation medium (330 mM sorbitol, 50 mM HEPES pH 7.5, 2 mM

EDTA, 1 mM MgCl₂, 5 mM ascorbic acid) using a polytron homogenizer. After filtration the homogenate was centrifuged at 760 g at 4 min, 4°C. The pellet was resuspended in washing buffer (5 mM sorbitol, 50 mM HEPES pH 7.5) and centrifuged again. The pellet was resuspended in TMK buffer (100 mM sorbitol, 50 mM HEPES pH 7.5, 5 mM MgCl₂) and the sample was incubated 10 min on ice, centrifuged and resuspended in a small volume of TMK buffer. Chlorophyll content was measured.

2.4.5 Solubilization of thylakoid membranes

For analysis of photosynthetic protein complexes via BN-PAGE thylakoid membranes according to 30 µg chlorophyll were pelleted at 3300 g, 3 min, 4°C, then solubilized in 70 µl ACA buffer with n-dodecyl β-D-maltoside (β-DM) (1.1% final concentration) for 10 min on ice. After 10 min centrifugation at 16000 g, 4°C supernatant was loaded on BN-PAGE.

2.4.6 Thylakoid membrane wash from *A. thaliana*

Thylakoids isolated as described in section 2.4.2, were sonicated on ice with three 1 min pulses applied at 5 min intervals. Immediately, broken thylakoids were mixed with different salt solutions (final concentration of 1 M NaCl, 100 mM Na₂CO₃, 3 mM urea or 1% LDS, respectively) and incubated for 30 min on ice. The samples were further centrifuged for 10 min at 10000 g and 4°C to separate the soluble and membrane fraction of the thylakoids.

2.4.7 Trypsin digestion of thylakoid membranes from *A. thaliana*

Intact thylakoids isolated as described in section 2.4.2 were diluted to a final concentration of 1 mg/ml of chlorophyll in 1 ml in digestion buffer (50 mM HEPES pH 8, 5 mM MgCl₂) and incubated for 15 min on ice. Afterwards, 20 µl of trypsin at 1 mg/ml was added to 1 ml of thylakoids (final trypsin concentration 20 µg/ml) and incubated on ice for 5, 10 and 15 min. The reaction was stopped by adding SDS-loading buffer.

2.4.8 *In vitro* import into chloroplasts from *P. sativum*

10 µg chlorophyll was used in a final reaction volume of 100 µl import buffer (330 mM sorbitol, 50 mM HEPES pH 7.6, 3 mM MgCl₂, 10 mM methionine, 10 mM cysteine, 0.2% BSA, 3 mM ATP) together with 4 µl ³⁵S labeled, reticulocyte lysate translated preprotein. Import was performed for indicated times at 25°C. Sample was loaded on 300 µl of 40% percoll solution to reisolate intact chloroplasts by centrifugation at 4500 g, 5 min, 4°C. Pellets were washed twice in 100 µl washing buffer (1100 g, 1 min, 4°C) then resuspended in SDS loading buffer, heated for 3 min at 95°C and loaded onto a SDS gel. Radioactive signals were detected by exposure overnight to BAS-MS phosphor imaging plates (FUJIFILM).

2.4.9 *In vivo* translation of proteins in *Arabidopsis* seedlings

Arabidopsis seedlings grown for 10 days on MS medium with sugar were taken and immersed into 50 µl of 1 mM KH₂PO₄. To this mix 30 µCi ³⁵S methionine (Perkin Elmer, Walluf, Germany) was added and vacuum infiltration was applied. Afterwards, samples were incubated at 25°C for the indicated time points with illumination (125 100 µmol / m²s). Subsequently, the buffer was discarded, and the seedlings were washed twice with 500 µl of Na₂CO₃. Finally, the seedlings were homogenized in 100 µl isolation buffer (330 mM sorbitol, 50 mM HEPES pH 7.5, 2 mM EDTA, 1 mM MgCl₂, 5 mM ascorbic acid) by using a pistil. The homogenate was then centrifuged for 3 min at 6000 g and 4 °C. The pellet was washed twice with washing buffer (5 mM sorbitol, 50 mM HEPES pH 7.5) by centrifuging the samples for 3 min at 6000 g and 4 °C. Finally, samples were used for photosynthetic protein complexes analysis via BN-PAGE as it is described in section 2.4.5. To separate soluble and membrane proteins, infiltrated seedlings were homogenized in 60 µl of 100 mM Na₂CO₃ by using a pistil and centrifuged for 15 min at 16000 g and 4 °C. The supernatant containing the soluble proteins was stored and the pellet was further washed with 100 µl of 20 mM Na₂CO₃ by centrifuging the samples for 15 min at 16000 g and 4 °C. The pellet was then resuspended in 50 µl of 100 mM Na₂CO₃. Soluble and membrane proteins were further separated by SDS-PAGE as described in section 2.3.6.

2.4.10 RNase A treatment

Soluble proteins from *A. thaliana* were isolated as described in section 2.3.4. The protein concentration was adjusted to 1.5 mg/ml in 5 ml. For RNase A treatment, 200 µl of RNase A (0.4 mg/ml) were added to 2 ml of the soluble proteins and the reaction was incubated for 1 h on ice. In parallel, 2 ml of soluble proteins were incubated with the addition of 50 U RibolockRI (Thermo Fisher Scientific). The proteins were further separated by loading 2 ml of the samples onto continuous sucrose gradients (5% -40%), which were centrifuged for 3 h at 100000 g and 4°C. The gradients were fractionated into 1 ml fractions and the proteins were precipitated by using TCA as described in section 2.2.8.

2.5 Plant biological methods

2.5.1 Plant growth conditions

Pea (*Pisum sativum*) was grown under long day conditions (14 h light / 10 h dark). *A. thaliana* WT Columbia ecotype (Col-0) and the mutant plants were grown either on soil or on half-strength MS (Murashige and Skoog) medium supplied with 1% sucrose and 1.2% agar-agar under controlled conditions in a growth chamber (16 h light / 8 h dark, 22°C, 100 µmol / m²s in fluorescent light conditions). For plants grown on soil; Seeds were sown and vernalized at 4°C in the dark for 2 days to synchronize germination. For sowing seed on sterile plates, seeds were surface-sterilized by washing once with 70% ethanol with 0.1% Tween-20 for 15 min and then thrice with 100% ethanol, dried before sowing. The plates were sealed and vernalized at 4°C for 2 days. For phenotyping analysis plants were grown on soil in long day condition (16 h light / 8 h dark, 22°C, 100 µmol / m²s in fluorescent light conditions).

2.5.2 Stable transformation of *A. thaliana* with *A. tumefacium*

400 ml LB medium was inoculated with preculture of transformed *A. tumefacium* strain GV3101 and grown over night. Cells were harvested by 20 min centrifugation at 1900 g, resuspended in Silwet medium (5% sucrose, 0.05% silwet L-77) and

adjusted to an OD600 of 0.8. Flowering *A. thaliana* plants were dipped for 5 sec in cell suspension. Seeds from transformed plants were selected on MS medium with 50 mg/l kanamycin or 15 mg/l hygromycin.

2.5.3 Transient transformation of *N. benthamiana*

Subcellular localization of proteins was analyzed by transient expression of GFP-fusion proteins in 3 - 4 weeks old *Nicotiana benthamiana* plants. *Agrobacterium tumefaciens* (AGL1) transformed with plasmid of interest was grown in LB medium with appropriate antibiotics. When cell density of 0.5 OD600 was reached, cells were pelleted (centrifugation: 15 min at 4000 rpm) and resuspended in infiltration medium (10 mM MgCl₂, 10 mM MES / KOH pH 5.6, 150 µM Acetosyringone) such that OD600 was 1. This cell suspension was incubated in dark for 2 h (rotating) and then used to infiltrate the abaxial surface of *Nicotiana benthamiana* leaves. Infiltrated plants were kept for two-three days before isolation of protoplast for observing the expression of GFP-fusion protein.

2.5.4 Isolation of protoplast from *N. benthamiana* for GFP localization

Nicotiana benthamiana leaves transiently expressing GFP-fusion proteins were used for isolation of protoplasts. The leaves cut approximately into 0.2 - 0.4 cm wide and 1 cm long stripes were incubated in 10 ml enzyme solution (1% Cellulase R10 and 0.3% Macerozyme R10) made in F-PIN medium (MS medium PC-vitamins [200 mg/l Myoinositol, 1 mg/l thiamin-HCl, 2 mg/l Ca-panthotenate, 2 mg/l nicotinic acid, 2 mg/l pyridoxin-HCl, 0.02 mg/l biotin, 1 mg/l 6-benzylaminopurin (BAP), 0.1 mg/l α -naphthaleneacetic acid (NAA)], 2 mM MES pH 5.8, 5 mM KNO₃, 1.5 mM CaCl₂, 0.75 mM MgSO₄, 0.625 mM KH₂PO₄, 20 mM NH₄-succinat, 80 g/l glucose [550 Osm]) for 2 h rotating in dark at 40 rpm on bench top shaker. After a short 1 min rotation at 80 rpm, the suspension was filtered through 100 µm Nylon-membrane and overlaid with 2 ml F-PCN medium (F-PIN, except instead of glucose, sucrose was added as the osmoticum). The gradient was centrifuged for 10 min at 70 g (slow deceleration) to separate intact protoplasts at the interface between the F-PIN and F-PCN media. The protoplasts were transferred to new tubes and washed with 10 ml W5 buffer

(centrifugation: 10 min at 50 g) and resuspended with 200 μ l of W5 (2 mM MES pH 5.8, 125 mM CaCl_2 , 5 mM KCl, 550 Osm glucose). To stain mitochondria, 5 μ l of Mitotracker orange (Thermo Fisher Scientific) were added and incubated in dark for 30 min. Protoplasts were then centrifuged at 100 g for 1 min at RT and resuspended in W5 buffer. GFP as well as Mitotracker orange fluorescence was observed with a TCS-SP5 confocal laser scanning microscope (Leica, Wetzlar, Germany).

2.5.5 Photosynthetic performance by pulse amplitude modulation analysis (PAM)

The kinetics of induction of chlorophyll *a* fluorescence in WT and mutant leaves was measured using a pulse-modulated fluorimeter (DUAL-PAM100; Walz). Leaves, dark adapted for at least 15 min, were used to analyze minimal (F_0) and maximal (F_m) fluorescence yields, the latter being determined by application of a saturating light pulse (1-s duration, 500 μ mol photons $\text{m}^{-2} \text{s}^{-1}$). The potential maximum quantum yield of PSII was measured as $(F_m - F_0)/F_m = F_v/F_m$ (Schreiber *et al.*, 1998). PSI yield in leaves was measured as absorption changes at 820 nm induced by saturating pulses and far-red light (12 W m^{-2} as measured with a YSI Kettering model 65 A radiometer) in the absence or presence of actinic light (650 nm, 20 and 250 μ mol $\text{m}^{-2} \text{s}^{-1}$) using the DUAL-PAM100 (Klughammer & Schreiber, 1994). Other parameters were calculated using the algorithms provided in the DUAL-PAM100 software (Walz).

2.6 Microscopy

2.6.1 Analysis of chloroplast ultrastructure

Sample preparation and imaging was performed by Prof. Dr. Andreas Klingl (Department of Biology I, Ludwig-Maximilian's-University Munich). Plant leaves were cut into small pieces (1 x 1 x 1 mm or smaller) in 75 mM cacodylate buffer containing 2 mM MgCl₂ and 2.5% glutaraldehyde. After over-pressure/normal pressure infiltration with the fixation buffer and storage of the samples overnight at 4°C, the samples were post-fixed with 1% osmium tetroxide for 1 h. This step was followed by dehydration in a graded acetone series: samples were successively incubated in 10% acetone for 15 min, 20% acetone supplemented with 1% uranyl acetate for 30 min and in 40, 60 and 80% acetone for 20 min each. Finally, the samples were put into 100% acetone at least twice (for 5 min, then overnight). Afterwards, the plant tissue was infiltrated with Spurr's resin and polymerized at 63°C for at least 16 h. After thin sectioning, the material was examined on a Zeiss EM 912 with an integrated OMEGA filter for transmission electron microscopy (TEM). The acceleration voltage was set to 80 kV and the microscope was operated in the zero-loss mode. Images were acquired using a 2k x 2k slow-scan CCD camera (TRS Tröndle Restlichtverstärkersysteme, Moorenweis, Germany).

3 Results

3.1 RV-1

3.1.1 Phylogenetic conservation of RV-1

The protein RV-1 (AT4g37920) was selected from a proteomics screen, which was performed earlier on chloroplasts from very young pea plants in the laboratory of Prof Jürgen Soll. Due to its prediction of a chloroplast transit peptide it was selected as a potential candidate involved in chloroplast biogenesis. Phylogenetic analysis in photosynthetic organisms revealed a clear conservation in higher plants (Figure 4).

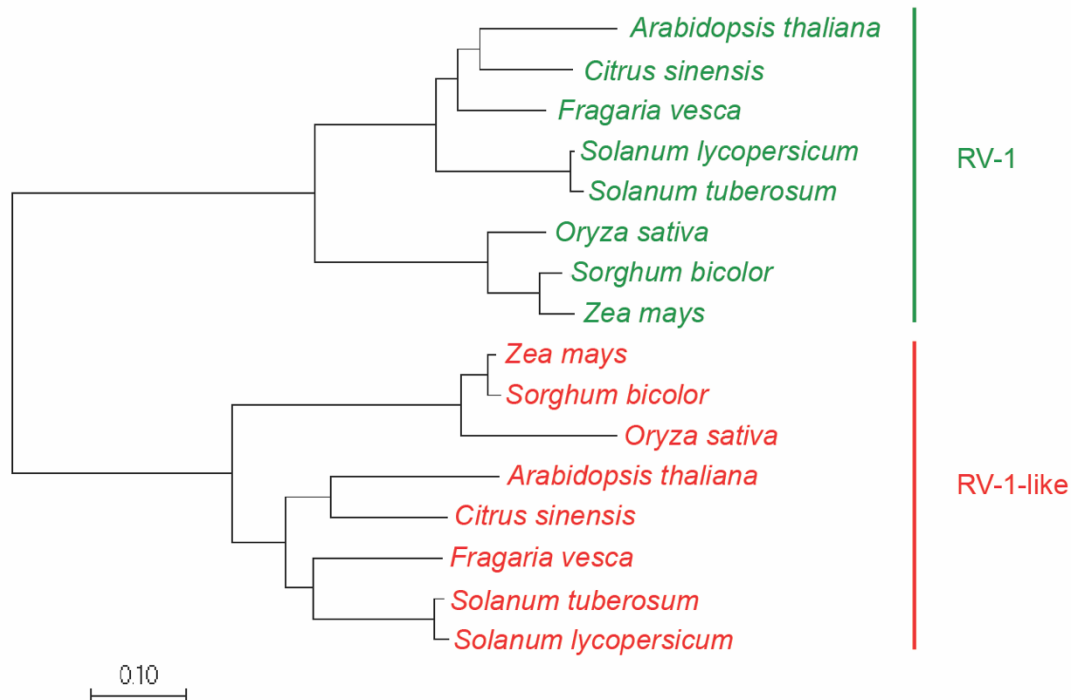


Figure 4. Evolutionary conservation of RV-1 and RV1-like. Phylogenetic tree of RV-1 and RV1-like protein sequences was constructed by the maximum likelihood method. The evolutionary distances were computed using the Jones-Taylor-Thornton (JTT) model. Represented in green are the species that contain at least one homolog of RV-1 and in red those with at least one homolog of RV1-like. Those species represented in black contain one gene homolog to both RV-1 and RV-1-like. Individual accession numbers are given in Material and methods.

Furthermore, an RV-1 paralog was identified, with a sequence identity of 41%, which was likewise found to be conserved in higher plants (Figure 4), we accordingly termed it RV-1-like (AT1G36320). Interestingly a search for conserved domains (with NCBI Blast) (Marchler-Bauer *et al.*, 2017) revealed the presence of a RelA/SpoT domain (accession TIGR00691), also called RSH for RelA and SpoT homologs. However, the domain is only conserved to a relatively low level (Bit Score 38.91, e-value 5.45×10^{-3} with RV-1). These proteins have been identified to control translation and RNA stability by synthesizing (p)ppGpp which inhibits translation (Potrykus & Cashel, 2008). Additionally, both RV-1 and RV-1-like have a distant homology with an RNase E protein from rice of 53% (within a stretch of 200 aminoacids in RV1, see black box in Figure 5) and 48% of identity (within 174 aminoacids) (accession BAD44933). This type of RNAses have been described to be involved in rRNA processing (Carpousis *et al.*, 2009) (Figure 5). Interestingly, no distinct homologs of both RV-1 and RV-1-like were found in cyanobacteria, algae or mosses.

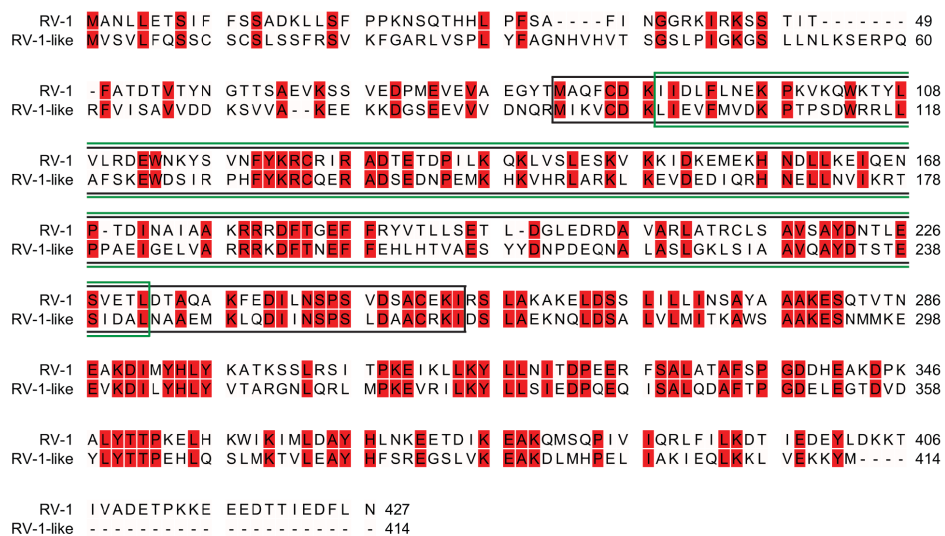


Figure 5. Amino acid conservation between RV-1 and RV-1-like. Protein sequences from *Arabidopsis thaliana* were aligned using BLASTp (Altschul *et al.*, 1997). Amino acids highlighted with red correspond to positions with identical residues for both proteins. The black box represents the domain found to be similar to an RNase E domain from a *Oryza sativa* protein (locus BAD44933). The green box represents the region with homology to the RelA/SpoT family domain (accession TIGR00691).

3.1.2 RV-1 localization in chloroplasts

To validate the localization of RV-1 (from *A. thaliana*) in chloroplasts, tobacco leaves were infiltrated with *Agrobacteria* bearing a construct for the over-expression of RV-1 fused to GFP at its C-terminus (Figure 6). The fluorescence of GFP in the protoplasts isolated from the infiltrated leaves was colocalized with the autofluorescence of chlorophyll from chloroplasts indicating its possible chloroplast localization.

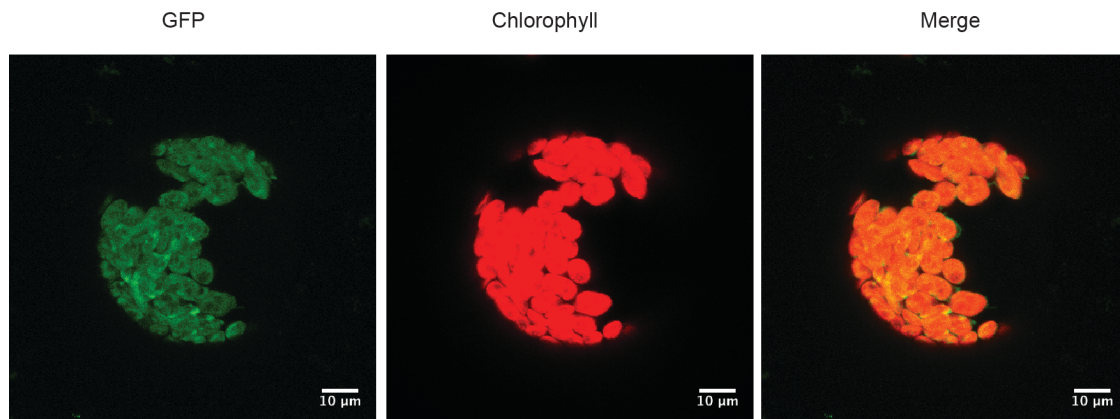


Figure 6. RV-1 protein is localized in chloroplasts. Tobacco leaves were infiltrated with *Agrobacteria* containing the vector of RV-1 fused to GFP. After two days of incubation, protoplasts were prepared from the infiltrated leaves and visualized with confocal microscopy.

Furthermore, in order to corroborate the chloroplast localization of RV-1 and to know the length of the mature form of the protein (mRV-1) *in-vitro* import analyses were performed. Therefore, chloroplasts from peas were isolated and the RV-1 precursor was synthesized *in-vitro* from the full CDS of *Arabidopsis* (pRV-1). Additionally, the chloroplast protein ferredoxin-NADP⁺-oxidoreductase (FNR), was used as a positive control. The precursor and mature forms for both proteins were identified by the radioactive signal of their polypeptides synthesized with methionine ³⁵S. In order to identify the mature form of each protein, chloroplasts subjected to

import were further treated with thermolysin for the digestion of non-imported precursors. As a result, the FNR protein showed a size shift corresponding to the cleavage of its TP to produce its mature form and validating the competence of the chloroplast to perform import. For RV-1, the import showed also a size shift from its precursor into a mature form of 45 kDa (Figure 7A). *In silico* analysis for RV-1 predicted a TP of 6.8 kDa (analysis done using ChloroP software) (Emanuelsson *et al.*, 1999), however the experimental data revealed that the true TP consists of about the first 34 aminoacids (with a size of 3.8 kDa). This result supports the *in-vivo* localization observed by the fluorescence of GFP fused to RV-1 indicating that it is indeed localized in the chloroplast.

Additionally, the mature form of RV-1 was heterologously over-expressed in *E. coli* and purified, from which antibodies were raised. Chloroplast sub-compartments were separated in order to identify RV-1 localization within the chloroplast. As expected, due to lack of hydrophobic regions on its sequence, RV-1 was found to be located in the stroma of chloroplasts (Figure 7B). The band obtained in the immunoblot matches with the size of the mature form of RV-1 of 45 kDa observed in the *in-vitro* import, thus corroborating the correct size of the protein. The distribution of RV-1 in the different subcompartments was observed by its accumulation in the stroma as it also does the protein fructose-1,6-bisphosphate (FBPase) which was used as a marker for stroma proteins. On the other hand, marker proteins for thylakoids as LHCbII, inner envelope TIC110 and outer envelope OEP37 showed the purity of the fractions indicating the absence of RV-1 in these

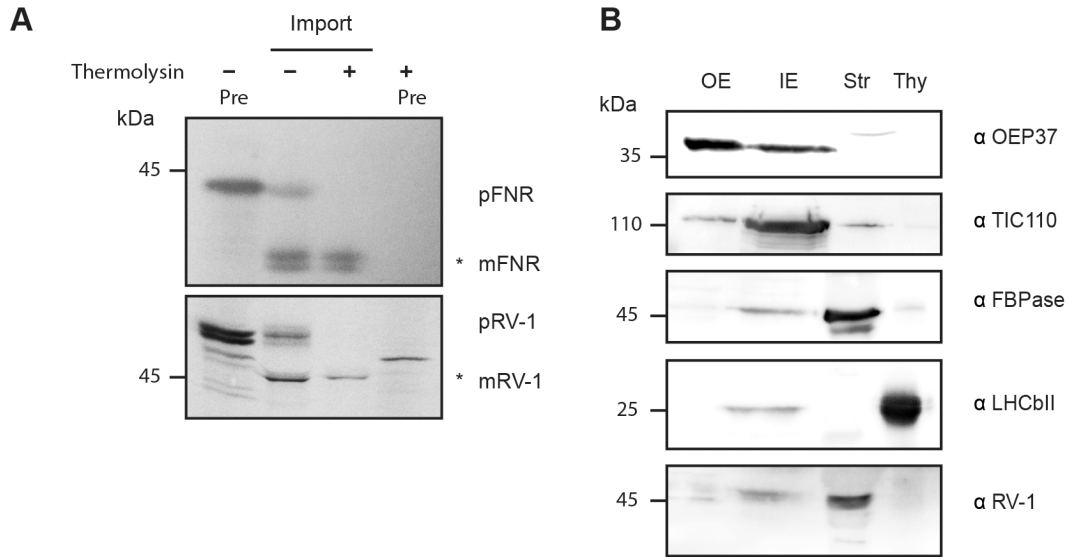


Figure 7. The protein RV-1 is localized in the stroma of chloroplasts. (A) Intact chloroplasts isolated from peas were used to perform import analyses by using *in-vitro* translated precursors (Pre) radiolabeled with methionine ³⁵S. After import, chloroplasts were treated with thermolysin to digest the fraction of precursor that was not imported. The stromal protein ferredoxin-NADP+-oxidoreductase (FNR) was used as positive control for import. Asterisks indicate the mature form for each protein after being imported into chloroplasts. **(B)** Chloroplasts from peas were isolated and their specific sub-compartment separated by using discontinuous sucrose gradients. Immunoblots were performed by using specific antibodies against RV-1 and maker proteins for each compartment; OEP37 (outer envelope, OE), TIC110 (inner envelope, IE), FBPase (stroma, Str) and LHCII (thylakoids, Thy).

3.1.3 Isolation of *rv-1* mutant lines

Two independent T-DNA insertion lines in the background of Col-0 (N347947 and N580811) were studied. The isolation of homozygous plants showed that the mutation on *RV-1* gene is seedling lethal, producing albino plants which can survive when grown on sugar till expanding their first true leaves but not producing seeds nor increasing size. A younger plant stage 14 days after germination with expanded cotyledons is shown in Figure 8A. The genotype of the lines was screened by performing PCR using different primer arrangements to amplify either the mutant or WT allele (Figure 8B). The WT PCR was performed by using primers flanking the

CDS region of the gene, whereas for the mutant PCR the insertion primer from GABI-Kat was used with either forward CDS primer (for the line N347947) or reverse CDS primer (for the line N580811) (Figure 8C upper panel). Furthermore, the line N347947 was complemented by transforming heterozygous plants with *Agrobacteria* bearing a construct for the over-expression of RV-1 under the control of the 35S promoter. The complementation line was checked by PCR for its homozygous mutant genotype along with the presence of the transgene (Figure 8C, lower panel). The PCR arrangement done by amplifying the mutant allele as explained above but in this case the WT PCR using CDS forward and reverse primers were used to amplify the transgene which was 35S::RV-1. In order to identify if the plants had heterozygous or homozygous genotype from the insertion, the WT PCR was repeated by using the forward CDS primer with a reverse primer annealing in the 3' UTR region which ensures amplification just in case the full sequence is present and differs in size from the previous PCR because of the additional intron sequences. The phenotype was completely restored in the complemented line (data not shown).

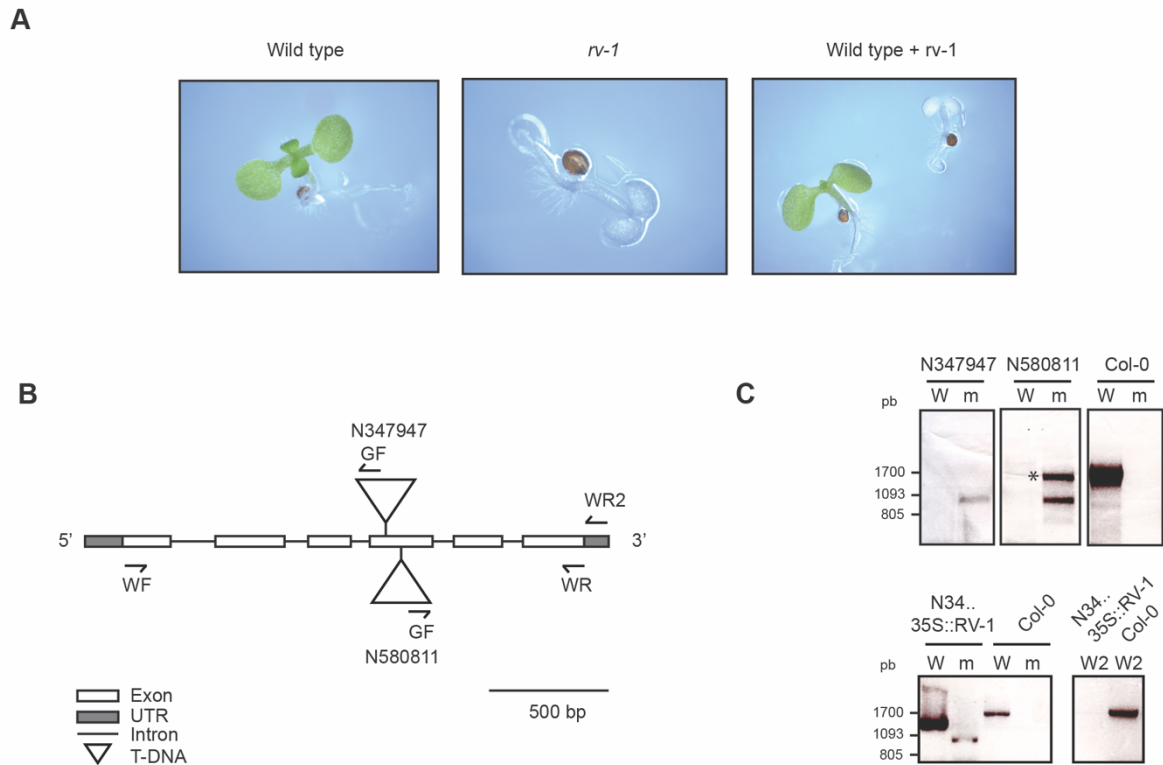


Figure 8. Homozygous *rv-1* mutant present pale phenotype. (A) Heterozygous seeds from the exon insertional line N347947 were sowed on MS plus 1% sugar plates for 2 weeks. The genotype of the plants was checked by PCR confirming the pale phenotype for the homozygous plants (N347947, *rv-1*). (B) Gene scheme represents the position of the insertion lines N347947 and N580811. The position of the primers used for genotyping are represented as arrows. (C) Genotyping was performed by using gDNA from lines N347947 and N580811 (upper panel). For line N347947, the mutant allele PCR (m) was performed by using the primers WF and GF on (A). The line N580811 was genotyped performing PCR for the mutant allele using WR and GF primers. The asterisk indicates an unspecific amplicon. WT PCR was performed using WF and WR primers (W). On the lower panel is shown the genotyping for the complementation of the line N347947. The WT PCR (W2) was performed by using WF and WR2 whereas the mutant PCR was performed as mentioned above.

From this point the line N347947 (henceforth referred to as *rv-1*) was used for further studies since both lines showed the same phenotype in homozygous mutants (data not shown). Ultrastructure images of chloroplasts on the homozygous *rv-1* showed an aberrant chloroplast morphology with the absence of thylakoid membranes. Overall aberrant chloroplasts in *rv-1* were strongly reduced in size in comparison to

WT (Figure 9). Accumulation of large vesicle was observed in every chloroplast and their sizes were also very different from one another.

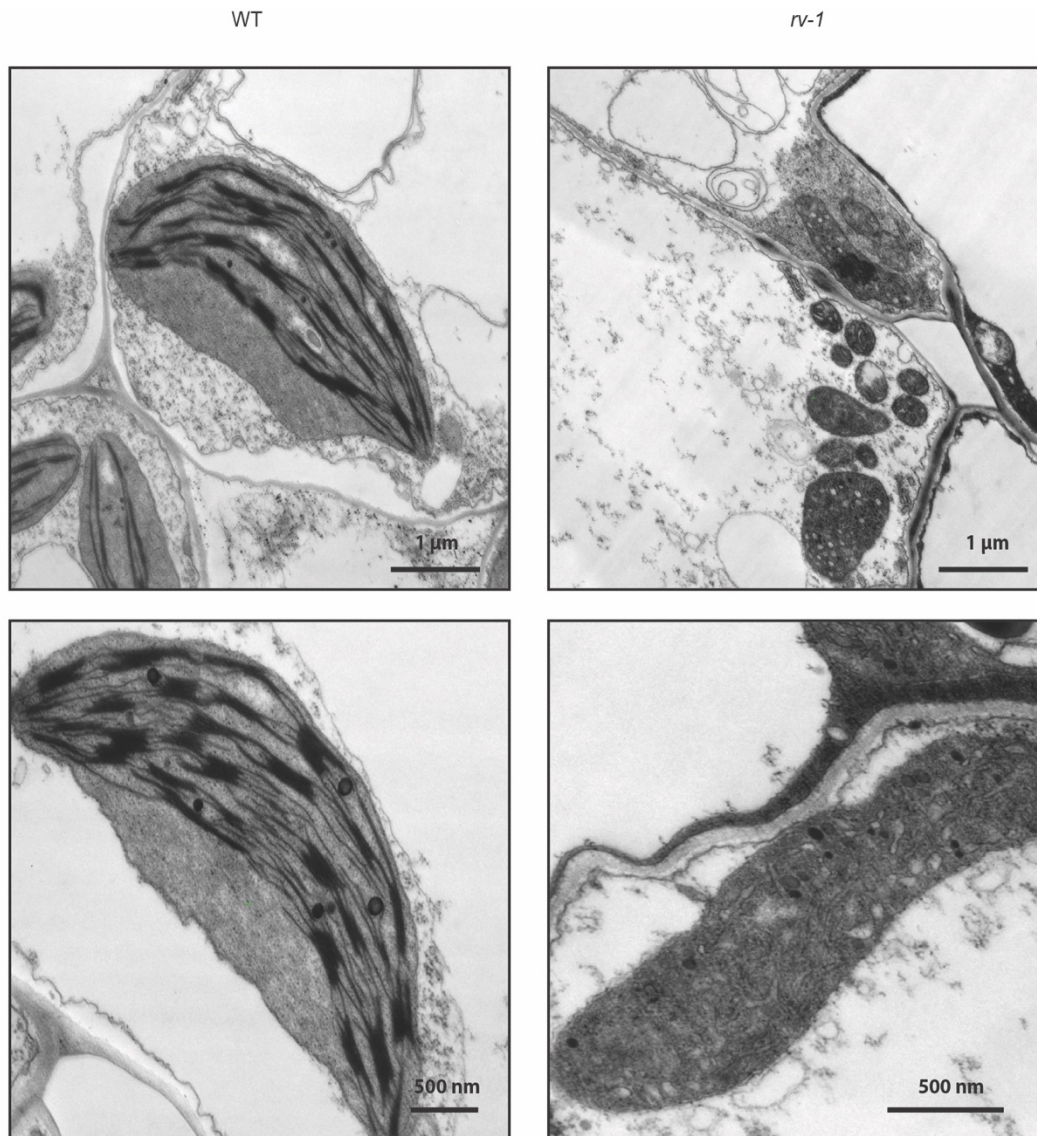


Figure 9. Homozygous *rv-1* mutant affected in chloroplast morphology. (D) Heterozygous seeds were sowed on MS plus 1% sugar for 3 weeks and true leaves from WT and homozygous plants (N347947, *rv-1*) were excised for electron microscopy analyses. Pictures taken by Prof Andreas Klingl.

3.1.4 Translation is impaired in *rv-1*

Since the homozygous mutant plants showed undeveloped chloroplasts and were albino, the ability to perform translation was assessed. Therefore, 21 days old seedlings were infiltrated with radiolabeled methionine ^{35}S and then incubated under light exposure for 20 min. Proteins were extracted from the seedlings and separated into soluble and membrane proteins. In the WT, translation of the large subunit of RubisCO was very prominent in the soluble fraction as well for the D1 subunit of PSII in the membrane fraction. Surprisingly, the mutant *rv-1* showed barely any translation in comparison to WT seedlings (Figure 10A). Interestingly, it could be observed in the CBB gel even a high reduction in RubisCO content compared with the total soluble proteins in the *rv-1* mutant as well for LHCs in the membrane fraction in comparison to WT. This observation posed the question about the absence or presence of plastid ribosomes. This was investigated by isolating total proteins from WT and *rv-1* mutant seedlings and performing immunoblots using specific antibodies against members of the 50S subunit of plastid ribosomes, RPL2 and RPL4. Interestingly, this showed the absence of these in the mutant *rv-1* seedlings compared to WT (Figure 10B). Since absence of thylakoid membranes was observed from ultrastructure pictures, the protein TIC110 present in the inner envelope of the chloroplast was used as a loading control and to monitor the presence of plastid ribosomes, two proteins of the large ribosomal subunit were for immunoblot analyses.

Furthermore, since ribosomes subunits are complexes of protein and rRNA, the presence of the rRNA was analyzed by isolating total RNA from WT and *rv-1* mutant seedlings. As expected, *rv-1* showed high reduction of the chloroplast rRNAs, both of the 30S and 50S ribosomal subunit, 16S and 23S rRNA, respectively. In comparison to WT levels (Figure 10C). However, the 25S and the 18S were even slightly more abundant in the mutant compared to WT indicating that the problem of translation or ribosomal stability relays on the plastid ribosomes.

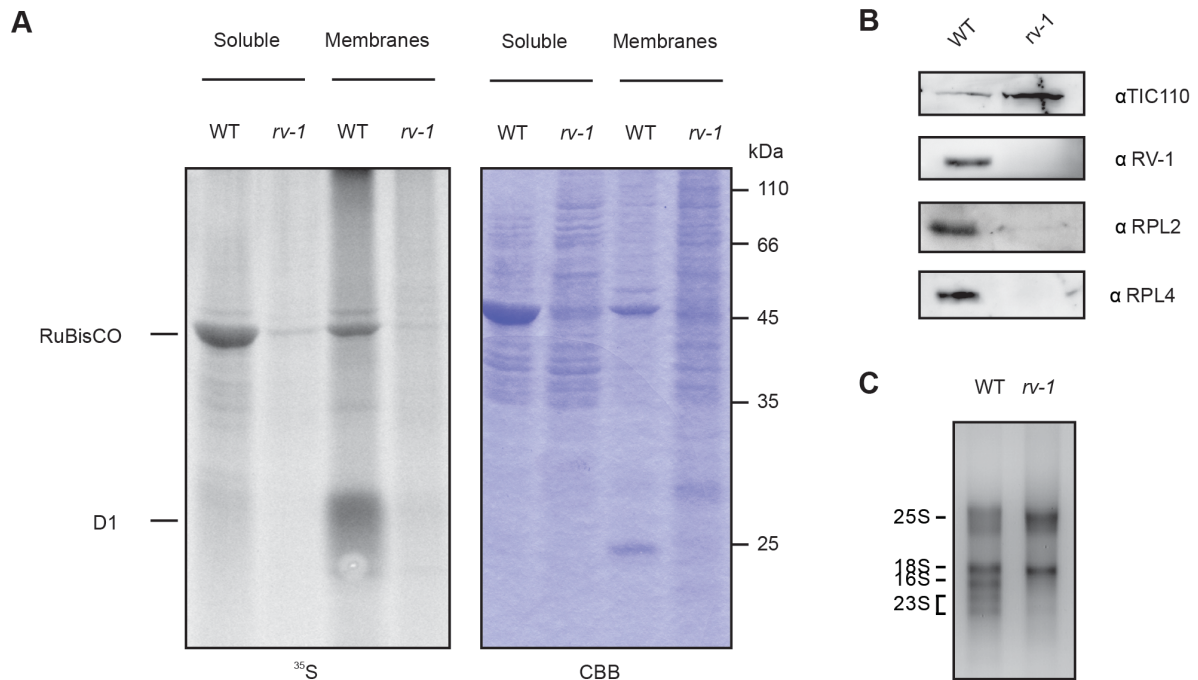


Figure 10. Homozygous *rv-1* mutant plants are impaired in protein translation and lack plastid ribosomes. (A) Heterozygous seeds were sowed on MS medium with 1% sugar for 4 weeks. WT and mutant seedlings (*rv-1*) were taken and infiltrated with radiolabeled methionine ³⁵S. The total soluble and membrane proteins of the plants were extracted to run an SDS-PAGE and the gel then exposed to phosphorimaging screen to visualize the labeled proteins. **(B)** Plants were grown on MS medium with 1% sugar for 4 weeks. Immunoblots were performed by extracting total protein content from WT and mutant plants and using specific antibodies against RV-1, TIC110 as loading control and RPL2 and RPL4 from the 50S subunits in chloroplast ribosomes. **(C)** Total RNA was isolated from WT and homozygous *rv-1* mutant plants and analyzed on agarose gel.

In order to discard the presence of the plastid rRNAs, northern blot analyses were performed by using specific probes for 16S and 23S rRNAs and fresh isolated RNA from Arabidopsis plants. Surprisingly, despite that in normal agarose gel analysis 16S and 23S rRNAs appeared absent, northern blots revealed that both rRNAs and their processed fragments are still present though in both cases the rRNAs are highly reduced (Figure 11).

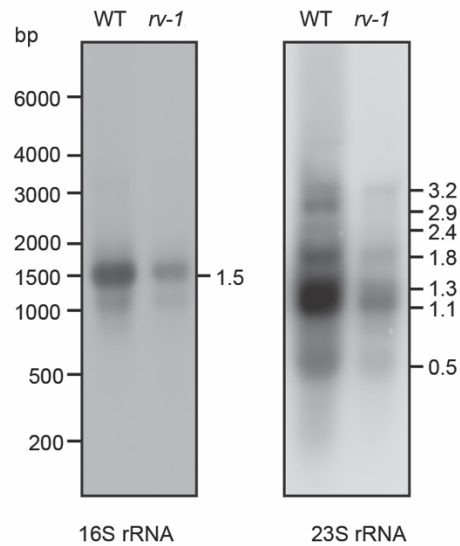


Figure 11. Homozygous *rv-1* mutant is highly reduced in 16S and 23S plastid rRNA. Total RNA isolated from homozygous pale *rv-1* mutant plants and WT, grown on MS plus sugar for three weeks, were used for northern blot analyses using specific probes against 16S and 23S rRNA. Northern blot performed by Dr. Steffen Heinz.

3.1.5 Analysis of a putative RNase activity of RV-1

Due to the, albeit distant, homologies to RNA binding and processing proteins the ability of RV-1 to either degrade or bind to RNA was assessed. Therefore, RV-1 fused to MBP was purified from over-expression in *E. coli* RIPL cells (Figure 12A). Interestingly, RV-1 was not able to degrade RNA isolated from WT plants nor DNA (Figure 12B). Since it is known that plastid rRNAs undergo steps of processing from precursors, putative specific RNase activity was tested by using plastid precursors rRNAs 16S and 23S. Likewise, these rRNAs were not susceptible to any degradation by RV-1 (Figure 12C).

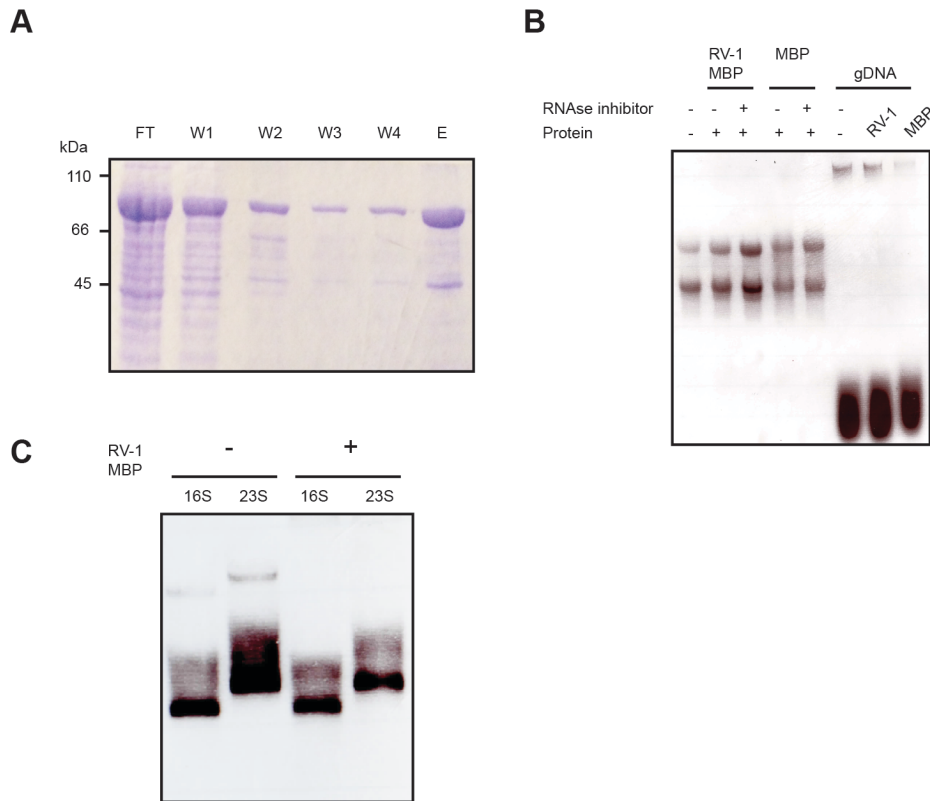


Figure 12. RV-1 does not present RNase activity. **(A)** Over-expression of RV-1 fused to MBP in RIPL cells and purified by Ni^{2+} beads. The fractions indicated in the SDS-PAGE gel correspond to flow through (FT), washes (W1, W2, W3 and W4) and elution (E). **(B)** Total RNA was isolated from 3 weeks old *Arabidopsis* plants and then used to performed RNAse assays by using purified RV-1 fused to MBP. As a negative control for RNAse activity was used the purified MBP protein. The RNA and DNAg (as negative control) were run on agarose gel. **(C)** *In-vitro* transcribed 16S and 23S chloroplasts rRNA were used to perform RNAse assays by using RV-1 fused to MBP. The RNAs were analyzed by running them on an agarose gel

Besides its putative RNase activity, the ability of RV-1 to bind RNA was tested by performing an electrophoretic mobility shift assay (EMSA) and using radiolabeled plastid 16S and 23S rRNAs. Interestingly, neither 16S nor 23S rRNAs could be targets for the putative RV-1 binding activity (Figure 13). As positive control, the protein PAC was used, which is known to bind 23S rRNA (Meurer *et al.*, 2017).

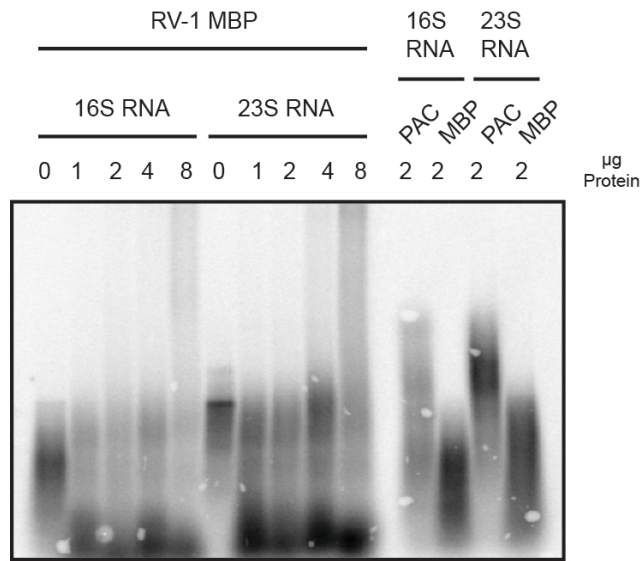


Figure 13. RV-1 does not bind to chloroplast rRNAs. Plastid rRNA 16S and 23S were cloned and *in vitro* synthesized by using radiolabeled UTP (α 32 P) to perform EMSA analysis. The recombinant protein RV-1 fused to MBP was freshly isolated used for binding assays with the synthesized RNAs by incubation of 30 min at RT. After this the samples were run in 1% agarose gels and transferred to a membrane by Northern Blot. As positive control the PAC protein was used and MBP as negative control.

Despite the evidence showing that RV-1 does not bind or degrade plastid rRNAs, its potential to bind to ribosomes was investigated further. Stroma samples from WT *Arabidopsis* plants treated with or without RNase A were separated onto continuous sucrose gradients. During RNase A treatment, ribosomes should be disassembled due to the absence of RNA thus shifting their distribution in a sucrose gradient. The same behavior would also be expected for proteins associated to those ribosomes. The gradients were separated into 12 fractions which were further precipitated with TCA to analyze their protein content performing immunoblots. The majority of RV1 accumulated in fractions with a very low sucrose concentration, suggesting this fraction of the protein is not part of a larger complex. However, a portion of RV1 was also found to accumulate at higher sucrose concentrations and in fact co-migrated with the ribosomal subunit RPL4. Interestingly, RV-1 was shifted upon RNase A treatment as was RPL4 (Figure 14). This indicates that even though RV-1 is not able to bind plastid rRNAs, it might be nevertheless associated to ribosomes.

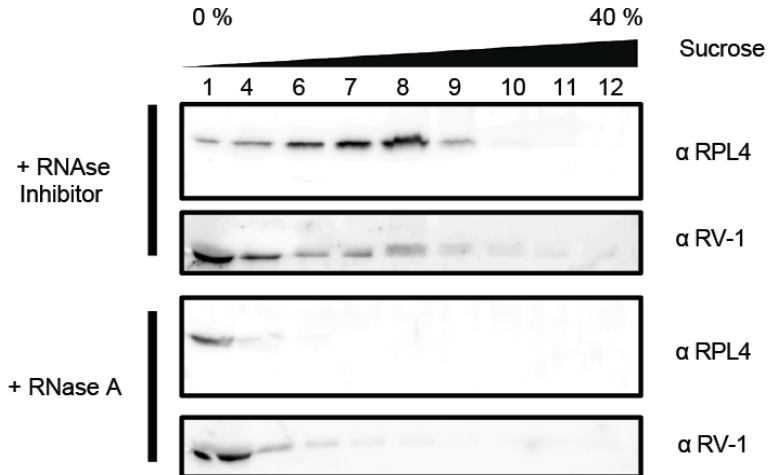


Figure 14. RV-1 forms RNAse A sensitive complexes that co-migrate with ribosomes. Stroma fractions from peas chloroplast were isolated and treated with RNase A or RNase inhibitor. These samples were separated in sucrose gradients for immunoblot analyses of the different fractions using specific antibodies against RV-1 and the 50S subunit of chloroplasts ribosomes RPL4.

In order to analyze the function of RV-1 in more detail, RNA interference (RNAi) lines for the *RV-1* gene were generated in Col-0 background. As expected, over-expressing RNAi lines were affected in greening of leaves as well as overall fitness of the plants. However, they reached adulthood and were able to produce seeds (Figure 15A). In order to verify that the phenotype correlates with a decrease in RV-1 levels, the down-regulation of RV-1 expression due to RNAi was tested by performing immunoblots. As expected, RV-1 is highly reduced in the RNAi mutant line in comparison to the WT, and therefore it validates the affected phenotype in the RNAi line (Figure 15B). Interestingly, when analyzing the ultrastructure of chloroplast of the RNAi line 1 in comparison to WT it is possible to observed severely affected chloroplast similar to Figure 9. Nevertheless, chloroplast containing thylakoid membranes are also observed though also affected with reduced grana stacks in comparison to WT (Figure 15C). These lines will be useful for further analysis to monitor their chloroplast function and content since they can grow on soil being able to produce enough plant material.

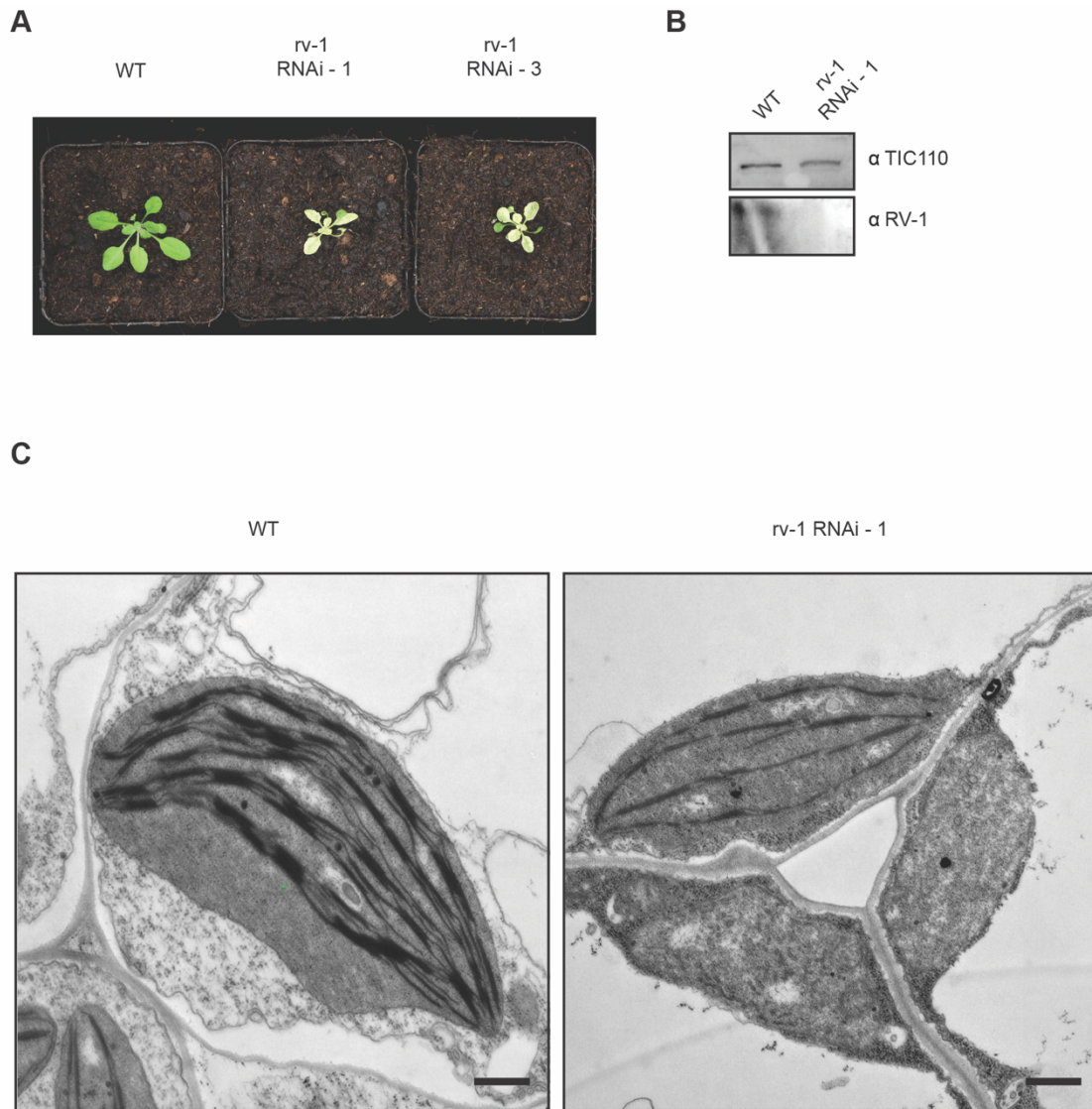


Figure 15. Down-regulation of RV-1 affects Arabidopsis plant development at all stages. (A) WT plants were stably transformed with a construction for down-regulation of RV1 expression by RNAi in the vector pOpOff2. Stable lines affected in their development were selected. Plants were grown on soil for 3 weeks and just two out of three survived to produced seeds. **(B)** Immunoblots were done by isolating total protein from the RNAi line 1 and WT plants. Specific antibodies were used to detect RV-1 and as loading control TIC110. **(C)** Arabidopsis plants from the RV-1 RNAi line 1 and WT were grown on soil for 3 weeks under long day conditions and their leaves were excised for electron microscopy analyses. The scale bars represent for each case 500 nm. Pictures taken by Prof Andreas Klingl.

3.1.6 Characterization of the RV-1-like gene

As mentioned above, RV-1 has a paralog, termed RV-1-like. *In-silico* analysis for its localization using the online server TargetP 1.1 showed chloroplast predicted TP (Emanuelsson *et al.*, 2000). Therefore, we proceeded to investigate the localization of RV-1-like experimentally. The expression of a RV-1-like-GFP fusion protein in tobacco leaves was analyzed. In addition to infiltrating leaves RV-1-like-GFP construct, protoplast extracted from those leaves were further treated with Mitotracker orange to visualize mitochondria on the microscope. Surprisingly, the GFP signal obtained did not colocalize with chlorophyll but with the mitotracker signal suggesting that RV-1-like is localized in the plant mitochondria (Figure 16).

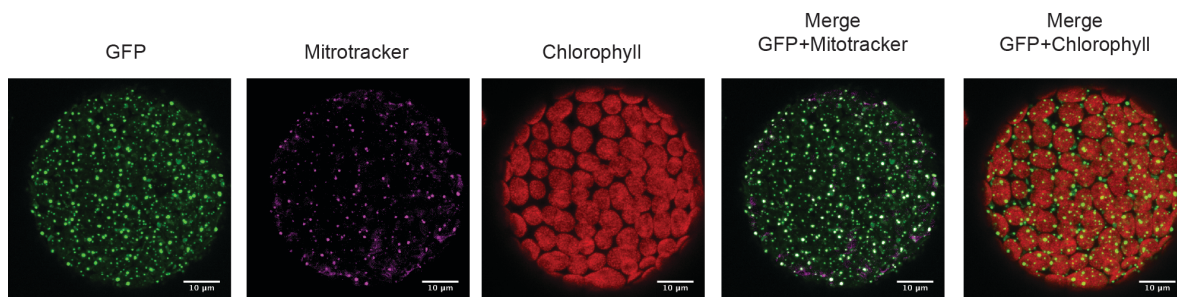


Figure 16. RV-1-like is localized in plant mitochondria. Tobacco leaves were infiltrated with *Agrobacterium* containing the vector of RV-1-like fused to GFP. After two days of incubation, protoplasts were prepared from the infiltrated leaves. Protoplasts were incubated with Mitotracker and then visualized with confocal microscopy.

In order to understand the relevance of RV-1-like for plant growth, a T-DNA mutant line, with the T-DNA located in the last exon of *RV-1-like* gene, was used for further studies (GK844F05, henceforth referred to as *rv-1-like*) (Figure 17A). Genotype analyses were performed with primers located at the fourth exon as forward and at the last exon as reverse for the WT PCR. On the other hand, for the mutant PCR it was used the forward GABI-kat primer with the forward primer at the fourth exon of *RV-1-like* gene. This showed that the heterozygous plants did not produce

homozygous individuals but rather a distribution of 50% WT and 50% heterozygous plants (analyzing around 50 individual plants). Therefore, the siliques of the heterozygous plants were analyzed in order to identify aborted embryos which might explain the absence of homozygous plants in the segregation of the heterozygous *rv-1-like* line. Indeed, the siliques from heterozygous *rv-1-like* plants showed empty spaces (Figure 17C). Furthermore, heterozygous *rv-1-like* showed a reduced amount of seeds per silique and an increased number of empty spaces or aborted embryos per silique (Table 6).

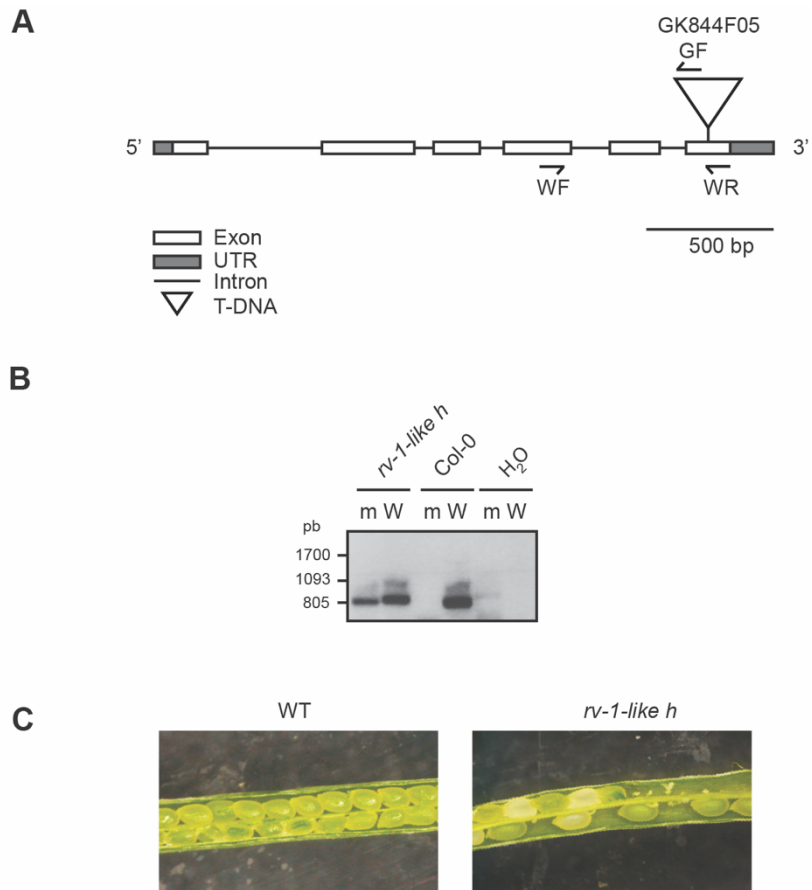


Figure 17. Homozygous mutant plants for RV-1-like are not viable. (A) Schematic representation of the *rv-1-like* gene. The T-DNA insertion site is indicated as a triangle. The primers used for genotyping are represented as arrows. **(B)** Genotyping of heterozygous *rv-1-like* plants. PCR was conducted using forward and Gabi-forward (GF) primers for the mutant PCR (m) and WF whereas the WT PCR with the primers WF and WR (W). **(C)** Heterozygous seeds for an insertion mutant line for *rv-1-like* were grown for 6 weeks. Siliques were taken and opened to observed aborted embryos.

Genotype	N° of seeds / Silique	Aborted embryos / Silique
WT	44.5 ± 1.2	0
<i>rv-1-like h</i>	20.5 ± 2 *	10 ± 0.6 *

Table 6. Heterozygous *rv1-like* mutant plants present aborted embryos and reduced seeds in their siliques. Seeds from the heterozygous mutant line (*rv-1-like h*) were sowed and plants grew for 6 weeks on soil. Heterozygous and WT plants were identified by genotyping them with PCR and the siliques were used to count their number of seeds as well as aborted embryos per silique. Asterisks represent significant differences ($P < 0.05$) in comparison to the WT based on the t-test. The mean of seeds and aborted embryos from 10 siliques taken from 3 independent plants are represented along with the SEMs.

The phenotype for RV-1 and RV-1-like demonstrated that both genes are essential for viability of the plant. Loss of function of RV-1 alters not just chloroplast morphology but also the plastid ribosomes stability or assembly which provides insight on its possible function. Whereas RV-1-like is most likely localized in the plant mitochondria but still impacting plant viability in its loss of function with the inability of producing homozygous individuals. However, the exact molecular function of both proteins remains to be investigated.

3.2 PG18

3.2.1 Characterization of PG18

Similar to RV1, PG18 (AT4G13200) was selected from the previously performed proteomic study. Interestingly, this protein was also found in a proteome analysis from PG of *Arabidopsis* (Lundquist *et al.*, 2012). It has no known protein domains and phylogenetic analysis showed that PG18 is conserved from higher plants to cyanobacteria (Figure 18).

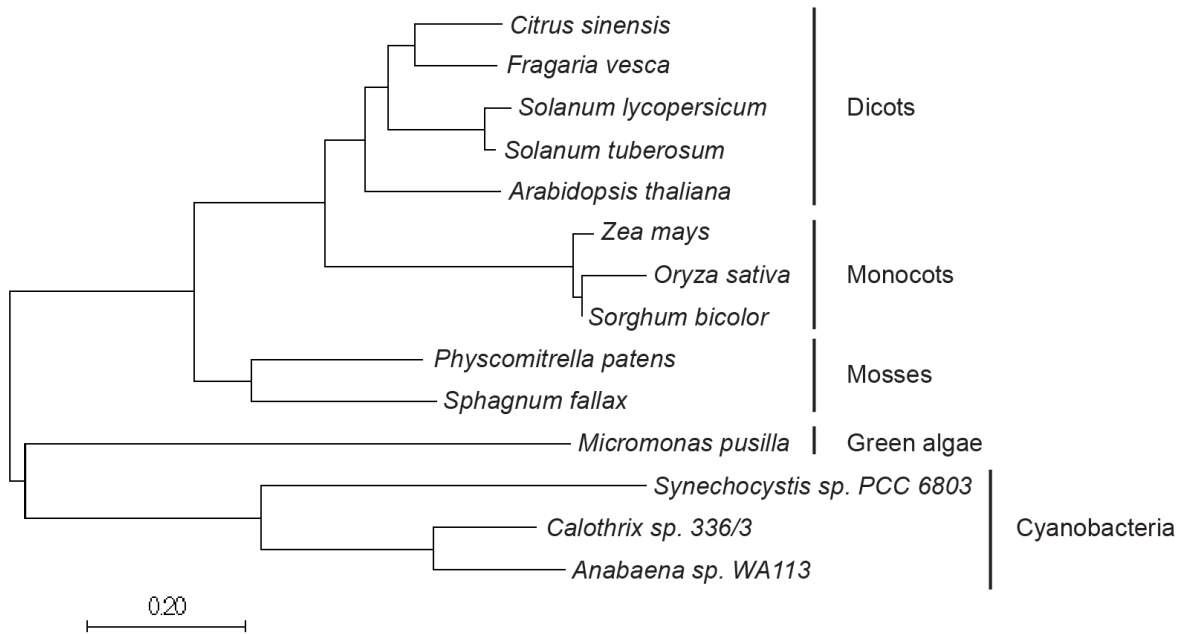


Figure 18. PG18 conservation in photosynthetic organisms. Phylogenetic tree showing homology of PG18 protein from cyanobacteria to higher plants. The phylogenetic tree was made by using distance-based method with the neighbor-joining algorithm and bootstrap value of 100.

In order to validate its chloroplast localization, transient over-expression of PG18-GFP fusion protein was performed under the control of the 35S promoter in tobacco leaves. Leaves were infiltrated with *Agrobacteria* containing the construct and protoplasts were isolated two days after the transfection. GFP, as well as chlorophyll autofluorescence, was detected in isolated protoplasts with a confocal laser-scanning microscope. The GFP signal was found exclusively in chloroplasts, where it appeared to form punctate structures (Figure 19A). In order to generate antibodies against PG18, the protein was over-expressed in *E. coli* RIPL cells and the purified protein was used to raised the specific antibodies. As PG18 did not show any hydrophobic region in its aminoacid sequence but it was found in PGs, the solubility of the protein was assesed by separating WT *Arabidopsis* total proteins in soluble and membrane fractions. Surprinsilgy, the PG18 protein was found exclusively in the membrane fraction using specific antibodies againts PG18 (Figure 19B).

Furthermore, in order to understand the association of PG18 with membranes, thylakoids were isolated and washed with several buffers. Then the membrane fraction was treated with 1 M NaCl, 0.1 M Na₂CO₃, and 3 M urea to ascertain whether PG18 is attached to the membrane by hydrophobic or electrostatic interactions and could therefore be removed by any of these agents (Figure 19C). Incubation with buffer (HEPES/KOH 5 mM, EDTA 5 mM, pH 7.5) served as a negative control and disruption of the membrane with 1% LDS was applied to achieve total solubilization of the membrane. Only the treatment with 1% LDS resulted in complete solubilization of PG18. However, a small amount of PG18 was found in the supernatant after treatment with 3 M urea (Figure 19C). To assess the efficiency of these treatments, the blot was probed with OE33 antiserum. OE33 is a peripheral luminal protein and is at least partially extracted by each of the agents mentioned above, as they all damage the integrity of the thylakoid membrane (Figure 19C) (Bhuiyan *et al.*, 2015). Cytochrome *f* (Cyt *f*) was used as an example of an integral membrane protein and, as expected, it is solubilized only by treatment with 1% LDS (Figure 19C). Several proteomics studies have identified PG18 in PGs (Friso *et al.*, 2004; Peltier *et al.*, 2004; Ytterberg *et al.*, 2006) and therefore it was set out to test this further. To this end, pea chloroplasts were fractionated into PGs and thylakoid membranes. Pea plants were chosen instead of *Arabidopsis* for this experiment because they provide larger amounts of leaf material. Thylakoid membranes and PGs were separated on a sucrose density gradient, and selected fractions were subjected to SDS-PAGE and subsequently probed with antisera against LHC1a as a thylakoid marker, plastoglobulin 35 (PGL35) as a PG marker and PG18 (Figure 19D). As revealed by the distribution of the PG marker protein PGL35, the PG fraction was not contaminated with thylakoids, and the majority of PG18 was also detected in this fraction. Since PGs are known to be associated with the thylakoid membrane (Austin *et al.*, 2006), it is not surprising that small amounts of both PG18 and PGL35 are detected in the thylakoid fraction. Additionally, in order to demonstrate that PG18 is located at the surface of the PGs, intact thylakoids and their associated PGs were treated with trypsin (Figure 19E). As expected, PG18 was completely digested – as was the alpha subunit of ATP synthase, which is exposed on the stroma side of the

thylakoids – while the luminal OE33 protein used as a control for thylakoid integrity remained intact. Taken together, the observed punctate structures of PG18-GFP, the sub-fractionation data, and the fact that PG18 has been assigned to PGs by mass spectrometric analyses (Lundquist *et al.*, 2012) led to the conclusion that PG18 is indeed a PG-localized protein. Considering that none of the PG proteins identified so far harbor transmembrane domains but are nevertheless most likely to be integrated into the lipid monolayer surface of PGs, the observation that PG18 behaves similarly to an integral membrane protein upon treatment with various chaotropic agents is compatible with the protein's localization to PGs.

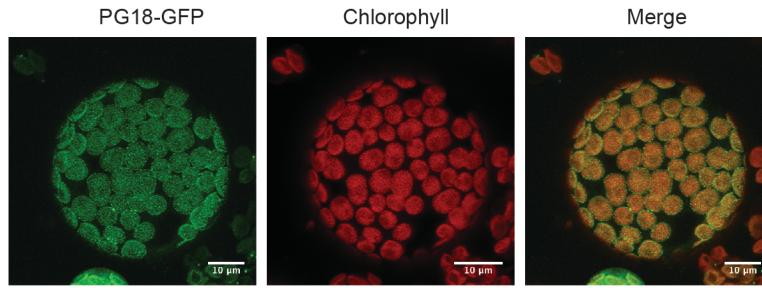
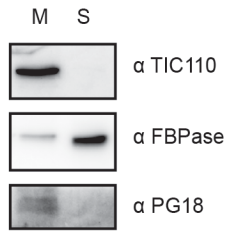
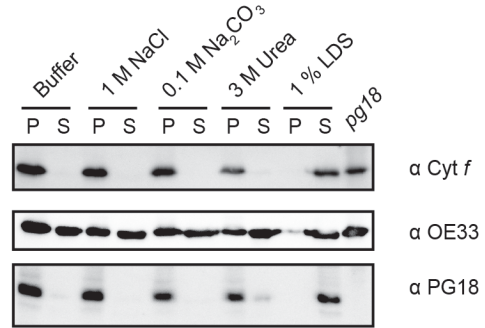
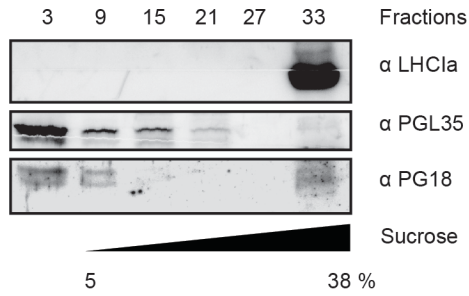
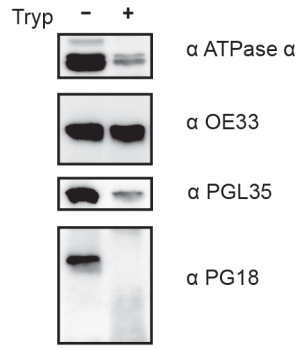
A**B****C****D****E**

Figure 19. PG18 is a membrane-associated protein in PGs. (A) Tobacco leaves were infiltrated with *Agrobacteria* containing a vector expressing PG18 fused to GFP (see Materials and methods). Protoplasts were prepared from the infiltrated leaves and visualized with confocal microscopy. **(B)** A total protein extract from *Arabidopsis* was separated into a membrane (M) and a soluble fraction (S). PG18 was detected on immunoblots using specific antibodies. Antibodies raised against TIC110 (a membrane protein marker) and FBPase (a soluble protein marker) were used as controls. **(C)** Disrupted *Arabidopsis* thylakoids were extracted with salt-containing buffers and separated into supernatant (S) and pellet (P) fractions by centrifugation. The samples were fractionated by SDS-PAGE and analyzed immunologically using antibodies specific for PG18, Cyt *f* and OE33, respectively. As a control for the specificity of the anti-PG18 antibody, isolated chloroplasts from the mutant line *pg18* were also loaded onto the gel. **(D)** Chloroplast membranes were isolated from 3-week-old peas. The samples were then further fractionated on a discontinuous sucrose gradient (the number of the fraction is indicated above each lane). Immunoblotting was performed and the blot was probed for the presence of the marker proteins for thylakoids (LHCA1) and plastoglobuli (PGL35). **(E)** *Arabidopsis* thylakoids were isolated from plants grown on soil for three weeks. Trypsin digestion of thylakoids was performed on ice for 10 min and the samples were analyzed after immunoblotting. An antiserum directed against the ATP synthase α subunit was used to ensure that the stromal side of the thylakoid was accessible to the enzyme, whereas the lumen protein OE33 served as a marker for the integrity of the thylakoids. PGL35 was used as a PG control.

3.2.2 Characterization of *pg18* mutant lines

Two independent T-DNA insertion lines in the background Col-0 (N442085 and N459729) were obtained (Figure 20A). The genotype of the line N442085 was screened by performing PCR (Figure 20B) and was then used for further studies (henceforth referred to as *pg18*). The WT PCR was performed by using forward and reverse primers flanking the full CDS sequence of PG18. Whereas for the mutant PCR it was assessed two combination of primers which was the GABI-kat forward primer with either the reverse or forward primer for the CDS sequence of PG18.

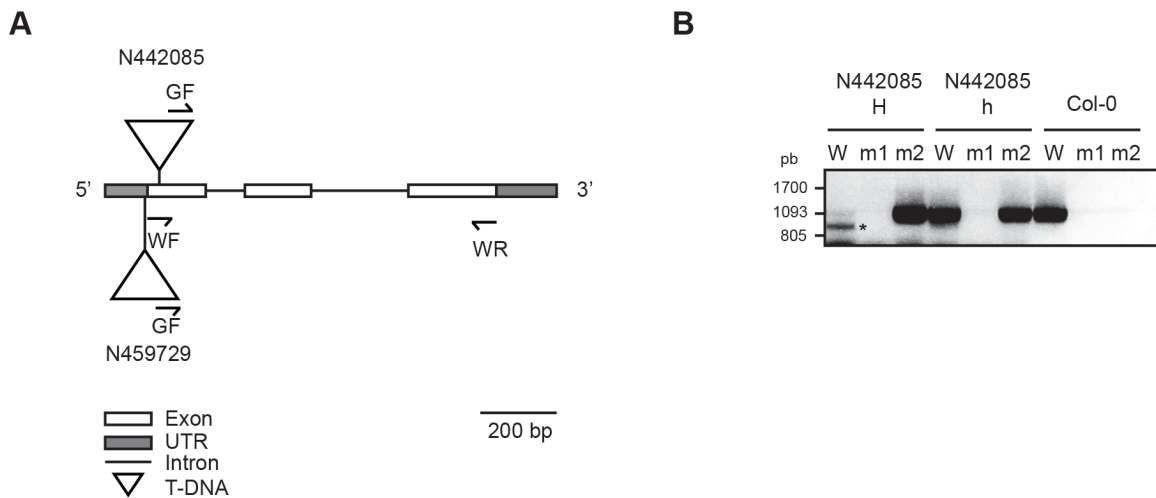


Figure 20. *pg18* mutant lines isolation. (A) Schematic representation of the *pg18* gene. The T-DNA insertion site is indicated as a triangle. The primers used for genotyping are represented as arrows. (B) Genotypification of *pg18* mutant plants (line N442085). WT PCR was conducted using the primers WF and WR (W). On the other hand, mutant PCR was done by using Gabi-forward primers (GF) with either WF (m1) or WR (m2) primers. The asterisk indicates an unspecific amplicon and the H indicates homozygous and h to heterozygous plant for the line N442085.

The mutant was viable on soil but displayed a pale green phenotype under normal lighting (NL) conditions (21°C, 120 $\mu\text{mol} / \text{m}^2\text{s}$ light, 16 / 8 h light / dark). Since it has been observed that PGs become more abundant under light stress (Zhang *et al.*, 2010), mutant plants were also exposed to increased light intensities (IL, 250 $\mu\text{mol}/\text{m}^2\text{s}$) for 3.5 days, following 17.5 days growth under NL conditions (Figure 21A). To ensure that the phenotype correlated with the disruption of the *PG18* gene, the mutant *pg18* line was complemented with a PG18-GFP fusion construct expressed under the control of a 35S promoter. A representative example of a complemented line is shown in Figure 21A. The knock-out of PG18 was verified at the protein level using the specific antiserum (Figure 21B). Total protein extracts of WT and *pg18* were probed with the PG18 antiserum, which detected a specific band at 18 kDa in the WT that was absent in the mutant. An antiserum raised against the chloroplast protein TIC110 was used as a loading control. In addition, proteins were extracted

from the complemented mutant line and likewise probed with PG18 antiserum. A protein of 45 kDa was detected, corresponding to the expected size of PG18-GFP. These results demonstrate the specificity of the generated antiserum, as well as successful complementation of the mutant. It has been reported that PG proteins are strongly expressed under increased light (IL) – with the exception of PG18 (Ytterberg *et al.*, 2006). To verify this, levels of PG18 in plants were monitored under NL and IL conditions. As expected, P18 is equally abundant in NL and IL plants, while expression of the core PG protein PGL35 increases upon exposure to high light levels (Figure 21C).

Since the pale phenotype indicated a defect in chloroplasts, the phenotype was analyzed at the ultrastructural level (Figure 21D). Interestingly, when examined at higher magnification, the stroma lamellae in *pg18* mutant chloroplasts are shorter and appear to be stacked, rather than present in single layers. Moreover, the stroma lamellae exhibit less branching between grana stacks, while the latter display a more compact organization and generally consist of more layers in the mutant than in the WT or the complemented line. This effect is observed under both NL and IL conditions, although it is more pronounced in IL (Figure 21D). In comparison to the WT, the cross-sectional area of *pg18* chloroplasts is significantly smaller under both conditions (Figure 21E). Interestingly, under both light conditions, PG abundance per chloroplast is also reduced in the mutant chloroplast in comparison to WT. The number of PGs increases under IL in the WT by 100%. Strikingly, this effect of exposure to IL is also observed in the mutant, in spite of the overall reduction in the numbers of PGs (Figure 21F).

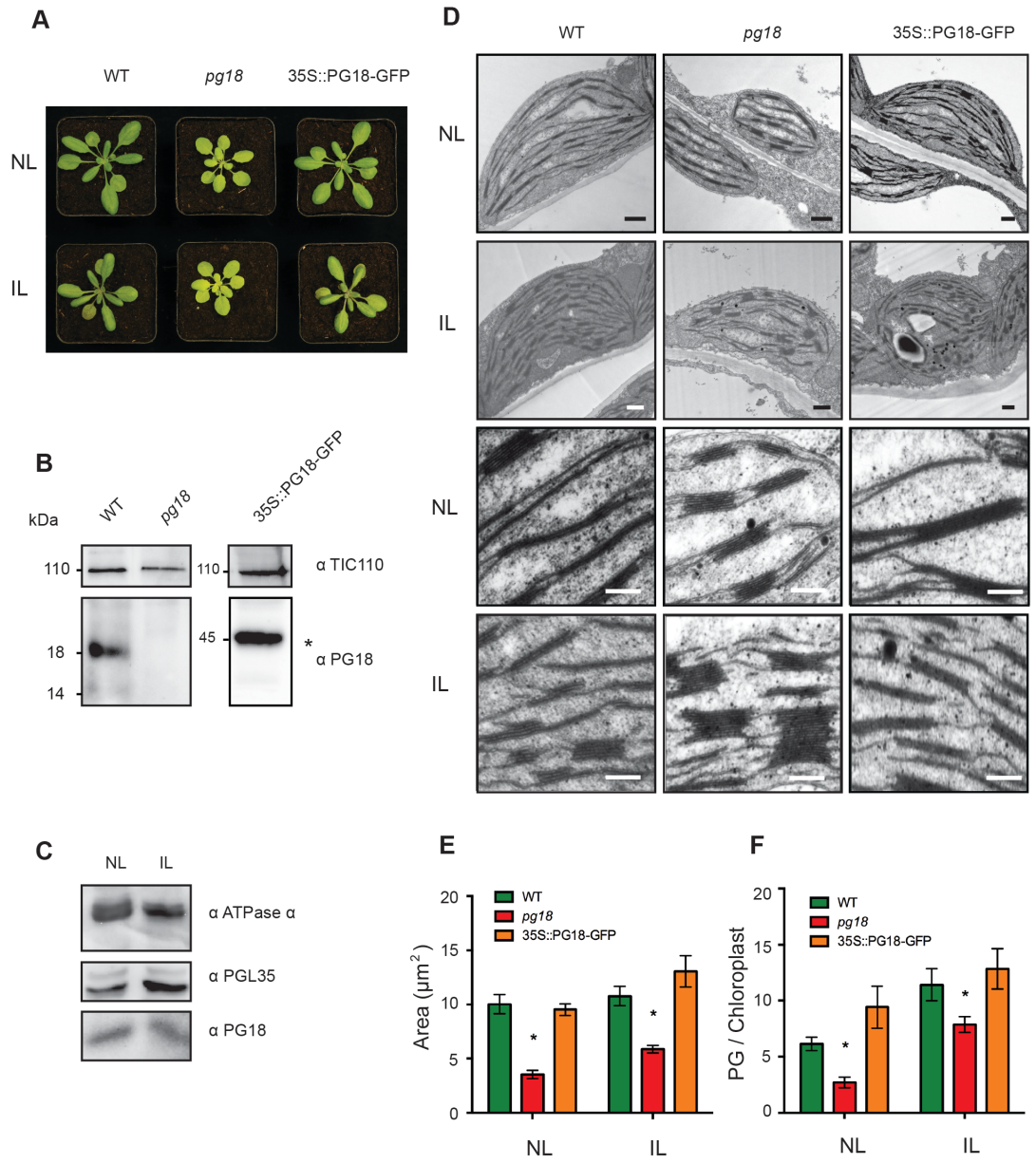


Figure 21. PG18 is required for normal development of *A. thaliana*. (A) WT, homozygous mutant (*pg18*) and complemented mutant plants (35S::PG18-GFP) were grown in long-day conditions for three weeks (normal light, NL) and for 17.5 days under 120 $\mu\text{mol photons m}^{-2} \text{s}^{-1}$ followed by 3.5 days under 250 $\mu\text{mol photons m}^{-2} \text{s}^{-1}$ (increased light, IL). (B) Total protein extracts from WT and *pg18* mutant plants were gel-fractionated and immunoblots were prepared. The PG18 protein was detected with specific antibodies. TIC110, a protein found in the inner envelope of the chloroplast was used as a loading control. The immunolabeled PG18-GFP is highlighted with an asterisk. (C) Total protein was extracted from plants grown under NL and IL conditions, and subjected to immunoblot analysis. The PG18 protein was detected using the specific antibodies mentioned above. The alpha subunit of the chloroplast ATP synthase was used as a loading control. Antibodies against PGL35 were used to show PG accumulation under IL relative to NL conditions. (D) Plants were grown in long-day conditions for three weeks under NL and IL as explained in (A), and the leaves were excised for electron microscopy. Scale bars represent 500 nm. Thylakoid ultrastructure zooms in plants grown on the panels below under NL or IL conditions. The scale bar corresponds to 200 nm. Pictures taken by Prof Andreas Klingl. (E) Quantification of chloroplast area (in μm^2). The bars represent standard error (SEM) and asterisks represent significant differences ($P < 0.05$) in comparison to the WT (Student's t-test). (F) Numbers of PGs per chloroplast. The bars represent the standard error (SEM) and asterisks represent significant differences ($P < 0.05$) relative to the WT based on the t-test.

3.2.3 *Arabidopsis pg18* mutant plants show symptoms of light stress

To assess differences in thylakoid pigments that might be related to the mutant phenotype, the pigment content of *pg18* leaves was analyzed. Chlorophylls *a* and *b* were indeed reduced in the mutant, in agreement with its pale green phenotype (20% and 36% reduction for chlorophylls *b* and *a* respectively); however, only the difference in chlorophyll *a* relative to the WT was significant (Figure 22A).

Analysis of carotenoid content revealed that β -carotene was significantly reduced in the *pg18* mutant compared to WT, irrespective of the lighting conditions during growth. In particular, the level of the protective carotenoid lutein was reduced in the mutant under IL conditions, whereas the neoxanthin content remained unchanged (Figure 22B). Further pigments related to photoprotection, specifically constituents of the xanthophyll cycle, were also analyzed. In WT plants under NL conditions, violaxanthin (Vx), which binds to light-harvesting complexes (LHCs), is by far the most abundant of these, but upon light stress this compound undergoes two de-

epoxidation steps to produce the intermediate antheraxanthin (Ax) and finally zeaxanthin (Zx). On the return of NL, this process is reversed, with epoxidation of Zx regenerating Vx. Interestingly, antheraxanthin (Ax) and zeaxanthin (Zx) levels were clearly increased in the mutant, suggesting a light stress response, although the pool of xanthophyll cycle pigments as a whole (the VAZ pool) was not markedly altered, except under IL conditions, where the mutant *pg18* showed a higher overall pigment content (Figure 22C). However, the ratio of the xanthophyll intermediates, which takes the de-epoxidation reactions into account reveals that both lighting conditions are associated with significantly higher levels of de-epoxidation in the *pg18* mutant than in WT (Figure 22C), suggesting that the mutant is more susceptible to light stress.

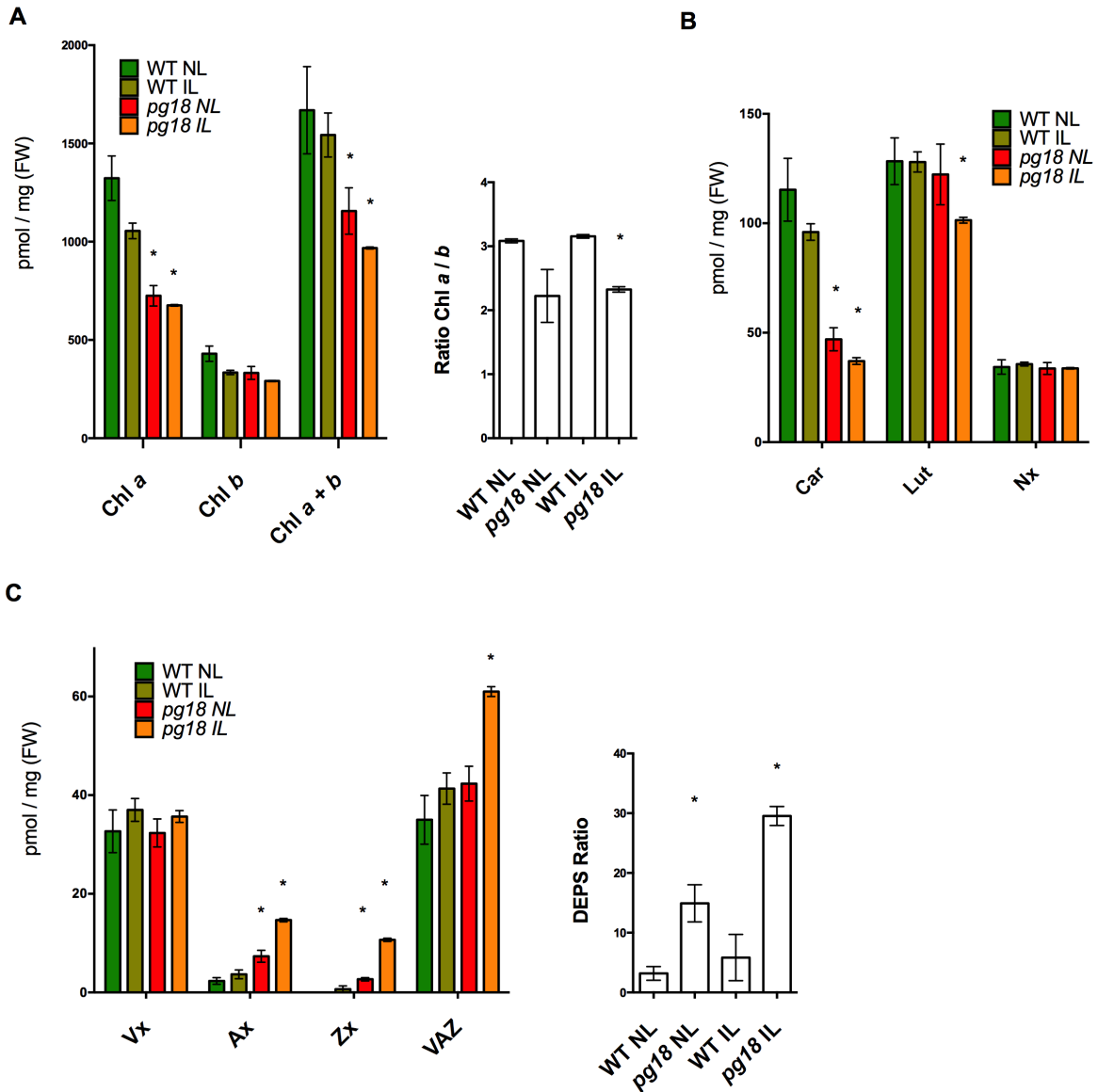


Figure 22. Pigment analysis of WT and *pg18* mutants. Pigments were isolated from 3-week-old *Arabidopsis* plants grown on a long-day photoperiod under NL and IL conditions. **(A)** Chlorophyll content was measured from plants grown under NL and IL conditions. Chlorophyll *a* and *b* levels were measured and the sum of the two is also represented. The ratio of chlorophyll *a* to Chl *b* is shown on the right. **(B)** Carotenoid content measured from plants grown under NL and IL conditions. The pigments analysed correspond to β -carotene (Car), lutein (Lu) and neoxanthin (Nx). **(C)** Xanthophyll content and de-epoxidation state (DEPS) of plants grown under NL and IL conditions. The pigments measured were violaxanthin (Vx), antheraxanthin (Ax) and zeaxanthin (Zx). VAZ represents their sum. The DEPS ratios (on the right) were calculated using the following formula: $(Zx + 0.5 * Ax) / (Vx + Ax + Zx) * 100$. Values on the Y-axis represent pmol per mg fresh weight (FW) of leaves. Asterisks represent significant differences ($P < 0.05$) in comparison to the WT based on the t-test. Error bars correspond to SEMs. Analyses performed by Dr Peter Jahns.

3.2.4 Photosynthetic performance is affected in *pg18* mutant plants

Since the ultrastructure of the chloroplast is altered in *pg18* mutant plants, their photosynthetic performance was analyzed by measuring the quantum yields of both photosystems in 3-week-old plants grown under NL and IL conditions using a pulse-amplitude modulated (PAM) fluorimeter. Both parameters are reduced in the *pg18* mutant, especially under high light intensities (Figure 23A and 23B). Moreover, the electron transport rate (ETR) was dramatically reduced by more than threefold in NL and about fivefold in IL in the mutant compared to the WT, which is an indication of much less efficient electron transport from PSII to PSI (Figure 23C). Interestingly, however, levels of nonphotochemical quenching (NPQ) in the *pg18* mutant were twice as high as in the WT, which is a symptom of light stress (Figure 23D).

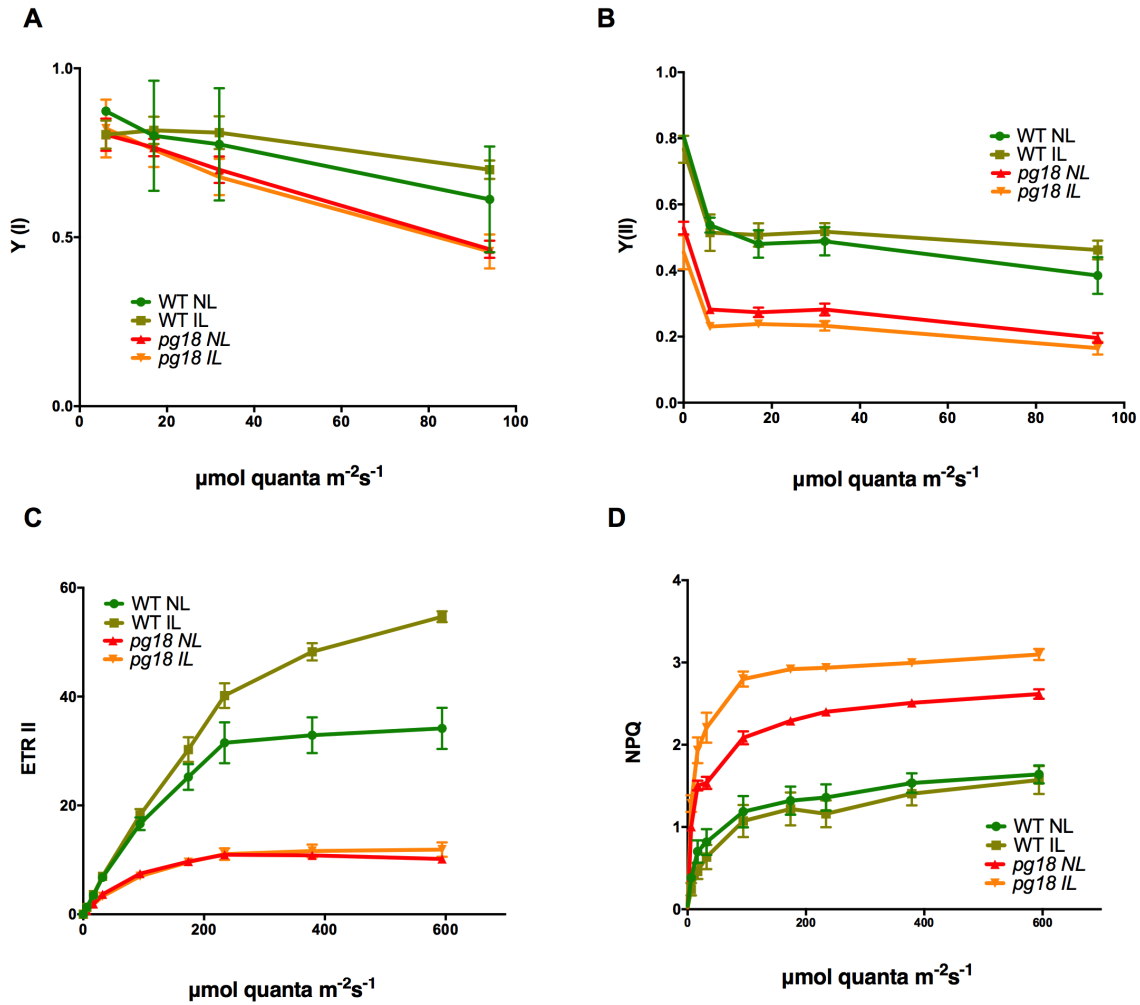


Figure 23. Loss of PG18 affects photosynthetic performance. *Arabidopsis* plants (3 weeks old) grown under NL and IL conditions were subjected to chlorophyll fluorescence analysis. **(A)** Quantum yields of photosystem I, Y(I). **(B)** Quantum yield of photosystem II, Y(II). **(C)** Electron transport rate (ETR) in $\mu\text{mol electrons m}^{-2}\text{s}^{-1}$. **(D)** Non-photochemical quenching (NPQ). Data represent mean values (\pm SEM), $n=3$.

Since the differences between WT and *pg18* plants follow the same trend regardless of whether they are grown and evaluated under NL or IL conditions their recovery from photo-inhibition of PSII was analyzed by measuring their Fv / Fm values. Interestingly, the degree of photo-inhibition after a 2-h exposure to 1000 $\mu\text{E m}^2 \text{s}^{-1}$ was the same for WT and *pg18* plants coming from NL as well for IL conditions. Likewise, their Fv / Fm values recovered with the same kinetics on return to normal light levels (Figure 24A). This indicates again that PSII is equally susceptible to photo-damage in both lines. Additionally, the translation efficiency was assessed to discard any effect on biogenesis of the different subunits of the photosynthetic complexes. *In-vivo* translation was performed by infiltrating young WT and mutant *pg18* plants with methionine ^{35}S and then incubating it for 20 min. Afterwards, thylakoids were isolated, and the photosynthetic complexes were separated in a Blue native gel. In line with the recovery experiment results, the translation rate for WT and *pg18* mutant did not show high differences indicating that the defects in photosynthetic parameters could come from the accumulation of the complexes (Figure 24B). Since the effect on ETR or low quantum yield for both photosystems might relate to stoichiometry or assembly of the different complexes in the thylakoid membrane, they were considered to be investigated in more detail.

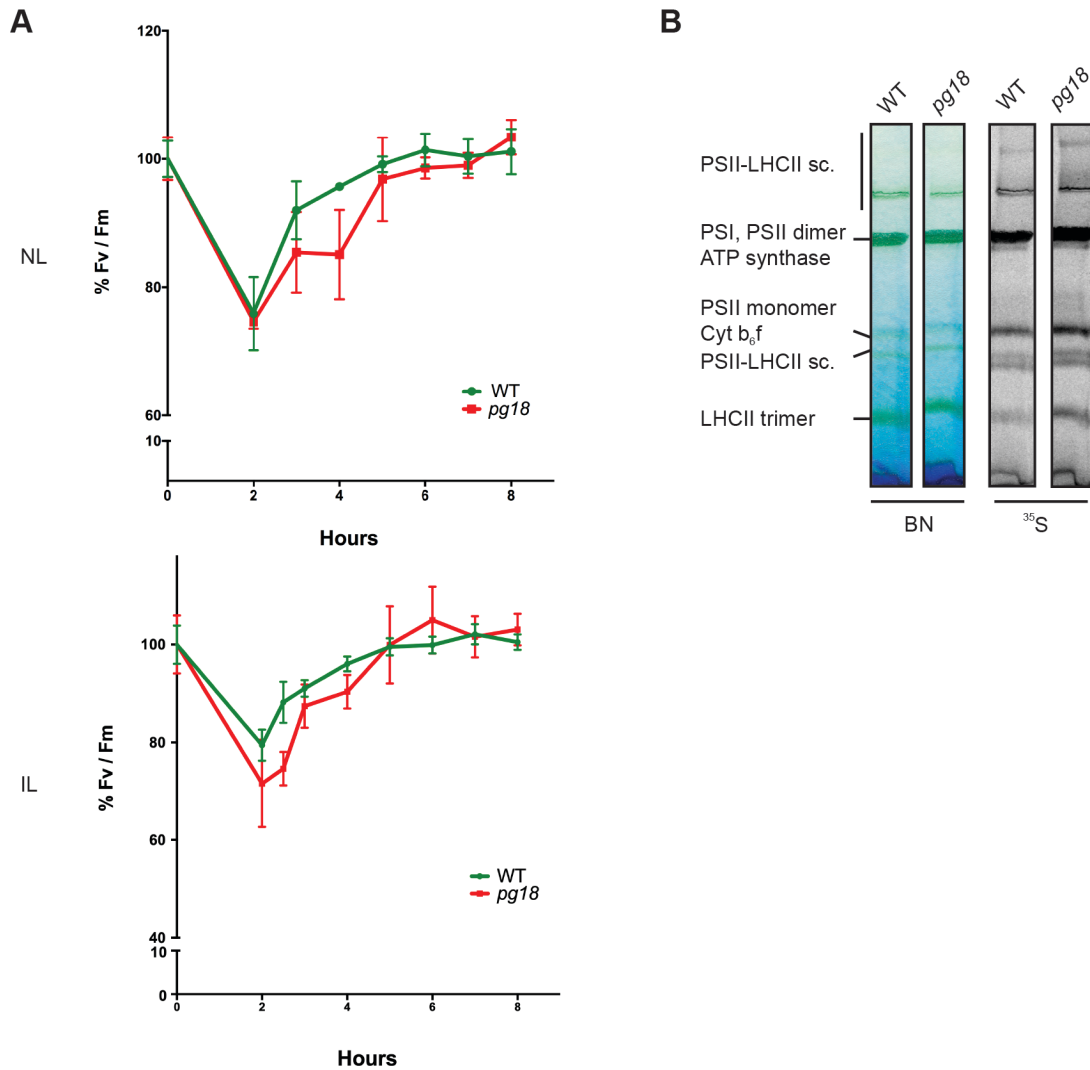


Figure 24. Loss of PG18 does not alter thylakoid complexes biogenesis and repair. (A) Arabidopsis plants of 3 weeks old grown under normal light (NL) and increased light (IL) were exposed to intense light ($1000 \mu\text{E m}^{-2} \text{s}^{-1}$) for two hours and recovery was performed under $30 \mu\text{E m}^{-2} \text{s}^{-1}$. PAM measurements were done in order to monitor the status of PSII of WT and the mutant plants of PG18 (*pg18*). Fv / Fm was 0.84 for WT and 0.58 for *pg18*. Values for Fv / Fm are represented as percentage and the error bars correspond to SEM. **(B)** WT and mutant *pg18* seeds were sowed on MS medium with 1% sugar for 4 weeks. Seedlings were taken and infiltrated with radiolabelled methionine ^{35}S and thylakoid were isolated to run Blue native gel. The gel was then exposed to a phosphoimaging screen to visualize the labelled proteins.

3.2.5 Loss of PG18 has an impact on the accumulation of thylakoid membrane complexes

In order to monitor abundance of the thylakoid membrane proteins in WT and *pg18*, immunoblot analysis was performed with antisera against subunits of the photosystems, the ATP synthase as well as the cytochrome *b₆f* complex. The results revealed that components of the ATP synthase (ATPase α and ATPase γ) as well as for the subunits of PSI PsaG, PsaD, PsaF and Lhca2 were reduced to approx. 70% of WT levels (Figure 25A). Moreover, mutant levels of Cyt *f* did not show differences compared to WT as well as for subunits of PSII except for LHCbII, which was surprisingly increased by 20%. To analyze the assembly status of thylakoid complexes, thylakoid membranes were solubilized with 1% β -dodecylmaltoside and separated in Blue native gels (BN) followed by a second dimension of SDS-PAGE. In accordance with the immunoblot results, the mutant *pg18* showed higher accumulation of LHCbs compared to WT and a slight reduction of ATP synthase and PSI subunits (Figure 25C).

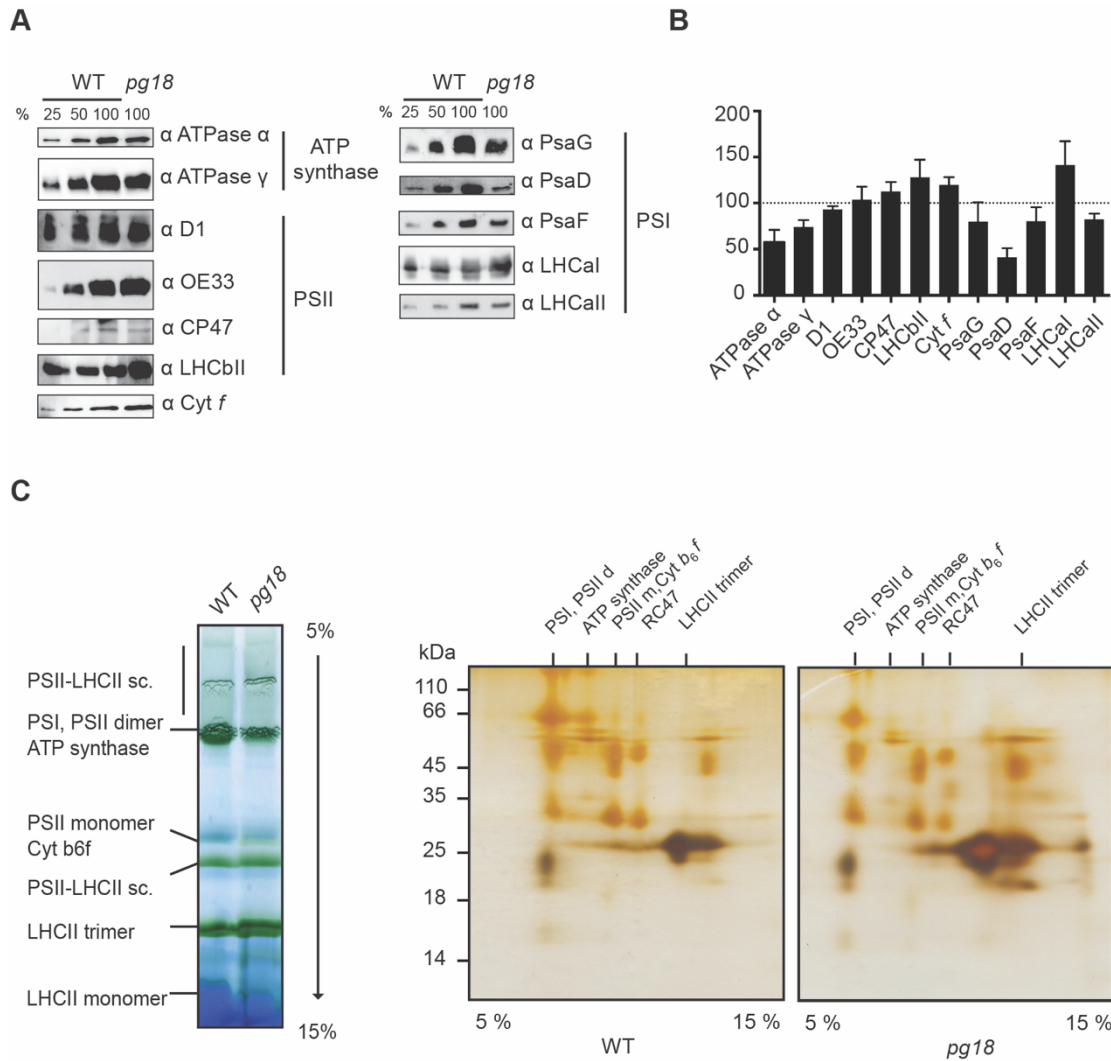


Figure 25. Loss of PG18 has an impact on the accumulation of thylakoid membrane complexes. (A) Thylakoids were isolated from plants grown on soil of three weeks old under long day conditions. Proteins in the thylakoid membranes were immunodetected by using antibodies against subunits of PSI, PSII, ATP synthase and the Cyt *b₆f* complex. Loading of 100% corresponds to 20 μ g protein and the same amount was loaded for the mutant. **(B)** Immunoblotting quantification using ImageJ. Each column represents percentage in relation to WT with mean value of three replicates for each case and the error bars represent SEM with $n = 3$. **(C)** Thylakoid membranes were isolated from *Arabidopsis* plants grown on MS sugar plates, and then solubilized with 1% (w/v) DM. BN-PAGE (left panel) was followed by separation of protein complexes in the second dimension by SDS/PAGE and silver staining (right panel).

4 Discussion

With the development of molecular biology techniques, there has been a rapid advance in gaining knowledge about the chemistry and the biology of photosynthesis. The last years have seen the development of techniques such as X-ray emission spectroscopy to understand the very steps that electrons follow when water is split by PSII (Gul *et al.*, 2015). In spite of the deep knowledge that has been collected around the photosynthetic complexes, undoubtedly there is still a lot to discover since mimicking photosynthesis has turned out to be very challenging (Rutherford & Moore, 2008). Furthermore, the biosynthesis of various complexes are quite different from one organism to another showing that despite their common principle they differ dramatically in assembly and therefore compatibility (Nickelsen & Rengstl, 2013). For instance, recently has been elucidated that a thylakoid region in cyanobacteria could be dedicated for PSII biogenesis and assembly (Nickelsen & Zerges, 2013). Additionally, in higher plants it has been identified that for the biosynthesis and assembly of the thylakoid complexes alone there are multiple nuclear encoded proteins required (Chi *et al.*, 2012; Schottler *et al.*, 2011; Schottler *et al.*, 2015). However, the focus over the past years has been on the protein level of the complexes neglecting how important the actual organization of these are and how they become organized and segregated in different portions of the thylakoid membranes. Attempts to understand the processes that are not just involved protein complexes assembly but also in the biogenesis of thylakoids as a whole have started with the observation of vesicles (Westphal *et al.*, 2001). In line with this idea, *in-silico* analyses have been done in order to identify candidates with homology to proteins known to participate in vesicle trafficking (Khan *et al.*, 2013). Unfortunately, there is still no protein clearly identified which plays a role specifically in vesicle trafficking inside the chloroplast making the process even more difficult to tackle. Whether or not vesicles play a role in the biogenesis of thylakoids, there are still unknown processes that require other ways to be approached for they thorough understanding.

4.1 RV-1

The unknown protein named RV-1 was successfully localized to chloroplasts and its mature form was identified by import experiments. Despite of not having close homologs with known domains, RV-1 is conserved in higher plants highlighting its relevance. Other green lineages like mosses and algae present distant homologs to RV-1 but not to RV-1-like. This suggests that in those lineages RV-1 might be dual targeted to chloroplast and mitochondria. When analyzing the mutant *rv-1* lines, the seedling lethal phenotype observed revealed its fundamental role in chloroplast biogenesis. In addition of not being able to produce seeds, homozygous *rv-1* plants were pale and present aberrant chloroplast morphology which indicates that the loss of RV-1 might be affecting a very initial step in chloroplast biogenesis. The lethal phenotype of homozygous *rv-1* plants was very surprising, taking into account that its paralog is as conserved as RV-1 is and therefore functional redundancy was initially expected. Interestingly, however, the cellular localization of RV-1-like showed that it is localized in the mitochondria. This observation revealed that probably *RV-1* and *RV-1-like* are derived from an ancestral gene which got duplicated and evolutionary distributed into both organelles. The absence of homologs in cyanobacteria or even non-photosynthetic prokaryotes posed the question about their ancestry from a conserved gene in endosymbiotic organisms or from a horizontal gene transfer followed by duplication. Furthermore, the *rv-1-like* mutant line also showed that RV-1-like might play a fundamental role in plant physiology since mutant siliques exhibited embryos abortion which is a typical phenotype for genes essential for plant mitochondria (Leon *et al.*, 2007; Yamaoka & Leaver, 2008). Thus, these observations suggest that both paralogs might have similar functions that are essential and shared between chloroplast and mitochondria.

In order to provide insights on the function of RV-1 which turned out to be essential for chloroplast biogenesis, the drastic reduction on plastid rRNAs exhibited by the *rv-1* mutant was investigated in detail. Since proteins like PAC known to participate in plastid rRNA maturation also present a similar phenotype with reduction or absence of processed rRNA (Meurer *et al.*, 2017), the distant homology of RV-1 to

an RNase E from rice was taken into account. RNase E proteins were first identified in *E. coli* playing a role in the processing of 5S rRNA (Ghora & Apirion, 1978). Later it was found that this family of proteins play similar role in other organisms such as *Arabidopsis* and *Synechocystis* (Horie *et al.*, 2007; Mudd *et al.*, 2008). It is known that RNase E proteins play a role not just in the maturation of RNA but also in the degradation of mRNA (Carpousis, 2007; Carpousis *et al.*, 2009). Thus, the putative RNase E activity of RV-1 was assessed with the unmaturation of plastid rRNAs namely 16S and 23S. However, no RNase activity was observed even when using total RNA extracted from young plants. Therefore, the ability to bind rRNA was tested again using as targets the plastid 16S and 23S rRNAs. EMSA analyses revealed that RV-1 does not have the ability to bind to any of these two rRNAs, whereas the protein PAC binds specifically 23S.

Moreover, RV-1 has a distant homology to RelA and SpoT proteins (RSHs). These proteins were characterized to cause inhibition of stable RNA accumulation provoked by amino acid starvation in *E. coli* (Cashel & Gallant, 1969). In prokaryotes it has been shown that RelA is responsible for the accumulation of the (p)ppGpp which causes failure of stable RNA accumulation (Alfoldi *et al.*, 1962; Potrykus & Cashel, 2008). Later it was shown that a RelA homolog SpoT was able to synthesize and degrade (p)ppGpp (Battesti & Bouveret, 2006; Seyfzadeh *et al.*, 1993). In *Arabidopsis*, RSHs have been already identified playing a role in chloroplast function and gene expression (Sugliani *et al.*, 2016). However, similar to the effect of (p)ppGpp in translation (English *et al.*, 2011), *rv-1* mutant seedling exhibited drastic reduction in *de-novo* translation of proteins. Furthermore, it has been shown that (p)ppGpp inhibits the activity of chloroplast translation *in-vitro* which could give a hint on RV-1 putative function (Nomura *et al.*, 2012). However, the distant homology to the RelA/Spot domain and the absence of homology to other RSH proteins makes the relation of RV-1 with RelA/Spot probably more evolutive than functional.

Since RV-1 could neither bind or process any of the plastid rRNA, it was hypothesized that it could bind to the ribosomes. The *rv-1* mutant plants showed absence of plastid ribosome proteins posing the question whether RV-1 could be related to the stability or assembly of these ribosomes. Surprisingly, experiments

performed by treating stroma with and without RNase shifted the distribution of RV-1 in a sucrose gradient separation which was also observed for one subunit of the plastid ribosome. This might imply that RV-1 could bind ribosomes similar to proteins such as PAC. In order to validate this hypothesis, RNA sequencing of pulled down RV-1 might provide its targets. Additionally, since the transit peptide of RV-1 is already known it could be assessed the chloroplast localization of the paralog RV-1-like protein and test its ability to rescue the *rv-1* mutant phenotype. Thus, the successful complementation of *rv-1* mutant by chloroplast *RV-1-like* could demonstrate their functional homology in chloroplast and plant mitochondria.

4.2 PG18

Several lines of evidence indicate that PGs play an important role in thylakoid development. Their number decreases during de-etiolation, while mutants with defects in thylakoid formation often accumulate larger numbers of PGs (Babiychuk *et al.*, 2008; Kroll *et al.*, 2001). Their function may consist in providing metabolites, such as carotenoids and prenylquinones. Additionally, they may be responsible for providing triglycerides for membrane lipid synthesis.

The protein with unknown domain identity named PG18 was investigated for its role in chloroplast biogenesis. PG18 is a protein of unknown function that was identified in PGs of higher plants by mass spectrometry (Lundquist *et al.*, 2012). With the help of a PG18-specific antiserum, it was confirmed that PG18 is indeed localized to PGs. Surprisingly, despite the absence of obvious hydrophobic regions in its sequence, PG18 behaves as a membrane protein. A previous study on the fibrillin PGL34, which likewise does not contain typical transmembrane domains, revealed that most deletion variants tested failed to localize to PGs when transiently expressed as GFP fusions (Vidi *et al.*, 2006). This suggests that the association of PG proteins with the PG monolayer might rely on their folded conformation rather than a particular hydrophobic domain.

The characterization of a loss-of-function mutant of PG18 clearly demonstrates that the lack of this protein has a severe impact on plant fitness throughout development. Mutant plants show a light green phenotype and are smaller than WT. Since PGs

have been shown to accumulate under light stress (Zhang *et al.*, 2010), it was assessed whether the mutant line exhibits a stronger phenotype under such conditions. Mutants for other PG proteins typically show enhanced phenotypes when subjected to light stress (Fatihi *et al.*, 2015; Porfirova *et al.*, 2002; Youssef *et al.*, 2010). However, the phenotype of *pg18* remained essentially the same under NL and IL conditions. This indicates that PG18 plays a more general role in chloroplast biogenesis. This notion is supported by the fact that *pg18* plants have smaller chloroplasts and fewer PGs per chloroplast than WT. Interestingly, the number of PGs was increased under IL conditions in both WT and *pg18* chloroplasts, although the latter always contained fewer PGs per chloroplast. This indicates that PG18 is not involved in promoting PG accumulation under light stress.

The pale green leaves of *pg18* plants point to a reduction in chlorophyll content. This assumption was verified by analyzing the chlorophyll content of leaves from plants grown under NL and IL conditions, and the most significant reduction was noted in chlorophyll *a*. The carotenoid fraction revealed a strong reduction in β -carotene in the *pg18* mutant compared to WT under both NL and IL conditions, whereas the reduction in lutein was statistically significant only under IL. PGs are known to play a role in carotenoid accumulation, for example in the chromoplasts of fruits and flowers (Steinmuller & Tevini, 1985), which are enriched in biosynthetic enzymes such as zeaxanthin epoxidase (ZDS) and lycopene- β cyclase (LYC- β) (van Wijk & Kessler, 2017). Therefore, a reduction in carotenoid content could be a reflection of PG dysfunction linked to changes in the activity of such enzymes.

Analysis of the pigments of the xanthophyll cycle in the *pg18* mutant showed that levels of the photoprotective pigments Ax and Zx were increased relative to WT, and further enhanced under IL conditions. These pigments are synthesized from Vx under light stress and serve as photoprotectants for PSII, binding to its LHC proteins and contributing to energy dissipation as heat (nonphotochemical quenching; NPQ) (Gilmore *et al.*, 1995). Thus, *pg18* mutant plants show symptoms of light stress even under normal light conditions, which probably explains the accumulation of larger grana stacks in their chloroplasts.

Chlorophyll fluorescence analyses showed that photosynthetic performance in general was affected, with both photosystems showing lower quantum yields than WT, and these deficits became more pronounced under increased light intensities. Taking into account the fact that levels of ATP synthase and PSI were reduced in the mutant plants, the reduction observed in ETR can be explained by an early saturation of the electron transport chain, since the Δ pH cannot be fully relaxed. Therefore, the early reduction and saturation of PSII and PSI might cause damage, which could also explain a further reduction in the abundances of both photosystems (Gilmore *et al.*, 1995). In accordance with an expected rise in lumen pH, NPQ levels were higher in the mutant than in the WT, which dissipates energy mainly from PSII (Horton *et al.*, 1996). This observation correlates with the high levels of Zx and Ax found in the mutant plants relative to WT. These pigments are known to modulate NPQ by deactivating excited states in the PSII antenna, and also acting as antioxidants in the thylakoid membrane (Havaux & Niyogi, 1999; Nilkens *et al.*, 2010). Complementation of the mutant line rescued both the photosynthetic activity and reduced pigment accumulation to WT levels (data not shown).

Moreover, to investigate the light sensitivity of PSII and the ability to repair it via *de novo* synthesis and incorporation of D1 under IL conditions, a light stress recovery analysis was performed. Strikingly, both WT and *pg18* were equally affected by light stress and both showed the same ability to recover. Thus, the pleiotropic effects on photosynthetic performance in *pg18* chloroplasts probably do not result from a PSII that is more sensitive to light, but rather from initial assembly defects or altered stoichiometry of the photosynthetic complexes. In line with this, analysis of the accumulation of thylakoid proteins revealed a reduction in the ATP synthase and PSI complexes. Concordantly with the reduction in PSI, levels of chlorophyll *a* were sharply reduced in the *pg18* mutant compared to the WT, which is also reflected in the fact that the ratio of chlorophyll *a* to *b* remains essentially the same under NL and IL conditions. Furthermore, our finding that the stroma lamellae are shorter and less branched in the *pg18* mutant than in WT correlates with the reduction in levels of PSI and ATP synthase, as less membrane area is available for their integration. Furthermore, the overall assembly of the complexes in the thylakoid membrane is

affected in the mutant *pg18*. Interestingly, there is a clear accumulation of LHC proteins in the mutant line which is compatible with the fact that *pg18* plants accumulate more photoprotective LHC-binding pigments like Zx (Johnson *et al.*, 2007). This effect can also be seen in the high level of NPQ seen in the *pg18* mutant, which is further enhanced under IL, in accordance with the increased levels of Zx in the mutant relative to WT under both NL and IL conditions. Hence, PG18 seems not to intervene in the assembly of any particular complex in the thylakoid membrane, but affects the composition of some of them, possibly by modulating the structural organization of the thylakoid membrane during its biogenesis.

Despite the lack of identifiable functional domains, which suggests that PG18 is not itself an enzyme, loss of PG18 has a significant impact on the composition and architecture of the thylakoid membrane. In light of the indications that PGs play an important role in mobilizing lipids for incorporation into the thylakoid membrane (Deruere, Romer, *et al.*, 1994; Simkin *et al.*, 2007), an alteration in PGs could be expected to affect thylakoid complexes, as has been observed when the lipid content of the thylakoid membrane is altered (Kansy *et al.*, 2014; Zhou *et al.*, 2009). Levels of the PG18 protein were not found to be specifically upregulated under stress conditions, nor does it accumulate to a greater extent in PGs isolated after high light treatment (Ytterberg *et al.*, 2006). These findings indicate that it is a constitutive component of PGs, possibly fulfilling a general role in PG maintenance or interacting with other PG proteins. This inference is supported by the observation that knockout mutants for other PG proteins do not show a phenotype under normal conditions. Phenotypes only become manifest when PG mutants are exposed to stresses, such as high light intensities (Avendano-Vazquez *et al.*, 2014; Fatihi *et al.*, 2015; Martinis *et al.*, 2013; Porfirova *et al.*, 2002; Singh *et al.*, 2010; Youssef *et al.*, 2010). Moreover, PG18 was also found in chromoplasts of red pepper (Ytterberg *et al.*, 2006), also suggesting that its function is not restricted to chloroplasts. Interestingly however, PG18 is phosphorylated, which might lead to conformational changes or otherwise have an impact on its activity, possibly depending on different developmental stages or stress conditions (Wang *et al.*, 2013).

In summary, investigation of the *pg18* mutant underlines the importance of PGs in the formation of thylakoid membranes. Elucidating its exact role will be a challenging task to address in the future.

5 Literature

- Albiniak, A. M., Baglieri, J., & Robinson, C. (2012). Targeting of luminal proteins across the thylakoid membrane. *J Exp Bot*, 63(4), 1689-1698. doi:10.1093/jxb/err444
- Alfoldi, L., Stent, G. S., & Clowes, R. C. (1962). The chromosomal site of the RNA control (RC) locus in *Escherichia coli*. *J Mol Biol*, 5, 348-355.
- Altschul, S. F., Madden, T. L., Schaffer, A. A., Zhang, J., Zhang, Z., Miller, W., & Lipman, D. J. (1997). Gapped BLAST and PSI-BLAST: a new generation of protein database search programs. *Nucleic Acids Res*, 25(17), 3389-3402.
- Aro, E. M., McCaffery, S., & Anderson, J. M. (1993). Photoinhibition and D1 Protein Degradation in Peas Acclimated to Different Growth Irradiances. *Plant Physiol*, 103(3), 835-843.
- Austin, J. R., 2nd, Frost, E., Vidi, P. A., Kessler, F., & Staehelin, L. A. (2006). Plastoglobules are lipoprotein subcompartments of the chloroplast that are permanently coupled to thylakoid membranes and contain biosynthetic enzymes. *Plant Cell*, 18(7), 1693-1703. doi:10.1105/tpc.105.039859
- Avendano-Vazquez, A. O., Cordoba, E., Llamas, E., San Roman, C., Nisar, N., De la Torre, S., . . . Leon, P. (2014). An Uncharacterized Apocarotenoid-Derived Signal Generated in zeta-Carotene Desaturase Mutants Regulates Leaf Development and the Expression of Chloroplast and Nuclear Genes in *Arabidopsis*. *Plant Cell*, 26(6), 2524-2537. doi:10.1105/tpc.114.123349
- Babiychuk, E., Bouvier-Nave, P., Compagnon, V., Suzuki, M., Muranaka, T., Van Montagu, M., . . . Schaller, H. (2008). Allelic mutant series reveal distinct functions for *Arabidopsis* cycloartenol synthase 1 in cell viability and plastid biogenesis. *Proc Natl Acad Sci U S A*, 105(8), 3163-3168. doi:10.1073/pnas.0712190105
- Balsera, M., Goetze, T. A., Kovacs-Bogdan, E., Schurmann, P., Wagner, R., Buchanan, B. B., . . . Bolter, B. (2009). Characterization of Tic110, a channel-forming protein at the inner envelope membrane of chloroplasts, unveils a response to Ca(2+) and a stromal regulatory disulfide bridge. *J Biol Chem*, 284(5), 2603-2616. doi:10.1074/jbc.M807134200
- Barsan, C., Zouine, M., Maza, E., Bian, W., Egea, I., Rossignol, M., . . . Pech, J. C. (2012). Proteomic analysis of chloroplast-to-chromoplast transition in tomato reveals metabolic shifts coupled with disrupted thylakoid biogenesis machinery and elevated energy-production components. *Plant Physiol*, 160(2), 708-725. doi:10.1104/pp.112.203679
- Bartsch, S., Monnet, J., Selbach, K., Quigley, F., Gray, J., von Wettstein, D., . . . Reinbothe, C. (2008). Three thioredoxin targets in the inner envelope membrane of chloroplasts function in protein import and chlorophyll metabolism. *Proc Natl Acad Sci U S A*, 105(12), 4933-4938. doi:10.1073/pnas.0800378105
- Battesti, A., & Bouveret, E. (2006). Acyl carrier protein/SpoT interaction, the switch linking SpoT-dependent stress response to fatty acid metabolism. *Mol Microbiol*, 62(4), 1048-1063. doi:10.1111/j.1365-2958.2006.05442.x

- Benning, C., Xu, C., & Awai, K. (2006). Non-vesicular and vesicular lipid trafficking involving plastids. *Curr Opin Plant Biol*, 9(3), 241-247. doi:10.1016/j.pbi.2006.03.012
- Benz, J. P., Stengel, A., Lintala, M., Lee, Y. H., Weber, A., Philippar, K., . . . Bolter, B. (2009). Arabidopsis Tic62 and ferredoxin-NADP(H) oxidoreductase form light-regulated complexes that are integrated into the chloroplast redox poise. *Plant Cell*, 21(12), 3965-3983. doi:10.1105/tpc.109.069815
- Bhuiyan, N. H., Friso, G., Poliakov, A., Ponnala, L., & van Wijk, K. J. (2015). MET1 is a thylakoid-associated TPR protein involved in photosystem II supercomplex formation and repair in Arabidopsis. *Plant Cell*, 27(1), 262-285. doi:10.1105/tpc.114.132787
- Bieri, P., Leibundgut, M., Saurer, M., Boehringer, D., & Ban, N. (2017). The complete structure of the chloroplast 70S ribosome in complex with translation factor pY. *EMBO J*, 36(4), 475-486. doi:10.15252/embj.201695959
- Brasier, M. D., Antcliffe, J., Saunders, M., & Wacey, D. (2015). Changing the picture of Earth's earliest fossils (3.5-1.9 Ga) with new approaches and new discoveries. *Proc Natl Acad Sci U S A*, 112(16), 4859-4864. doi:10.1073/pnas.1405338111
- Cardona, T. (2018). Early Archean origin of heterodimeric Photosystem I. *Heliyon*, 4(3), e00548. doi:10.1016/j.heliyon.2018.e00548
- Carpousis, A. J. (2007). The RNA degradosome of Escherichia coli: an mRNA-degrading machine assembled on RNase E. *Annu Rev Microbiol*, 61, 71-87. doi:10.1146/annurev.micro.61.080706.093440
- Carpousis, A. J., Luisi, B. F., & McDowall, K. J. (2009). Endonucleolytic initiation of mRNA decay in Escherichia coli. *Prog Mol Biol Transl Sci*, 85, 91-135. doi:10.1016/S0079-6603(08)00803-9
- Cashel, M., & Gallant, J. (1969). Two compounds implicated in the function of the RC gene of Escherichia coli. *Nature*, 221(5183), 838-841.
- Chaal, B. K., Mould, R. M., Barbrook, A. C., Gray, J. C., & Howe, C. J. (1998). Characterization of a cDNA encoding the thylakoidal processing peptidase from Arabidopsis thaliana. Implications for the origin and catalytic mechanism of the enzyme. *J Biol Chem*, 273(2), 689-692.
- Chan, K. X., Phua, S. Y., Crisp, P., McQuinn, R., & Pogson, B. J. (2016). Learning the Languages of the Chloroplast: Retrograde Signaling and Beyond. *Annu Rev Plant Biol*, 67, 25-53. doi:10.1146/annurev-arplant-043015-111854
- Chi, W., Ma, J., & Zhang, L. (2012). Regulatory factors for the assembly of thylakoid membrane protein complexes. *Philos Trans R Soc Lond B Biol Sci*, 367(1608), 3420-3429. doi:10.1098/rstb.2012.0065
- Chigri, F., Hormann, F., Stamp, A., Stammers, D. K., Bolter, B., Soll, J., & Vothknecht, U. C. (2006). Calcium regulation of chloroplast protein translocation is mediated by calmodulin binding to Tic32. *Proc Natl Acad Sci U S A*, 103(43), 16051-16056. doi:10.1073/pnas.0607150103
- Chou, M. L., Chu, C. C., Chen, L. J., Akita, M., & Li, H. M. (2006). Stimulation of transit-peptide release and ATP hydrolysis by a cochaperone during protein import into chloroplasts. *J Cell Biol*, 175(6), 893-900. doi:10.1083/jcb.200609172
- Cunningham, F. X., Jr., Tice, A. B., Pham, C., & Gantt, E. (2010). Inactivation of genes encoding plastoglobuli-like proteins in Synechocystis sp. PCC 6803 leads to a

- light-sensitive phenotype. *J Bacteriol*, 192(6), 1700-1709. doi:10.1128/JB.01434-09
- Danielsson, R., Albertsson, P. A., Mamedov, F., & Styring, S. (2004). Quantification of photosystem I and II in different parts of the thylakoid membrane from spinach. *Biochim Biophys Acta*, 1608(1), 53-61.
- De Marais, D. J. (2000). Evolution. When did photosynthesis emerge on Earth? *Science*, 289(5485), 1703-1705.
- de Vries, J., & Archibald, J. M. (2017). Endosymbiosis: Did Plastids Evolve from a Freshwater Cyanobacterium? *Curr Biol*, 27(3), R103-R105. doi:10.1016/j.cub.2016.12.006
- Demarsy, E., Lakshmanan, A. M., & Kessler, F. (2014). Border control: selectivity of chloroplast protein import and regulation at the TOC-complex. *Front Plant Sci*, 5, 483. doi:10.3389/fpls.2014.00483
- Deruere, J., Bouvier, F., Steppuhn, J., Klein, A., Camara, B., & Kuntz, M. (1994). Structure and expression of two plant genes encoding chromoplast-specific proteins: occurrence of partially spliced transcripts. *Biochem Biophys Res Commun*, 199(3), 1144-1150. doi:10.1006/bbrc.1994.1350
- Deruere, J., Romer, S., d'Harlingue, A., Backhaus, R. A., Kuntz, M., & Camara, B. (1994). Fibril assembly and carotenoid overaccumulation in chromoplasts: a model for supramolecular lipoprotein structures. *Plant Cell*, 6(1), 119-133. doi:10.1105/tpc.6.1.119
- Douzery, E. J., Snell, E. A., Baptiste, E., Delsuc, F., & Philippe, H. (2004). The timing of eukaryotic evolution: does a relaxed molecular clock reconcile proteins and fossils? *Proc Natl Acad Sci U S A*, 101(43), 15386-15391. doi:10.1073/pnas.0403984101
- Dumas, L., Chazaux, M., Peltier, G., Johnson, X., & Alric, J. (2016). Cytochrome b 6 f function and localization, phosphorylation state of thylakoid membrane proteins and consequences on cyclic electron flow. *Photosynth Res*, 129(3), 307-320. doi:10.1007/s11220-016-0298-y
- Eckhardt, U., Grimm, B., & Hortensteiner, S. (2004). Recent advances in chlorophyll biosynthesis and breakdown in higher plants. *Plant Mol Biol*, 56(1), 1-14. doi:10.1007/s11103-004-2331-3
- Egea, I., Barsan, C., Bian, W., Purgatto, E., Latche, A., Chervin, C., . . . Pech, J. C. (2010). Chromoplast differentiation: current status and perspectives. *Plant Cell Physiol*, 51(10), 1601-1611. doi:10.1093/pcp/pcq136
- Emanuelsson, O., Nielsen, H., Brunak, S., & von Heijne, G. (2000). Predicting subcellular localization of proteins based on their N-terminal amino acid sequence. *J Mol Biol*, 300(4), 1005-1016. doi:10.1006/jmbi.2000.3903
- Emanuelsson, O., Nielsen, H., & von Heijne, G. (1999). ChloroP, a neural network-based method for predicting chloroplast transit peptides and their cleavage sites. *Protein Sci*, 8(5), 978-984. doi:10.1110/ps.8.5.978
- Enami, K., Ozawa, T., Motohashi, N., Nakamura, M., Tanaka, K., & Hanaoka, M. (2011). Plastid-to-nucleus retrograde signals are essential for the expression of nuclear starch biosynthesis genes during amyloplast differentiation in tobacco BY-2 cultured cells. *Plant Physiol*, 157(1), 518-530. doi:10.1104/pp.111.178897

- English, B. P., Hauryliuk, V., Sanamrad, A., Tankov, S., Dekker, N. H., & Elf, J. (2011). Single-molecule investigations of the stringent response machinery in living bacterial cells. *Proc Natl Acad Sci U S A*, *108*(31), E365-373. doi:10.1073/pnas.1102255108
- Farber, A., Young, A. J., Ruban, A. V., Horton, P., & Jahns, P. (1997). Dynamics of Xanthophyll-Cycle Activity in Different Antenna Subcomplexes in the Photosynthetic Membranes of Higher Plants (The Relationship between Zeaxanthin Conversion and Nonphotochemical Fluorescence Quenching). *Plant Physiol*, *115*(4), 1609-1618.
- Fatihi, A., Latimer, S., Schmollinger, S., Block, A., Dussault, P. H., Vermaas, W. F., ... Basset, G. J. (2015). A Dedicated Type II NADPH Dehydrogenase Performs the Penultimate Step in the Biosynthesis of Vitamin K1 in *Synechocystis* and *Arabidopsis*. *Plant Cell*, *27*(6), 1730-1741. doi:10.1105/tpc.15.00103
- Flores-Perez, U., & Jarvis, P. (2013). Molecular chaperone involvement in chloroplast protein import. *Biochim Biophys Acta*, *1833*(2), 332-340. doi:10.1016/j.bbamcr.2012.03.019
- Friso, G., Giacomelli, L., Ytterberg, A. J., Peltier, J. B., Rudella, A., Sun, Q., & Wijk, K. J. (2004). In-depth analysis of the thylakoid membrane proteome of *Arabidopsis thaliana* chloroplasts: new proteins, new functions, and a plastid proteome database. *Plant Cell*, *16*(2), 478-499. doi:10.1105/tpc.017814
- Froehlich, J. E., Benning, C., & Dormann, P. (2001). The digalactosyldiacylglycerol (DGDG) synthase DGD1 is inserted into the outer envelope membrane of chloroplasts in a manner independent of the general import pathway and does not depend on direct interaction with monogalactosyldiacylglycerol synthase for DGDG biosynthesis. *J Biol Chem*, *276*(34), 31806-31812. doi:10.1074/jbc.M104652200
- Gaude, N., Brehelin, C., Tischendorf, G., Kessler, F., & Dormann, P. (2007). Nitrogen deficiency in *Arabidopsis* affects galactolipid composition and gene expression and results in accumulation of fatty acid phytyl esters. *Plant J*, *49*(4), 729-739. doi:10.1111/j.1365-313X.2006.02992.x
- Ghora, B. K., & Apirion, D. (1978). Structural analysis and in vitro processing to p5 rRNA of a 9S RNA molecule isolated from an rne mutant of *E. coli*. *Cell*, *15*(3), 1055-1066.
- Gilmore, A. M., Hazlett, T. L., & Govindjee. (1995). Xanthophyll cycle-dependent quenching of photosystem II chlorophyll a fluorescence: formation of a quenching complex with a short fluorescence lifetime. *Proc Natl Acad Sci U S A*, *92*(6), 2273-2277.
- Greenwood, A. D., Leech, R. M., & Williams, J. P. (1963). The osmiophilic globules of chloroplasts: I. Osmiophilic globules as a normal component of chloroplasts and their isolation and composition in *Vicia faba* L. *Biochimica et Biophysica Acta*, *78*(1), 148-162. doi:doi.org/10.1016/0006-3002(63)91620-2
- Gross, J., & Bhattacharya, D. (2009). Reevaluating the evolution of the Toc and Tic protein translocons. *Trends Plant Sci*, *14*(1), 13-20. doi:10.1016/j.tplants.2008.10.003
- Gul, S., Ng, J. W., Alonso-Mori, R., Kern, J., Sokaras, D., Anzenberg, E., ... Yano, J. (2015). Simultaneous detection of electronic structure changes from two elements of a bifunctional catalyst using wavelength-dispersive X-ray emission spectroscopy

- and in situ electrochemistry. *Phys Chem Chem Phys*, 17(14), 8901-8912. doi:10.1039/c5cp01023c
- Hanahan, N. (1985). Techniques for transformation of E. coli. *DNA cloning*, 1, 109-135.
- Hansmann, P., & Sitte, P. (1982). Composition and molecular structure of chromoplast globules of *Viola tricolor*. *Plant Cell Rep*, 1(3), 111-114. doi:10.1007/BF00272366
- Havaux, M., & Niyogi, K. K. (1999). The violaxanthin cycle protects plants from photooxidative damage by more than one mechanism. *Proc Natl Acad Sci U S A*, 96(15), 8762-8767.
- Heins, L., Mehrle, A., Hemmler, R., Wagner, R., Kuchler, M., Hormann, F., . . . Soll, J. (2002). The preprotein conducting channel at the inner envelope membrane of plastids. *EMBO J*, 21(11), 2616-2625. doi:10.1093/emboj/21.11.2616
- Hinnah, S. C., Wagner, R., Sveshnikova, N., Harrer, R., & Soll, J. (2002). The chloroplast protein import channel Toc75: pore properties and interaction with transit peptides. *Biophys J*, 83(2), 899-911. doi:10.1016/S0006-3495(02)75216-8
- Hirsch, S., Muckel, E., Heemeyer, F., von Heijne, G., & Soll, J. (1994). A receptor component of the chloroplast protein translocation machinery. *Science*, 266(5193), 1989-1992.
- Horie, Y., Ito, Y., Ono, M., Moriwaki, N., Kato, H., Hamakubo, Y., . . . Asayama, M. (2007). Dark-induced mRNA instability involves RNase E/G-type endoribonuclease cleavage at the AU-box and SD sequences in cyanobacteria. *Mol Genet Genomics*, 278(3), 331-346. doi:10.1007/s00438-007-0254-9
- Horton, P., Ruban, A. V., & Walters, R. G. (1996). Regulation of Light Harvesting in Green Plants. *Annu Rev Plant Physiol Plant Mol Biol*, 47, 655-684. doi:10.1146/annurev.arplant.47.1.655
- Jahns, P., & Holzwarth, A. R. (2012). The role of the xanthophyll cycle and of lutein in photoprotection of photosystem II. *Biochim Biophys Acta*, 1817(1), 182-193. doi:10.1016/j.bbabi.2011.04.012
- Johnson, M. P., Havaux, M., Triantaphylides, C., Ksas, B., Pascal, A. A., Robert, B., . . . Horton, P. (2007). Elevated zeaxanthin bound to oligomeric LHCII enhances the resistance of Arabidopsis to photooxidative stress by a lipid-protective, antioxidant mechanism. *J Biol Chem*, 282(31), 22605-22618. doi:10.1074/jbc.M702831200
- Johnson, M. P., Zia, A., & Ruban, A. V. (2012). Elevated DeltapH restores rapidly reversible photoprotective energy dissipation in Arabidopsis chloroplasts deficient in lutein and xanthophyll cycle activity. *Planta*, 235(1), 193-204. doi:10.1007/s00425-011-1502-0
- Kansy, M., Wilhelm, C., & Goss, R. (2014). Influence of thylakoid membrane lipids on the structure and function of the plant photosystem II core complex. *Planta*, 240(4), 781-796. doi:10.1007/s00425-014-2130-2
- Kato, Y., & Sakamoto, W. (2010). New insights into the types and function of proteases in plastids. *Int Rev Cell Mol Biol*, 280, 185-218. doi:10.1016/S1937-6448(10)80004-8
- Keegstra, K., & Yousif, A. E. (1986). Isolation and characterization of chloroplast envelope membranes. In *Methods in Enzymology* (Vol. 118, pp. 316-325): Academic Press.

- Kerr, R. A. (2005). Earth science. The story of O₂. *Science*, *308*(5729), 1730-1732. doi:10.1126/science.308.5729.1730
- Kessler, F., Blobel, G., Patel, H. A., & Schnell, D. J. (1994). Identification of two GTP-binding proteins in the chloroplast protein import machinery. *Science*, *266*(5187), 1035-1039.
- Khan, N. Z., Lindquist, E., & Aronsson, H. (2013). New putative chloroplast vesicle transport components and cargo proteins revealed using a bioinformatics approach: an Arabidopsis model. *PLoS One*, *8*(4), e59898. doi:10.1371/journal.pone.0059898
- Kikuchi, S., Oishi, M., Hirabayashi, Y., Lee, D. W., Hwang, I., & Nakai, M. (2009). A 1-megadalton translocation complex containing Tic20 and Tic21 mediates chloroplast protein import at the inner envelope membrane. *Plant Cell*, *21*(6), 1781-1797. doi:10.1105/tpc.108.063552
- Kim, D. H., & Hwang, I. (2013). Direct targeting of proteins from the cytosol to organelles: the ER versus endosymbiotic organelles. *Traffic*, *14*(6), 613-621. doi:10.1111/tra.12043
- Kirchhoff, H. (2008). Molecular crowding and order in photosynthetic membranes. *Trends Plant Sci*, *13*(5), 201-207. doi:10.1016/j.tplants.2008.03.001
- Klughammer, C., & Schreiber, U. (1994). An improved method, using saturating light pulses, for the determination of photosystem I quantum yield via P700 ⁺-absorbance changes at 830 nm. *Planta*, *192*(2), 261-268.
- Kobayashi, K. (2016). Role of membrane glycerolipids in photosynthesis, thylakoid biogenesis and chloroplast development. *J Plant Res*, *129*(4), 565-580. doi:10.1007/s10265-016-0827-y
- Kobayashi, K., Kondo, M., Fukuda, H., Nishimura, M., & Ohta, H. (2007). Galactolipid synthesis in chloroplast inner envelope is essential for proper thylakoid biogenesis, photosynthesis, and embryogenesis. *Proc Natl Acad Sci U S A*, *104*(43), 17216-17221. doi:10.1073/pnas.0704680104
- Kouranov, A., Chen, X., Fuks, B., & Schnell, D. J. (1998). Tic20 and Tic22 are new components of the protein import apparatus at the chloroplast inner envelope membrane. *J Cell Biol*, *143*(4), 991-1002.
- Kovacheva, S., Bedard, J., Patel, R., Dudley, P., Twell, D., Rios, G., . . . Jarvis, P. (2005). In vivo studies on the roles of Tic110, Tic40 and Hsp93 during chloroplast protein import. *Plant J*, *41*(3), 412-428. doi:10.1111/j.1365-313X.2004.02307.x
- Kroll, D., Meierhoff, K., Bechtold, N., Kinoshita, M., Westphal, S., Vothknecht, U. C., . . . Westhoff, P. (2001). VIPP1, a nuclear gene of Arabidopsis thaliana essential for thylakoid membrane formation. *Proc Natl Acad Sci U S A*, *98*(7), 4238-4242. doi:10.1073/pnas.061500998
- Kumar, S., Stecher, G., & Tamura, K. (2016). MEGA7: Molecular Evolutionary Genetics Analysis Version 7.0 for Bigger Datasets. *Mol Biol Evol*, *33*(7), 1870-1874. doi:10.1093/molbev/msw054
- Laemmli, U. K. (1970). Cleavage of structural proteins during the assembly of the head of bacteriophage T4. *Nature*, *227*(5259), 680-685.
- Lake, J. A., Larsen, J., Tran, D. T., & Sinsheimer, J. S. (2018). Uncovering the Genomic Origins of Life. *Genome Biol Evol*, *10*(7), 1705-1714. doi:10.1093/gbe/evy129

- Langenkamper, G., Manac'h, N., Broin, M., Cuine, S., Becuwe, N., Kuntz, M., & Rey, P. (2001). Accumulation of plastid lipid-associated proteins (fibrillin/CDSP34) upon oxidative stress, ageing and biotic stress in Solanaceae and in response to drought in other species. *J Exp Bot*, *52*(360), 1545-1554.
- Leon, G., Holuigue, L., & Jordana, X. (2007). Mitochondrial complex II Is essential for gametophyte development in Arabidopsis. *Plant Physiol*, *143*(4), 1534-1546. doi:10.1104/pp.106.095158
- Lundquist, P. K., Poliakov, A., Bhuiyan, N. H., Zybailov, B., Sun, Q., & van Wijk, K. J. (2012). The functional network of the Arabidopsis plastoglobule proteome based on quantitative proteomics and genome-wide coexpression analysis. *Plant Physiol*, *158*(3), 1172-1192. doi:10.1104/pp.111.193144
- Marchler-Bauer, A., Bo, Y., Han, L., He, J., Lanczycki, C. J., Lu, S., . . . Bryant, S. H. (2017). CDD/SPARCLE: functional classification of proteins via subfamily domain architectures. *Nucleic Acids Res*, *45*(D1), D200-D203. doi:10.1093/nar/gkw1129
- Martinis, J., Glauser, G., Valimareanu, S., & Kessler, F. (2013). A chloroplast ABC1-like kinase regulates vitamin E metabolism in Arabidopsis. *Plant Physiol*, *162*(2), 652-662. doi:10.1104/pp.113.218644
- Martinis, J., Glauser, G., Valimareanu, S., Stettler, M., Zeeman, S. C., Yamamoto, H., . . . Kessler, F. (2014). ABC1K1/PGR6 kinase: a regulatory link between photosynthetic activity and chloroplast metabolism. *Plant J*, *77*(2), 269-283. doi:10.1111/tpj.12385
- Meurer, J., Schmid, L. M., Stoppel, R., Leister, D., Brachmann, A., & Manavski, N. (2017). PALE CRESS binds to plastid RNAs and facilitates the biogenesis of the 50S ribosomal subunit. *Plant J*, *92*(3), 400-413. doi:10.1111/tpj.13662
- Miquel, M., & Browse, J. (1992). Arabidopsis mutants deficient in polyunsaturated fatty acid synthesis. Biochemical and genetic characterization of a plant oleoyl-phosphatidylcholine desaturase. *J Biol Chem*, *267*(3), 1502-1509.
- Miyagishima, S. Y. (2011). Mechanism of plastid division: from a bacterium to an organelle. *Plant Physiol*, *155*(4), 1533-1544. doi:10.1104/pp.110.170688
- Morre, D. J., Sellden, G., Sundqvist, C., & Sandelius, A. S. (1991). Stromal low temperature compartment derived from the inner membrane of the chloroplast envelope. *Plant Physiol*, *97*(4), 1558-1564.
- Mudd, E. A., Sullivan, S., Gisby, M. F., Mironov, A., Kwon, C. S., Chung, W. I., & Day, A. (2008). A 125 kDa RNase E/G-like protein is present in plastids and is essential for chloroplast development and autotrophic growth in Arabidopsis. *J Exp Bot*, *59*(10), 2597-2610. doi:10.1093/jxb/ern126
- Muhlethaler, K. (1959). Entwicklung und Struktur der Proplastiden. *The Journal of Cell Biology*, *6*(3), 507-512. doi:10.1083/jcb.6.3.507
- Mullet, J. E. (1993). Dynamic regulation of chloroplast transcription. *Plant Physiol*, *103*(2), 309-313.
- Nickelsen, J., & Rengstl, B. (2013). Photosystem II assembly: from cyanobacteria to plants. *Annu Rev Plant Biol*, *64*, 609-635. doi:10.1146/annurev-arplant-050312-120124
- Nickelsen, J., & Zerges, W. (2013). Thylakoid biogenesis has joined the new era of bacterial cell biology. *Front Plant Sci*, *4*, 458. doi:10.3389/fpls.2013.00458

- Nilkens, M., Kress, E., Lambrev, P., Miloslavina, Y., Muller, M., Holzwarth, A. R., & Jahns, P. (2010). Identification of a slowly inducible zeaxanthin-dependent component of non-photochemical quenching of chlorophyll fluorescence generated under steady-state conditions in *Arabidopsis*. *Biochim Biophys Acta*, *1797*(4), 466-475. doi:10.1016/j.bbabi.2010.01.001
- Nomura, Y., Takabayashi, T., Kuroda, H., Yukawa, Y., Sattasuk, K., Akita, M., . . . Tozawa, Y. (2012). ppGpp inhibits peptide elongation cycle of chloroplast translation system in vitro. *Plant Mol Biol*, *78*(1-2), 185-196. doi:10.1007/s11103-011-9858-x
- Peltier, J. B., Ytterberg, A. J., Sun, Q., & van Wijk, K. J. (2004). New functions of the thylakoid membrane proteome of *Arabidopsis thaliana* revealed by a simple, fast, and versatile fractionation strategy. *J Biol Chem*, *279*(47), 49367-49383. doi:10.1074/jbc.M406763200
- Ponce-Toledo, R. I., Deschamps, P., Lopez-Garcia, P., Zivanovic, Y., Benzerara, K., & Moreira, D. (2017). An Early-Branching Freshwater Cyanobacterium at the Origin of Plastids. *Curr Biol*, *27*(3), 386-391. doi:10.1016/j.cub.2016.11.056
- Porfirova, S., Bergmuller, E., Tropf, S., Lemke, R., & Dormann, P. (2002). Isolation of an *Arabidopsis* mutant lacking vitamin E and identification of a cyclase essential for all tocopherol biosynthesis. *Proc Natl Acad Sci U S A*, *99*(19), 12495-12500. doi:10.1073/pnas.182330899
- Potrykus, K., & Cashel, M. (2008). (p)ppGpp: still magical? *Annu Rev Microbiol*, *62*, 35-51. doi:10.1146/annurev.micro.62.081307.162903
- Richly, E., & Leister, D. (2004). An improved prediction of chloroplast proteins reveals diversities and commonalities in the chloroplast proteomes of *Arabidopsis* and rice. *Gene*, *329*, 11-16. doi:10.1016/j.gene.2004.01.008
- Roberts, D. R., Thompson, J. E., Dumbroff, E. B., Gepstein, S., & Mattoo, A. K. (1987). Differential changes in the synthesis and steady-state levels of thylakoid proteins during bean leaf senescence. *Plant Mol Biol*, *9*(4), 343-353. doi:10.1007/BF00014909
- Rockholm, D. C., & Yamamoto, H. Y. (1996). Violaxanthin de-epoxidase. *Plant Physiol*, *110*(2), 697-703.
- Rosado-Alberio, J., Weier, T. R., & Stocking, C. R. (1968). Continuity of the chloroplast membrane systems in *zea mays* 1968. *Plant Physiol*, *43*(9), 1325-1331.
- Rottet, S., Besagni, C., & Kessler, F. (2015). The role of plastoglobules in thylakoid lipid remodeling during plant development. *Biochim Biophys Acta*, *1847*(9), 889-899. doi:10.1016/j.bbabi.2015.02.002
- Rutherford, A. W., & Moore, T. A. (2008). Mimicking photosynthesis, but just the best bits. *Nature*, *453*, 449. doi:10.1038/453449b
- Sambrook, J., & Russell, D. W. (2001). *Molecular cloning : a laboratory manual* (3rd ed.). Cold Spring Harbor, N.Y.: Cold Spring Harbor Laboratory Press.
- Schackleton, J. B., & Robinson, C. (1991). Transport of proteins into chloroplasts. The thylakoidal processing peptidase is a signal-type peptidase with stringent substrate requirements at the -3 and -1 positions. *The Journal of Biological Chemistry*, *266*(5), 2152-2156.
- Schnell, D. J., Kessler, F., & Blobel, G. (1994). Isolation of components of the chloroplast protein import machinery. *Science*, *266*(5187), 1007-1012.

- Schottler, M. A., Albus, C. A., & Bock, R. (2011). Photosystem I: its biogenesis and function in higher plants. *J Plant Physiol*, *168*(12), 1452-1461. doi:10.1016/j.jplph.2010.12.009
- Schottler, M. A., Flugel, C., Thiele, W., & Bock, R. (2007). Knock-out of the plastid-encoded PetL subunit results in reduced stability and accelerated leaf age-dependent loss of the cytochrome b6/f complex. *J Biol Chem*, *282*(2), 976-985. doi:10.1074/jbc.M606436200
- Schottler, M. A., Toth, S. Z., Boulouis, A., & Kahlau, S. (2015). Photosynthetic complex stoichiometry dynamics in higher plants: biogenesis, function, and turnover of ATP synthase and the cytochrome b6/f complex. *J Exp Bot*, *66*(9), 2373-2400. doi:10.1093/jxb/eru495
- Schreiber, U., Bilger, W., Hormann, H., & Neubauer, C. (1998). *Chlorophyll fluorescence as a diagnostic tool: Basics and some aspects of practical relevance*.
- Schunemann, D. (2007). Mechanisms of protein import into thylakoids of chloroplasts. *Biol Chem*, *388*(9), 907-915. doi:10.1515/BC.2007.111
- Schwenkert, S., Soll, J., & Bolter, B. (2011). Protein import into chloroplasts--how chaperones feature into the game. *Biochim Biophys Acta*, *1808*(3), 901-911. doi:10.1016/j.bbamem.2010.07.021
- Seyfzadeh, M., Keener, J., & Nomura, M. (1993). spoT-dependent accumulation of guanosine tetraphosphate in response to fatty acid starvation in Escherichia coli. *Proc Natl Acad Sci U S A*, *90*(23), 11004-11008.
- Shih, P. M. (2015). Photosynthesis and early Earth. *Curr Biol*, *25*(19), R855-859. doi:10.1016/j.cub.2015.04.046
- Simkin, A. J., Gaffe, J., Alcaraz, J. P., Carde, J. P., Bramley, P. M., Fraser, P. D., & Kuntz, M. (2007). Fibrillin influence on plastid ultrastructure and pigment content in tomato fruit. *Phytochemistry*, *68*(11), 1545-1556. doi:10.1016/j.phytochem.2007.03.014
- Singh, D. K., Maximova, S. N., Jensen, P. J., Lehman, B. L., Ngugi, H. K., & McNellis, T. W. (2010). FIBRILLIN4 is required for plastoglobule development and stress resistance in apple and Arabidopsis. *Plant Physiol*, *154*(3), 1281-1293. doi:10.1104/pp.110.164095
- Singh, D. K., & McNellis, T. W. (2011). Fibrillin protein function: the tip of the iceberg? *Trends Plant Sci*, *16*(8), 432-441. doi:10.1016/j.tplants.2011.03.014
- Slack, C. R., Roughan, P. G., & Balasingham, N. (1977). Labelling studies in vivo on the metabolism of the acyl and glycerol moieties of the glycerolipids in the developing maize leaf. *Biochem J*, *162*(2), 289-296.
- Solymosi, K., & Schoefs, B. (2010). Etioplast and etio-chloroplast formation under natural conditions: the dark side of chlorophyll biosynthesis in angiosperms. *Photosynth Res*, *105*(2), 143-166. doi:10.1007/s11120-010-9568-2
- Sperling, U., Franck, F., van Cleve, B., Frick, G., Apel, K., & Armstrong, G. A. (1998). Etioplast differentiation in Arabidopsis: both PORA and PORB restore the prolamellar body and photoactive protochlorophyllide-F655 to the cop1 photomorphogenic mutant. *Plant Cell*, *10*(2), 283-296.
- Steinmuller, D., & Tevini, M. (1985). Composition and function of plastoglobuli : I. Isolation and purification from chloroplasts and chromoplasts. *Planta*, *163*(2), 201-207. doi:10.1007/BF00393507

- Stiller, J. W. (2007). Plastid endosymbiosis, genome evolution and the origin of green plants. *Trends Plant Sci*, 12(9), 391-396. doi:10.1016/j.tplants.2007.08.002
- Stoppel, R., & Meurer, J. (2012). The cutting crew - ribonucleases are key players in the control of plastid gene expression. *J Exp Bot*, 63(4), 1663-1673. doi:10.1093/jxb/err401
- Sugliani, M., Abdelkefi, H., Ke, H., Bouveret, E., Robaglia, C., Caffarri, S., & Field, B. (2016). An Ancient Bacterial Signaling Pathway Regulates Chloroplast Function to Influence Growth and Development in Arabidopsis. *Plant Cell*, 28(3), 661-679. doi:10.1105/tpc.16.00045
- Suzuki, J. Y., Sriraman, P., Svab, Z., & Maliga, P. (2003). Unique architecture of the plastid ribosomal RNA operon promoter recognized by the multisubunit RNA polymerase in tobacco and other higher plants. *Plant Cell*, 15(1), 195-205.
- Tevini, M., & Steinmuller, D. (1985). Composition and function of plastoglobuli : II. Lipid composition of leaves and plastoglobuli during beech leaf senescence. *Planta*, 163(1), 91-96. doi:10.1007/BF00395902
- Tikkanen, M., Nurmi, M., Kangasjarvi, S., & Aro, E. M. (2008). Core protein phosphorylation facilitates the repair of photodamaged photosystem II at high light. *Biochim Biophys Acta*, 1777(11), 1432-1437. doi:10.1016/j.bbabi.2008.08.004
- Timmis, J. N., Ayliffe, M. A., Huang, C. Y., & Martin, W. (2004). Endosymbiotic gene transfer: organelle genomes forge eukaryotic chromosomes. *Nat Rev Genet*, 5(2), 123-135. doi:10.1038/nrg1271
- Toyota, M., Ikeda, N., Sawai-Toyota, S., Kato, T., Gilroy, S., Tasaka, M., & Morita, M. T. (2013). Amyloplast displacement is necessary for gravisensing in Arabidopsis shoots as revealed by a centrifuge microscope. *Plant J*, 76(4), 648-660. doi:10.1111/tpj.12324
- Trosch, R., & Jarvis, P. (2011). The stromal processing peptidase of chloroplasts is essential in Arabidopsis, with knockout mutations causing embryo arrest after the 16-cell stage. *PLoS One*, 6(8), e23039. doi:10.1371/journal.pone.0023039
- van Wijk, K. J., & Kessler, F. (2017). Plastoglobuli: Plastid Microcompartments with Integrated Functions in Metabolism, Plastid Developmental Transitions, and Environmental Adaptation. *Annu Rev Plant Biol*, 68, 253-289. doi:10.1146/annurev-arplant-043015-111737
- Vidi, P. A., Kanwischer, M., Baginsky, S., Austin, J. R., Csucs, G., Dormann, P., . . . Brehelin, C. (2006). Tocopherol cyclase (VTE1) localization and vitamin E accumulation in chloroplast plastoglobule lipoprotein particles. *J Biol Chem*, 281(16), 11225-11234. doi:10.1074/jbc.M511939200
- Voet, D., Voet, J. G., & Pratt, C. W. (2008). *Fundamentals of biochemistry : life at the molecular level* (3rd ed.). Hoboken, NJ: Wiley.
- Vom Dorp, K., Holzl, G., Plohm, C., Eisenhut, M., Abraham, M., Weber, A. P., . . . Dormann, P. (2015). Remobilization of Phytol from Chlorophyll Degradation Is Essential for Tocopherol Synthesis and Growth of Arabidopsis. *Plant Cell*, 27(10), 2846-2859. doi:10.1105/tpc.15.00395
- Vothknecht, U. C., & Westhoff, P. (2001). Biogenesis and origin of thylakoid membranes. *Biochim Biophys Acta*, 1541(1-2), 91-101.

- Waegemann, K., Eichacker, S., & Soll, J. (1992). Outer envelope membranes from chloroplasts are isolated as right-side-out vesicles. *Planta*, *187*(1), 89-94. doi:10.1007/BF00201628
- Wang, P., Xue, L., Batelli, G., Lee, S., Hou, Y. J., Van Oosten, M. J., . . . Zhu, J. K. (2013). Quantitative phosphoproteomics identifies SnRK2 protein kinase substrates and reveals the effectors of abscisic acid action. *Proc Natl Acad Sci U S A*, *110*(27), 11205-11210. doi:10.1073/pnas.1308974110
- Westphal, S., Soll, J., & Vothknecht, U. C. (2001). A vesicle transport system inside chloroplasts. *FEBS Lett*, *506*(3), 257-261.
- Westphal, S., Soll, J., & Vothknecht, U. C. (2003). Evolution of chloroplast vesicle transport. *Plant Cell Physiol*, *44*(2), 217-222.
- Yalovsky, S., Paulsen, H., Michaeli, D., Chitnis, P. R., & Nechushtai, R. (1992). Involvement of a chloroplast HSP70 heat shock protein in the integration of a protein (light-harvesting complex protein precursor) into the thylakoid membrane. *Proc Natl Acad Sci U S A*, *89*(12), 5616-5619.
- Yamaoka, S., & Leaver, C. J. (2008). EMB2473/MIRO1, an Arabidopsis Miro GTPase, is required for embryogenesis and influences mitochondrial morphology in pollen. *Plant Cell*, *20*(3), 589-601. doi:10.1105/tpc.107.055756
- Youssef, A., Laizet, Y., Block, M. A., Marechal, E., Alcaraz, J. P., Larson, T. R., . . . Kuntz, M. (2010). Plant lipid-associated fibrillin proteins condition jasmonate production under photosynthetic stress. *Plant J*, *61*(3), 436-445. doi:10.1111/j.1365-313X.2009.04067.x
- Ytterberg, A. J., Peltier, J. B., & van Wijk, K. J. (2006). Protein profiling of plastoglobules in chloroplasts and chromoplasts. A surprising site for differential accumulation of metabolic enzymes. *Plant Physiol*, *140*(3), 984-997. doi:10.1104/pp.105.076083
- Zbierzak, A. M., Kanwischer, M., Wille, C., Vidi, P. A., Giavalisco, P., Lohmann, A., . . . Dormann, P. (2009). Intersection of the tocopherol and plastoquinol metabolic pathways at the plastoglobule. *Biochem J*, *425*(2), 389-399. doi:10.1042/BJ20090704
- Zhang, R., Wise, R. R., Struck, K. R., & Sharkey, T. D. (2010). Moderate heat stress of Arabidopsis thaliana leaves causes chloroplast swelling and plastoglobule formation. *Photosynth Res*, *105*(2), 123-134. doi:10.1007/s11120-010-9572-6
- Zhou, F., Liu, S., Hu, Z., Kuang, T., Paulsen, H., & Yang, C. (2009). Effect of monogalactosyldiacylglycerol on the interaction between photosystem II core complex and its antenna complexes in liposomes of thylakoid lipids. *Photosynth Res*, *99*(3), 185-193. doi:10.1007/s11120-008-9388-9
- Zoschke, R., & Bock, R. (2018). Chloroplast Translation: Structural and Functional Organization, Operational Control, and Regulation. *Plant Cell*, *30*(4), 745-770. doi:10.1105/tpc.18.00016

CURRICULUM VITAE

PERSONAL INFORMATION

Given name	Roberto Andres
Family name	Espinoza Corral
Date of Birth	24/05/1988
Nationality	Chile

EDUCATION

April 2015 - to date	PhD student Project "Protein import in chloroplasts", Supervisor Prof. Dr. Soll, Fakultät für Biologie, L Ludwig-Maximilians-Universität München.
October 2010 – August 2014 (Valparaiso, Chile)	Professional degree of Biochemist Pontificia Universidad Católica de Valparaiso
March 2006 – October 2010 (Valparaiso, Chile)	Degree in Biochemistry Pontificia Universidad Católica de Valparaiso
2002 – 2005 (Iquique, Chile)	Secondary education Cambridge Academy school (Iquique, Chile)
1994 – 2001 (Iquique, Chile)	Primary education American College school (Iquique, Chile)

SCIENTIFIC CONTRIBUTIONS

CONFERENCES

24-28 th June 2018 (Uppsala, Sweden)	First European Congress on Photosynthesis research, ePS-1.
3-7 th September 2017 (Konstanz, Germany)	XVIII Annual meeting of the international society of endocytobiology German section (ISE-G).
12-16 th May 2013 (Rosario, Santa Fé, Argentina)	8th International Conference for Plant Mitochondrial, Biology (ICPMB).

PUBLICATIONS

Restovic F., **Espinoza-Corral R.**, Gomez I., Vicente-Carbajosa J., Jordana X. (2017) An active mitochondrial complex II present in mature seeds contains an embryo-specific iron-sulfur subunit regulated by ABA and bZIP53 and is involved in germination and seedling establishment, *Frontiers in Plant Science*, 8, art. no. 277.

Veröffentlichungen

Teile dieser Arbeit sind ebenfalls zur Veröffentlichung vorgesehen. Folgendes Manuskript ist eingereicht:

Espinoza-Corral R., Heinz S., Klingl A., Jahns P., Lehmann M., Meurer J., Nickelsen J., Soll J., Schwenkert S. (2019) Plastoglobular protein 18 is involved in chloroplast function and thylakoid formation.

Eidesstattliche Versicherung

Ich versichere hiermit an Eides statt, dass die vorgelegte Dissertation von mir selbstständig und ohne unerlaubte Hilfe angefertigt wurde. Ich habe weder anderweitig versucht, eine Dissertation einzureichen oder eine Doktorprüfung durchzuführen, noch habe ich diese Dissertation oder Teile derselben einer anderen Prüfungskommission vorgelegt.

München, den 26.03.2019

Roberto Espinoza-Corral

Danksagung

Este trabajo, como también las enseñanzas que han guiado mi vida por altos y bajos se las debo a mi familia, a mi cultura, a Dios y a mis hermanos y hermanas de la vida. Creo que nadie pensó entre nosotros que algo como esto pasaría, donde tras generaciones de trabajo duro y muchas veces represión y discriminación, el tiempo en que nuestro trabajo y esfuerzo se recompense con el debido reconocimiento llegue en nación extranjera. Lo anteriormente dicho no es un reconocimiento al esfuerzo del que escribe, porque es poco o nada comparado con el sacrificio de mis ancestros a los que les debo todo, sea a ustedes los que aun viven mi admiración y agradecimiento eterno, a mi abuelo Héctor y mis abuelas Nelly y Carmen. Mi profundo y eterno agradecimiento a mis padres Roberto y Elisa por enseñarme, cuidarme y darme aquellos valores que nos han forjado a luchar donde sea que tengamos que trabajar. A mi hermana Cristina por su apoyo incondicional que me ha dado fuerzas para soportar lo que nos ha llegado de la vida. A mis hermanos y hermanas de la vida, son tantos que con esto espero me disculpen, pero los llevo siempre en mi corazón, a cada uno de ustedes y espero sus hijos sean luego aquellos quienes demuestren al mundo la riqueza de nuestro continente y nuestra cultura.

My family has expanded since I went abroad, for all those brothers and sisters who started this journey with me, I wish you all the success. To the family I meet in Germany and please excuse me if I cannot name all of you, I want to give thanks for your support and for making me feel once again at home. That also applies for the laboratory I worked in, for all my brothers and sisters who gave me support and a minute to exchange not just science but real and honest conversations and our life, I would like to express my gratitude. To my brothers Ahmed, Daniel, sisters Li, Tamy, Renuka, Annabel, Franka, Manali, etc., please excuse me if I am not mentioning all of you. Real scientific development and understanding does not go anywhere but backwards without freedom, that is why I want to deeply give thanks to Serena for her supervision, support and constructive criticism, if I am a better scientist later a lot is because of her. I would like to also give thanks for the opportunity that Prof. Soll gave me to pursue my scientific carrier in his lab. Moreover, I would like to apologize to every single person I have annoyed and for the mistakes I have made, to those who felt I was rude or said wrong words, please forgive me for those moments, for all the headaches I have meant and for my faults. Finally, I would just express my gratitude for this opportunity in life and those who made it possible.

“In this modern day, when material goals and selfish aims dominate the scene of human effort, this high professional ideal of self-sacrifice and self-less devotion to one’s fellowmen may appear too remote, its demands too severe. But man is not meant to live for himself alone. He exists with others and for others, and it is this sense of social consciousness which distinguishes him from all other beings. And this goal can and will be attained by those who realize the tremendous potential of spiritual strength and their stay in striving ceaselessly for the attainment of this high objective” Negus Nagast, Haile Selassie I, July the 11th, 1958, Addis Ababa.